University of Messina

THESIS FOR THE DEGREE OF PHILOSOPHIAE DOCTOR

PHD COURSE IN APPLIED BIOLOGY AND EXPERIMENTAL MEDICINE

CURRICULUM IN BIOLOGICAL AND ENVIRONMENTAL SCIENCES

XXXVI PROGRAM

SSD BIO/07

Biological and ecological aspects of a native population of *Ruditapes decussatus* from the Lagoon of Capo Peloro (Messina – Italy): a multidisciplinary study

PhD candidate

Sergio Famulari

Supervisor

Professor Nunziacarla Spanò

Coordinator: Professor Nunziacarla Spanò

ACADEMIC YEAR 2022-2023

Acknowledgements

The realisation of this study would not have been possible without the contribution, preparation, and spirit of cooperation of the entire research team Lab StREAM (Laboratorio per lo Studio, la Ricerca e l'Esplorazione dell'Ambiente Marino) from the University of Messina. For this reason, I would first like to thank my supervisor, Professor Nunziacarla Spanò, for creating and always supporting this great team.

Special thanks are addressed to Professors Gioele Capillo and Serena Savoca, for their constant support, for sharing their experience in the field and for the constructive discussions that have never been lacking over all these years. I would also like to thank Professor Marco Albano and Dr. Claudio Gervasi for their valuable involvement during the molecular analyses.

I could not be more grateful to Dr. Sabrina Natale for her sincere friendship and for her invaluable involvement and support during all the sampling, laboratory analyses and drafting stages required to carry out this study.

Sincere gratitude is extended to all members of the research team Lab StREAM, Dr. Claudio D'Iglio, Professor Davide Di Paola, Dr. Dario Di Fresco, Dr. Alex Carnevale, Dr. Mariachiara Costanzo, Dr. Tosin Afeniforo, Dr. Shabab Hussain, Dr. Laura Saccardi. In particular, I would like to express my gratitude to Dr. Dario Di Fresco and Dr. Laura Saccardi for their help during the sampling and laboratory analysis phases, as well as to Dr. Claudio D'Iglio, with whom I shared this PhD course from the first to the last day.

It is a pleasure to thank the research team of Professors Fabio Marino and Carmelo Iaria for their fruitful cooperation.

Finally, my deepest gratitude is for my family to whose unceasing support I owe the achievement of this goal.

Table of contents

Index of figures

Index of tables

Abstract

The grooved carpet shell clam (*Ruditapes decussatus* – Linnaeus, 1758) is a bivalve mollusc belonging to the family Veneridae. The farming of this species of high commercial value has deep roots in the local culture of the city of Messina (Sicily – Italy), boasting a centuries-old tradition as one of the main activities in the Lagoon of Capo Peloro, along with mussel farming. Following the introduction into the Italian market of the Indo-Pacific congeneric species, *Ruditapes philippinarum* (Adams & Reeve, 1850), the native populations of grooved carpet shell clams has significantly declined, mostly due to the greater resistance and adaptability that characterise the allochthonous species, as well as frequent hybridization events. These aspects, together with the considerable technical difficulties related to the controlled reproduction of these molluscs, make it challenging to conducts investigations necessary to learn more about the natural population distribution of *R. decussatus* in the Mediterranean Sea. In this perspective, the following research has been developed, aimed to describe through a multidisciplinary approach a native population of grooved carpet shell clams living in the lagoon of Capo Peloro (Messina). The main goal is to preserve this species and fully reintroduce it into national shellfish farming activities as a niche product, using the traditional techniques employed in Capo Peloro lagoon since ancient times as an integrated model of sustainable shellfish farming. In the past, the accurate and consistent management of areas designated for mollusc production indeed ensured the maintenance of delicate ecosystem balances, leading to an improvement in water quality and the preservation of high biodiversity rates in these areas.

1. Introduction

1.1 The ancient origins of bivalve molluscs farming

It is likely that bivalve molluscs were among the first aquatic organisms to be extensively exploited by human as food source. These benthic animals can be found on both hard and soft bottoms, often in a few centimetres of water or even left exposed by the tides, being therefore much easier to catch than other edible organisms such as crustaceans and fishes. The exploitation of this aquatic resources was thus part of the basis of the economy that characterized the first human settlements during ancient times, before agriculture and animal husbandry development. For this reason, clear signs of this old activity have been discovered worldwide. The most famous example, due to its impressiveness and the scientific interest that its discovery has aroused, is certainly represented by the piles of shells and bones found along the east coast of Denmark towards the beginning of 19th century. The so called *"kioekkenmoedlinger"* (literally "kitchen leftovers" in ancient Danish language) were often up to 300 meters long, 60 meters wide and up to 3 meters high. Other similar finds dating back to about 10000 years ago were discovered in Japan, North Africa, Brazil, Cuba, Georgia, Portugal, and France, confirming the ubiquity of this human activity since ancient times. Many of these heaps were brought to light not only on seacoasts but even near rivers and lakes, revealing a crucial point for the history of shellfish farming: humans probably began to make the harvesting of molluscs more fruitful, by introducing these animals in particularly favourable environments and controlling the productive cycle of the resource. Evidence of the above were found even within the intertidal zone along the northwest coast of North America, where the natives built up clam gardens about 3500 years ago, composed of a rock wall positioned at the low tide mark and a flattened terrace (N. F. Smith et al., 2019). It is therefore clear that bivalve molluscs cultivation evolved independently worldwide, although starting from the same observations and insights, during different periods.

1.2 The history of shellfish farming in Italy

Regarding Italy, the history of shellfish farming is deeply rooted in the ancient civilizations that once thrived along its coastlines. The practice can be traced back to the time of the Romans and Greeks (Marzano, 2013), who recognized the value of these marine resources: oyster beds were established in the Gulf of Naples and nearby the city of Brundisium (today called Brindisi – Puglia),

where cultivation techniques for bivalve molluscs began to take shape, albeit on a relatively small scale compared to what would come in later centuries. The Middle Ages marked a significant turning point in the history of bivalve molluscs farming in Italy. Coastal communities, particularly those in the northern areas such as Venice and the Adriatic coast, began to recognize the economic potential of cultivating bivalve molluscs, exploiting the favourable characteristics of the lagoon environments. With a growing demand for these seafood, fishermen and coastal dwellers experimented with new methods to increase their production. Shallow ponds and lagoons were transformed into specially designed farming areas, providing a controlled environment for the cultivation of bivalves. This period saw the emergence of innovative techniques, such as constructing wooden stakes and placing them in the lagoon beds to serve as substrates for bivalves. These simple structures provided ideal surfaces for the bivalves to grow, enabling farmers to increase their yields and meet the growing demand. As consequence, several strategies of government were adopted for the preservation of lagoon environment and for the management of its biological resources, controlling any potentially harmful human activity through minutely detailed regulations. These policies were based on surprisingly modern principles, such as a clear description of the equipment to be used for different type of fishing, the minimum size of specimens to be caught and prohibitions on fishing during pre-reproductive periods of several organisms, as well as the identification of special protected areas of particular importance for juveniles' development. Such intense legislative activity affected the emerging cooperatives of operators in fishing sector and the trade in the final products, showing an overall advanced understanding of the principles underlying the correct management of these renewable resources. During the Renaissance, Italy experienced a flourishing of arts, culture, and scientific discoveries. This period also had a profound impact on the development of bivalve molluscs farming. Scholars and scientists began to study the biology and ecology of these organisms, contributing to a deeper understanding of their life cycles and environmental requirements. This newfound knowledge was shared among communities, further improving the techniques and practices of bivalve molluscs farming. Coastal regions such as Tuscany, Liguria, and Campania (Lovatelli et al., 2008) became centres of innovation and expertise of these practices. Farmers refined their methods, including the creation of artificial habitats, such as mussel rafts, which allowed for efficient cultivation in open waters. These rafts consisted of floating platforms on which ropes or nets were suspended, providing favourable substrates for the bivalves. This technique proved to be highly successful and remains widely used nowadays.

1.3 The heritage of traditional bivalve molluscs farming in the Capo Peloro Lagoon (Messina – Sicily)

Located in the north-eastern corner of Sicily (38°15'57" N, 15°37'50" E), where the Ionian and Tyrrhenian seas meet (Mazzola et al., 2010; D'Iglio et al., 2021), the Lagoon of Capo Peloro is historically renowned for its rich biodiversity, natural beauty, and traditional bivalve mollusc farming practices (Figure 1).

Figure 1 - Lagoon of Capo Peloro and the Strait of Messina seen from above (38°15'57" N, 15°37'50" E) Sicily – Italy

© ANTONINO BARTUCCIO 2021

This peculiar environment has been recognized as "Heritage of ethno-anthropological interest" (Declaratory Measure 1342/88, 1988), being a site of ancient and traditional productive activities related to shellfish farming (bivalves, mainly mussels and clams). It is also a Natural Reserve established by the Sicilian Region (D.A. 21/06/01, 2001), as well as Site of Community Importance (SIC) according to Directive 92/43/CEE and Special Protection Zone (ZPS) according to Directive 79/409/CEE (Sanfilippo et al., 2022). The lagoon of Capo Peloro is composed by three closely related physiographic units: two brackish ponds commonly named Ganzirri and Faro, the hills, and the Capo Peloro sand tongue (Antonioli et al., 2004). These two semi-closed basins are connected by the canal "Margi" (Albano et al., 2021; D'iglio et al., 2022). Moreover, the presence of several canals that allows the communication with the surrounding sea is essential for small exchanges of water that occur daily, following the tidal pattern (Manganaro et al., 2011).

However, the salinity of lakes waters does not exclusively depend on the connections with the sea, being the result of the interaction between rainwater conveyed in underground aquifers mainly fed by the hills, and marine waters (Manganaro et al., 2011). From an ecological point of view, this transitional environment is particularly relevant, especially because of the strong correlation with the Strait of Messina, globally known for its peculiar habitats (Butman & Raymond, 2011; Capillo et al., 2018; Savoca et al., 2020; D'Iglio et al., 2023). The Lake Ganzirri, also known as "Large marsh", is a brackish coastal basin that covers an area of 34 ha, with a registered maximum depth of 7 m and a total water volume of 106 m^3. Viewed from above, it has the appearance of a long (1670 m) and narrow (on average ~200 m) stream tube parallel to the Ionian coast (Manganaro et al., 2011), communicating with the Strait of Messina through the canal "Carmine" and with Lake Faro through the canal "Margi" (Sanfilippo et al., 2022). The Lake Faro, also named "Small marsh", has a smaller extension, covering an area of 26 ha with an almost circular shape (~500 m of diameter). This small meromictic marine coastal lagoon (Silvestro et al., 2017) has about 3 m average depth, reaching 30 m in its central part. There are two main canals through which the small marsh communicates with the surrounding sea: the "English" canal and the canal "Faro". The first one is an artificial canal only periodically opened during summer, connecting the Lake Faro with the Tyrrhenian Sea while the latter allows the continuous communication with the Straits of Messina (Manganaro et al., 2009). Regarding the geological formation of this area, it is likely that the lagoon of Capo Peloro was originated by tectonic movements in the Strait of Messina during Pliocene and Pleistocene (Barrier, 1995). This hypothesis was supported by data collected through radiocarbon dating, sedimentological and paleontological analysis performed during stratigraphical and geomorphological surveys that proved the relative change in sea level (Antonioli et al., 2004). Several models of shoreline barrier development were proposed by different authors (Chillemi, 1995; C. Bottari & Carveni, 2009) to date the formation of brackish ponds along the coastline. More specifically, it has been estimated that the formation of the large marsh dates to 3000-2500 BC (A. Bottari et al., 2005). The current conformation of Capo Peloro sand tongue and Lake Faro is more recent, being the result of a concentric accumulation of Eolian sand and shoreline sand around the eastern border of the small marsh during the late Holocene, shaped over time by the combined action of currents and waves (Antonioli et al., 2004). Traditional bivalve mollusc farming in the lagoon of Capo Peloro has deep historical roots, holding an immense socio-cultural significance specially for inhabitants of these areas. The practice dates back centuries, with local communities relying on the abundant lagoon

resources for sustenance and trade. Several archaeological findings brought to light in Ganzirri area suggest that human settlements took place from 5000 BP, during the early stage of sand accumulation (Biddittu et al., 1979). Moreover, historical evidence dating to Greek and Roman times proved the existence of a natural harbour exploited for its strategic position since the 1st century BC, as confirmed by the discovery of temple foundations and other archaeological materials during the excavations for the construction of canals by the Bourbons in more recent times (Solino, 1864; Biddittu et al., 1979). According to historical documents (Aricò, 1999; Buceti, 2004), fishing and hunting activities were regularly carried out by local communities in Capo Peloro lagoon, along with the swordfish fishing in the Strait of Messina, a fashionable hobby particularly appreciated by aristocracy since the 16th century (Manganaro et al., 2011). Between the late 18th century and the early 19th century, the keen interest in exploiting fishery resources, along with the military needs related to the British occupation, led to the construction of several canals to connect the brackish ponds to each other and to the surrounding sea (Manganaro et al., 2009). The first empirical data on temperature, salinity, and oxygen of Lakes Ganzirri and Faro dates to the end of 19th century and the beginning of 20th century (Carazzi, 1897; Ficalbi, 1898; Terni, 1901; Sanzo, 1904), proving the spread of scientific interest in the lagoon of Capo Peloro. More accurate and complete documentation dates to about the middle of the last century, with pioneering studies that report data still comparable to the latest (Mazzarelli, 1938; Lo Giudice, 1940; Dulzetto, 1942; Abruzzese & Genovese, 1952; Crisafi, 1954; Cavaliere, 1963). Special attention was also paid to the shellfish farming in this area (Ficalbi, 1898), mainly focusing on the sanitation of brackish ponds waters (Caselli, 1901; Terni, 1901), the health safety of edible bivalve molluscs (Sanzo, 1904), and the potential spread of infectious diseases related to human consumption (Gamberini, 1920). Shellfish cultivation activities have been regularly carried out in the Lake Ganzirri until 1981, after which, due to heavy pollution condition and waters contamination by pathogenic prokaryotes (Alonzo et al., 1979, 1981), the activities have been definitively forbidden (Sanfilippo et al., 2022; Regional Decree June 2, 1981; Directive 95/70/CE). In later years, the monitoring on hygienic conditions of waters (Ciaccio, 1983; Delia et al., 1984) and on environmental quality (Cortese et al., 2000; Bergamasco et al., 2005; Mazzola et al., 2010b) was carried out and regular controls are still performed periodically to reintroduce bivalves farming. Nowadays, shellfish harvesting is practiced by a local cooperative in the large marsh, where native species live (mainly *Ruditapes decussatus, Polititapes aureus, Cerastoderma glaucum*). However, the “production cycle” is discontinuous due to the considerable variability of

climate, oxygenation of waters, salinity and algal trophism. Rearing and cultivation of bivalve molluscs (mainly *Mytilus galloprovincialis* and *Ruditapes philippinarum*) are still widely practiced in Lake Faro, with an estimated mean cultivated biomass of ~300 t per year (Manganaro et al., 2011). However, contrary to common beliefs, shellfish farming activities carried out only provide for acclimatization and fattening of specimens generally coming from different areas of Italy (i.e., Venetian Lagoon, region of Marche, Trieste, and region of Emilia Romagna) and from Spain or other foreign areas during some periods of the year. There are currently five molluscs distribution centres operating in Faro area (of which one is also a shellfish purification centre) that are responsible for ensuring the suitability for human consumption of bivalve molluscs.

1.4 Shellfish aquaculture in modern times

In recent decades, Italy's bivalve molluscs farming industry has gained international recognition for its high-quality products and sustainable practices. Stricter regulations have been implemented to protect coastal ecosystems and ensure the production of healthy and safe seafood. Italy's favourable climate and waters, as well as the commitment to sustainable aquaculture have certainly contributed to its position as a leading producer of bivalve molluscs. Nowadays the shellfish farming represents the main productive system of Italian aquaculture, reaching 62,7 % of national production in 2016 with a total of 93252.8 tons mainly produced in Veneto, Emilia-Romagna, and Puglia (Antonini et al., 2019). According to the European Market Observatory for Fisheries and Aquaculture Products (EUMOFA), the Italian shellfish farming represents the 16 % of Community aquaculture, showing a decreasing trend after the increases recorded between 2012 and 2013. This leading sector has an estimated value close to 2/3 of national production (PROGRAMMA OPERATIVO NAZIONALE FEAMPA 2021-2027) , followed by salmonids (mainly trout – 22 %) and marine fishes (almost 11 % in total) (Figure 2). As reported by the census of the Italian Ministry of Agriculture, among 973 aquaculture production systems active in 2017, 385 were for shellfish farming. The regional analysis follows the productive structure of Italian aquaculture: as expected, most employees are in Veneto and Emilia Romagna, followed by Puglia and Sardegna, where the main mollusc farms are located, outside the area between the mouths of the Po and Adige rivers. Towards the end of 2019, the Chambers of Commerce reported a total of 5921 employees in aquaculture industry, almost half of whom (2919) were concentrated in the provinces of Rovigo and Ferrara, where the main Italian shellfish

farms are present (Table 1). The national production is based almost exclusively on mussels (*Mytilus galloprovincialis*), Manila clams (*Ruditapes philippinarum*) and to a lesser extent on oysters (*Ostrea edulis* and *Magallana gigas*). With a harvest of 50,000 tons per year, Italy is the top European producer and the second largest in the world of carpet shell clams. Limited quantities of grooved carpet shell clams (*Ruditapes decussatus*) are harvested from natural beds in Sardinia and Sicily, where restrictions are applied to resource management (Lovatelli. et al., 2008).

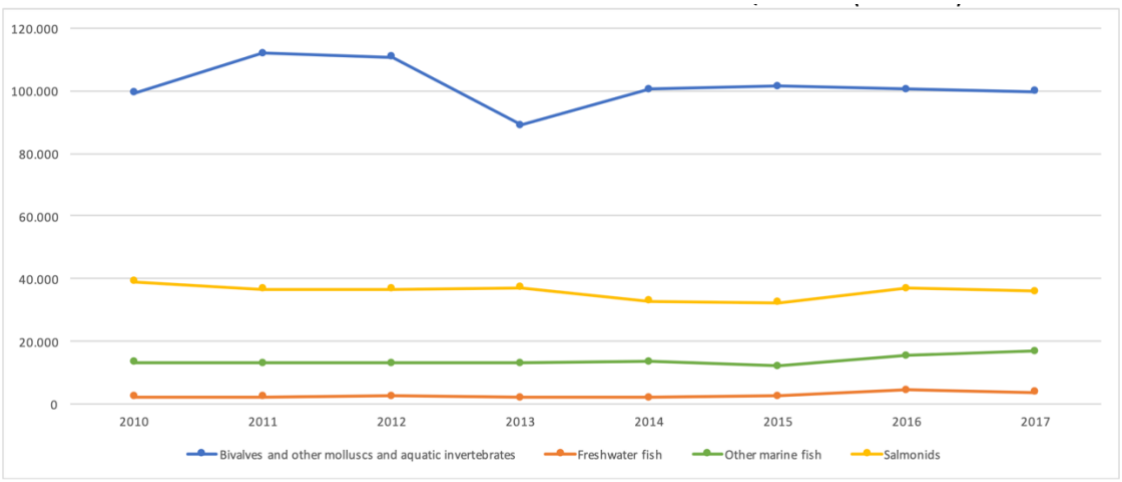

Figure 2 - Production trends of the main aquaculture fields (tonnes) from 2010 to 2017: the production of aquatic invertebrates, bivalves and other molluscs is significantly higher than the other main fish products (source - EUMOFA processing of data from Eurostat, FAO, FEAP and national administrations)

Region	N. employees 2014	N. employees 2019	Variation 2014/2019
Abruzzo	46	38	-17%
Basilicata	12	8	-33%
Calabria	18	26	44%
Campania	77	79	3%
Emilia-Romagna	1331	1722	29%
Friuli-Venezia Giulia	201	211	5%
Lazio	115	124	8%
Liguria	76	92	21%
Lombardia	239	140	-41%
Marche	173	177	2%
Molise	10	8	-20%
Piemonte	84	74	-12%
Puglia	442	458	4%
Sardegna	265	394	49%
Sicilia	212	212	0%
Toscana	94	186	98%
Trentino-Alto Adige	95	123	29%
Umbria	29	33	14%

Valle d'Aosta	3	3	0%
Veneto	1707	1813	6%
Total ITALY	**5229**	**5921**	**-13%**

Table 1 - Comparison of human resources employed in aquaculture fields in 2014 and 2019 by region (source: Chamber System, Open Data Explorer)

1.5 Fishing and breeding of Ruditapes spp.

Bivalve molluscs belonging to the genus *Ruditapes* are subject to community, national, and regional constraints on the minimum catch size, while there are no regulations on the fishing period (Cannas, 2010). The EC legislation has established the threshold value of 25 mm for minimum catch size, a provision also recognised in Italy with the Presidential Decree n. 1639, 02/10/1968, and subsequent amendments. The retail sale of the finished product is regulated by the Decree law n. 530, 30/12/1992 (implementing EEC Directive 91/492), which establish the health regulations applicable to the production and marketing of live bivalve molluscs, including the maximum algal biotoxin content (Decision n. 2002/225/EC, 15/03/2002). According to these regulations, only bivalves reared and harvested in areas classified for this purpose may be marketed, based on the following scale:

- **Class A**: molluscs from these areas can be used for direct human consumption without undergoing any sanitization process.
- **Class B:** molluscs from these areas must undergo a purification process before being marketed.
- **Class C:** molluscs from these areas must be housed for not less than two months in waters of class A.

As for the study area, the waters of Lake Faro are currently rated A, while class C is still assigned to the waters of Lake Ganzirri, despite the regular controls carried out to reintroduce traditional bivalve breeding, as mentioned in the previous paragraphs. Techniques but especially the tools used for the ancient practice of clam fishing in Italy have undergone a remarkable evolutionary process over the years, moving from simple hand tools such as knifes, rakes, and sieves to more sophisticated mechanical tools (e.g., hydraulic and vibrating dredge, mechanical sieves). Capture performance is obviously different for each tool, with significant improvements due to the transition from manual to mechanised harvesting systems. A brief description of the mainly used tools, which are not always approved by the regulations, is provided below (Cannas, 2010). The

use of the hydraulic dredge, which is very popular for fishing for the striped Venus clam, *Chamelea gallina* (Linnaeus, 1758), is prohibited in lagoon waters, due to the significant losses of fine materials and the damage caused to benthic stands (Pranovi & Giovanardi, 1995). However, it has been widely misused in the Manila clam fishery. As provided by Ministerial Decree 21/07/1998, this tool is in the shape of a metal parallelepiped resting on the seabed, mounted on boats that must have a maximum length between perpendiculars of 10 meters and a weight less than 10 tons. A series of nozzles placed on the upper part of the tool emit pressurized water that enters the substrate and collects the buried molluscs from the seabed. The vibrating dredge is a specific type of rake that differs from the hydraulic dredge in the mechanism of separating the bivalves from the sediment, which is achieved through an eccentric mass placed on the dredge that, as it rotates, causes it to vibrate. The mechanical rake (known in Italy as “rusca”) began as an evolution of traditional hand tools, refined over time according to the growing needs of professional fishermen. The "rusca" is mounted on a boat which laterally features a special net and an outboard motor. It is made up of a metal frame with two openings: a pentagonal mouth equipped with a V-shaped blade at the base, on the opposite side, a second rectangular opening that connects to the net. Between the two openings, on the bottom and sides of the tool, a metal grid is placed. The "rusca" operates near the auxiliary outboard motor located on one side of the boat, whose function is to remove sediment from the bottom and push the catch into the frame. This method allows for almost continuous work. While the slow advance of the boat allows the blade of the "rusca" to penetrate the sediment to collect buried bivalves, two skids placed at the base of the frame prevent the structure from sinking. The “turbo-blowing rusca” is another tool that evolved from hand rakes. The operation of this small dredge relies on a complex system of pipes and a gasoline-powered collection pump that pushes pressurized seawater into the gear. The crate or towed dredge consists of an iron mesh structure installed on two skids and towed by a motorboat. At the rear of the crate is a net bag for collecting the product. There is a V-shaped blade in the mouth that allows it to sink into the ground, and the turbulence produced by the propeller of the outboard motor, placed at the level of the bottom, is used for harvesting. To use this rather dangerous tool, two operators are required: the first on board who controls the outboard whose propeller moves the seabed, the second standing on the box whose weight keeps it sunk into the sediment. Despite significant advances in technology, hand tools and traditional techniques are still widely used in regions where mechanical means are not allowed (e.g., Sardinia) or in small local shellfish farming settings. The manual rake takes different shapes

and sizes depending on the area but generally consists of a mesh case fitted with conical metal teeth about 15 cm long and a long handle. It is used mainly on foot by operators equipped with diving suits and, when necessary, short stilts. Hand fishing is practiced with gloves and boots on the thigh to collect various marine and lagoon fossorial species. Animals are identified by the holes formed by siphons using a rudimentary mirror, a box whose bottom is fitted with glass. The animal is extracted by sticking a knife into the sediment perpendicular to the bottom. In cases where the bottom is very compact and the density of shellfish considerable, fishing is done with shovel and sieve. Like all human activities, the harvesting of bivalve molluscs, whether by hand or by mechanical means, can have negative consequences on the environment. More specifically, removal of large amounts of sediment can damage delicate juvenile stages by burying them at excessive depth or bringing them to the surface, thus making them more vulnerable to predation and causing high mortality (Bald et al., 2003; Borja et al., 2007). In addition, increased water turbidity due to sediment movement can have negative effects on the health of shellfish populations, such as lower growth and reproduction rates and increased mortality (Goulletquer P. & Bacher C., 1988). Today, breeding is a practice that essentially concerns the species *R. philippinarum,* well established in the Mediterranean area for decades and characterized by higher yields than the native species, as discussed above. As described by Helm M.M. & Pellizzato M. (1990), breeding under controlled conditions involves the selection of breeding stock and the composition of release batches, primarily based on the phenotypic characteristics most demanded by the market and the level of acclimatization of the specimens. Spawning stock conditioning requires some control of key water parameters (especially temperature and salinity) and can be carried out either in flowing or "still water" systems. Supplementary food, mainly consisting of phytoplanktonic species such as *Isochrysis galbana, Tetraselmis suecica, Dunaliella tertiolecta, Chaetoceros spp., Thalassiosira spp., Skeletonema costatum, Phaeodactylum ssp.,* should be given regularly, taking care to select the most suitable microalgae based on the stage of development and size of the clams. Gamete release can be achieved by two methods: the mass emission and individual emission. The former is mainly practiced commercially to obtain as many eggs and sperm as possible, while the latter is followed to select individual phenotypes for breeding. This is followed by the collection of fertilized eggs using special sieves with a mesh size of 25 µm. Larval development occurs best at temperatures between 18° and 28°C and salinity between 26‰ and 33‰. The optimal temperature is between 23° and 26°C, as higher temperatures increase problems with bacterial infections, while at lower temperatures larval

development is very slow. During larval metamorphosis stages, it is very important to conduct regular water changes and use appropriate aerators to ensure optimal oxygenation and gentle movement of water. Under favourable environmental conditions, larvae settlement occurs after about three weeks. The juveniles can then be moved first to a “still-water” system, and subsequently to a running water system that basically relies on a continuous water flow from above (“down-welling system”) or below (“up-welling system”) and on the use of special sieves that can retain the young clams within them, facilitating the handling. Bivalves weaning (size 2-3 mm to 10 mm) is certainly the most critical stage of the entire production cycle, during which the highest mortality rates occur. The transition from the controlled to the natural environment requires special attention, especially in the choice of the pre-fattening site on which the economic success of shellfish farming primarily depends. The salinity of the water should always be between 20‰ and 35‰, avoiding sudden changes, with a temperature above 10°C for at least 6-8 months of the year. Regarding the bottom substrate, it should preferably be sandy or muddy-sandy, while the current flow should be constant and never more than 50 cm/sec (Helm M.M. & Pellizzato M., 1990).

1.6 Research goals

The main purpose of this research is to deepen the knowledge of the natural population of *Ruditapes decussatus* living in the lagoon of Capo Peloro (Messina – Italy) through a multidisciplinary approach, to preserve it and fully reintroduce it to the national market as a niche product of traditional venerid farming activities of the Peloritan area. The importance of the grooved carpet shell clam in this area is not only related to economic value and ancient heritage. In the past, the careful and constant management of bivalve mollusc production areas ensured the preservation of delicate ecosystem balances, resulting in improved water quality and maintenance of high rates of biodiversity in these areas. These issues, along with the serious threat posed by the introduction of allochthonous species such as *R. philippinarum*, inspired this research, whose main goals are listed more specifically below:

- Studying the population structure of the species *R. decussatus* living in the Lake Faro of Capo Peloro lagoon
- Evaluation of intraspecific ecomorphological differences through shell shape analysis
- Genetic identification of the species under study through specific molecular analysis

- Studying the gonadal development related to the seasons through histological assessment
- Evaluation of the occurrence of plastic debris ingested by the clams analysed

2. Biological and ecological aspects of *Ruditapes decussatus* (Linnaeus, 1758)

2.1 General remarks on bivalve molluscs

2.1.1 The shell

The following paragraphs are based upon the texts by Gosling (2015), Cesari & Pellizzato (1990), and De Vico & Carella (2012).

The name of this invertebrates comes from their main characteristic, that is the constant presence of the shell composed by two distinct valves hinged together by elastic ligaments and interlocking teeth. The contraction of strong adductor muscles, located in dorsal position, together with the relaxation of the above-mentioned ligaments, enable the closing and opening of the valves respectively, whose main function is to protect the soft body of the animal (Figure 3).

A: Heart
B: Pericardium
C: Posterior adductor muscle
D: Anterior adductor muscle
E: Exhalant siphon
F: Inhalant siphon
G: Gills
H: Anus
I: Mantle adge
J: Gonad
K: Byssus gland

L: Foot
M: Digestive gland
N: Labial palps
O: Stomach
P: Esophagus
Q: Mouth
R: Gland of the crystalline style
S: Gut
T: Cardinal teeth
U: Ligament

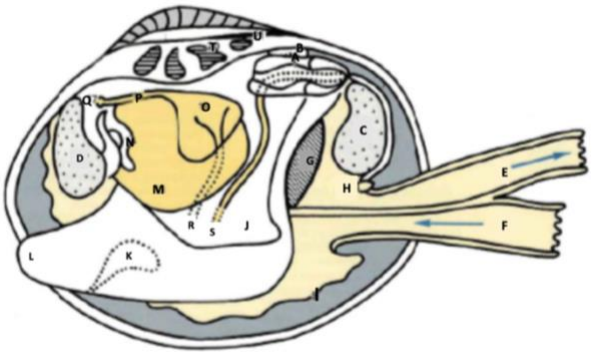

Figure 3 - Anatomy of Ruditapes spp.

In addition, the shell acts as a skeleton for muscles attachment and, in borrowing species, it prevents the infiltration of mud and sand in the mantle cavity. As in all other molluscs, bivalve shell is secreted by the mantle (also known as pallium), and its main component is calcium carbonate, mainly in the form of calcite and aragonite. The intake of calcium ions occurs from the surrounding environment or from the diet. The assimilated ions are sent through the bloodstream to the mantle and then to the extrapallial liquid between shell and mantle. This is the site where the deposition of carbonate calcium crystals occurs in an organic matrix, mainly composed of a

complex assemblage of hydrophobic silk protein (Polysaccharide β-chitin) and hydrophilic proteins, many rich in aspartic acid (Addadi et al., 2006). More than 95% of shell weight is represented by the mineral component, while 1-5% represents the organic matrix. Basing on the arrangement of calcium crystals it is possible to distinguish three layers that make up the shell (Figure 4).

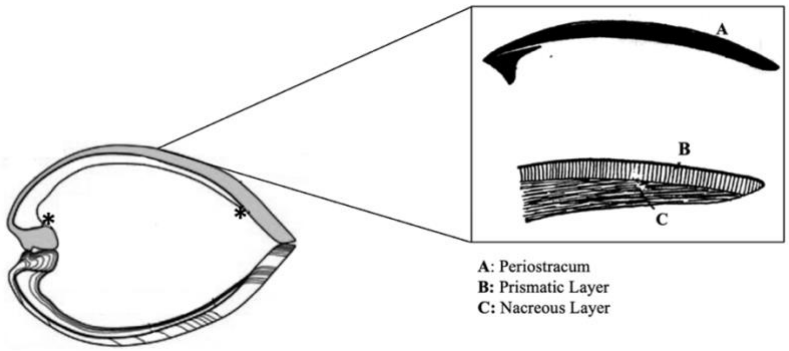

Figure 4 - Morpho-structural characteristics of Bivalves shell: (*) Pallial lines where the mantle is attached to the shell. The Periostracum (A) is the outermost layer; the middle layer is called Prismatic Layer (B), while the innermost is named Nacreous Layer (C)

The outermost is called periostracum, a thin layer made of a fibrous insoluble protein named conchiolin. This interfacial layer separates the calcareous shell from the environment (Chi et al., 2023). The thickness of periostracum can often be reduced by mechanical damage, diseases, epibionts and/or parasites. The prismatic structure, made up of calcium crystalized prisms perpendicularly aligned to the shell surface, forms the middle layer. The nacreous inner layer generally consists of aragonite lamellae parallel to the internal surface of the shell and arranged in layers, separated by a matrix of elastic biopolymers of chitin and silk-like proteins (Marin & Luquet, 2004). These proteins are essentials for mineralization processes and in recent years several genes that code for nacreous and prismatic layers proteins in bivalve shells were identified (Inoue et al., 2010; Jackson et al., 2010). The periostracum and the prismatic layer are secreted by the outer mantle, while the general mantle surface secretes the nacreous inner layer. Several techniques are used to study the microstructure of the shell, such as scanning and transmission electron microscopy (Bevelander & Nakahara, 1969; Kobayashi & Samata, 2006; Nudelman et al., 2008), X-ray and electron diffraction patterns (Levi-Kalisman et al., 2001; Jacob et al., 2008). Moreover, the chemical composition of shell was described for several bivalve species, using analytical methods such as secondary ion mass spectrometry (Shirai et al., 2008), electron probe microanalysis, and laser ablation inductively coupled plasma mass spectrometry (Jacob et al.,

2008). The construction of the shell begins during the early stages of larval development through ectodermal cells located in the dorsal region of the embryo. A second larval shell secreted by the mantle follows soon after, while the secretion of the more calcified adult shell begins after metamorphosis. The small fluid-filled space between the periostracum and the epithelial cell of the mantle is the site where the shell growth takes place. Here all the precursors for mineralization are released by cells, such as mineral ions extruded from the cytoplasm and organic components of the matrix secreted by exocytosis (Marin & Luquet, 2005). The addition of materials from the mantle edge allows the growth of the circumference of the shell, while the growth in thickness depends on materials deposition from the general mantle surface. The point where the growth stages begin is called “umbo” and the embryonic shell is generally visible in the umbonal area. In many bivalve species, the growth patterns lead to the formation of dark “rings” or “bands” on the external shell surface that form as annual periodic event. The analysis of these growth rings was historically used for age determination (Weymouth, 1922; Stevenson & Dickie, 1954; Merrill et al., 1966; Wilbur & Yonge, 2013). However, this method may lead to discordant or incomplete age determination (Ropes, 1987). Thus, the examination of the internal dark growth lines called “annuli”, alternating with light growth-increment deposits, provides a more reliable age determination. The internal depositional features represent a well-preserved record of growth, being less affected by destructive environmental conditions than the shell external surface. Although sectioning the valves can be considered a time-consuming procedure, it can make the age determination much easier. Moreover, the preparation of acetate peels of sectioned shells can better expose the internal annuli (Ropes, 1987). The external features of valves remain valuable tools for the specific and supra-specific taxonomy. The shape and sculptural pattern of the outer surface, the number, morphology and arrangement of the hinge teeth, the position of ligaments, the arrangement and number of muscle scars, are consistently used for the identification of several bivalve mollusc taxa.

2.1.2 The mantle

The internal organs of this molluscs are surrounded by the pallial cavity, bounded externally by two flaps of the mantle that form the two valves. The connective tissues with haemolymph vessels, nerves and muscles are the main components of the mantle, that is generally thin and transparent in most species, except for the edges that usually show a dark pigmentation. This is

probably a protection mechanism against the potentially harmful effects of solar radiation (Seed, 1976). The mantle edges are composed of three folds: the external one secretes the shell, the middle one is involved in sensory functions, and the internal muscular one controls the water flow in the mantle cavity. The numerous cilia present in the latter play a key role in directing the particles from the surrounding environment towards the gills, where the sorting occurs. Similarly, the waste materials are diverted by cilia along the rejection tracts, and they are periodically discharged out of the mantle cavity by a sudden and strong closing of shell valves, through the exhalant opening. A series of muscle fibers located in the inner fold, connect the mantle to the shell. The pallial line of attachment runs in a semicircle close to the shell margins. In many bivalve mollusc families, the mantle is also the site where the gametogenesis occurs, as well as a site for nutrient reserves storage, mainly glycogen. Although other organs such as gills and digestive glands are considered as more important sites for contaminants bioaccumulation, the mantle also plays a key role in these processes, specially related to heavy metals (Zuykov et al., 2013; Wang & Lu, 2017). Further modifications and morphological adaptations of the mantle edges are related to the habitats and the living habits. In deep-burrowing species, the margins of the pallium are completely fused together, except for the front opening, and the inhaling and exhaling opening located in the rear end. The latter have an elongated shape, forming extensible siphons primarily used for feeding. The extension is mediated by water or haemolymph pressure in mantle cavity, while the retraction is controlled by inner muscles. As already mentioned, the middle fold is mainly involved in sensory functions, showing short tentacles rich in tactile cells and chemoreceptors in most species. These are concentrated on the tips of siphons in digging species. The mantle is also the site where symbiotic organisms of some clam species can be found. All the products resulting from the photosynthetic activity of these organisms (mainly zooxanthellae) can be partially used by the host as source of nutrients (Hernawan, 2008; Maboloc et al., 2015; Kirkendale & Paulay, 2017). It is well known that bivalve molluscs can produce pearls in response to the penetration of foreign matter or to the presence of parasitic larva between the mantle and the shell. This self-defence mechanism leads to encapsulation of the alien object through the deposition of nacreous layers around it. Despite all bivalve molluscs are potentially able to produce pearls, only those made by species with an inner mother-of-pearl layer have a high commercial value (Taylor & Strack, 2008). Nowadays, pearls production is mainly artificially induced by inserting a small foreign body in the mantle tissues.

2.1.3 The foot

Most of the species belonging to the Bivalvia class exhibit laterally compressed body and foot. In particular, the foot often shows the shape of an axe (e.g., family Veneridae), due to dilatation caused by blood pressure. This peculiar conformation, long way different from the one suitable for the typical crawling of gastropods, is instead adapted for burrowing in sandy and muddy substrates, where many species of bivalves spend most of their life cycle. The foot first appears when bivalve larvae are about 200 µm long and become functional during the developmental stage that precedes settlement and metamorphosis, with an approximate shell length of 260 µm (Bayne, 1971). The foot structure consists of a central haemolymph space surrounded by several layers of longitudinal muscles. Numerous cilia cover the ventral surface, and different kinds of glands with specific function for attachment and crawling are present on mussel foot (Lane & Nott, 1975). One of the main functions is the production of the byssus filaments used by many species of bivalve molluscs for the attachment to the substrates. After a period of planktonic life, the larvae slowly descend to the sea bottom and, once the favourable conditions are found, the production of byssus is stimulated, and the metamorphosis takes place. This is also valid for species living buried in muddy and sandy substrates that initially use the byssus filaments for attachment to sediment particles. When a burrowing mollusc finds a suitable substrate, it immediately begins to dig into it through a series of coordinated activities (also known as "digging cycles"), which are mainly the result of haemolymph pressure and muscle contraction in the foot. During the first phase of a digging cycle, the two valves are slightly opened to allow the extrusion of foot, with which the animal probes and pushes the surrounding sand thanks to alternating contractions and relaxation of several muscles. When the foot is totally extruded from the shell, the valves begin to close, due to the contraction of the adductor muscles. Thanks to the closure, part of the water is expelled from the pallial cavity, thus helping the burrowing activities. The shell closure also increases the pressure on the residual water and haemolymph, acting as a hydrostatic skeleton that allows a better anchoring into the substrate. Due to muscles contraction, the shell is subsequently pushed down into the sediment through a rocking effect. Once the molluscs have well penetrated the substrate, the valves open thanks to the relaxation of adductor muscle, and the pedal expansion is lost. There follows a static period during which the animal continues to test the surrounding sediment with the foot. Burrowing molluscs can return to the surface if it is necessary, pushing against the anchored side of the foot or turning around for digging upwards

(Trueman, 1967). Smaller specimens usually dig faster than larger ones of the same species (Tallqvist, 2001), and the burrowing performance also depends on the grain size of sediment (Nel et al., 2001) and other factors, such as low temperature (Donn & Els, 1990), hypoxia and surface algal layer (Tallqvist, 2001). In addition, this complex behaviour can be seriously affected by sediment toxicity, being therefore a valuable bioassay to evaluate substrate contamination (Bonnard et al., 2009; Boldina-Cosqueric et al., 2010).

2.1.4 The gills

The gills are highly specialized and their main function, apart from breathing, is feeding by water filtering. All bivalve molluscs feed on suspended or deposited particles, mainly composed of phytoplankton and dead or alive microorganisms. This type of feeding habits requires an impressive volume of incoming water from which nutrients can be assimilated. For this purpose, the movement of branchial cilia can generate relatively strong current that force the intake of the surrounding water into the pallial cavity. Due to the abundant mucous secretions, the particles are trapped and subsequently directed to the cephalic region, where the labial palpi sort the introduced material. The waste particles are then expelled as a mixture of particles and mucus trough the exhaling siphon. Among primitive bivalves (or "Protobranchs"), the gills are only involved in breathing, and food particles are accumulated with sediment in the mantle cavity to be periodically ejected. Most of modern bivalves are also known as "Lamellibranchs" due to their peculiar branchial structure. One of the main morphological characteristics of these animals is the advanced development of the gills, also known as ctenidia, located in the pallial cavity on both sides of the foot. The two pairs of lamellar gills that composed the branchial system show a large curtain-like structure, and they are suspended from the ctenidial axis that is fused along the dorsal margins of the pallium. Branchial nerves and haemolymph vessels are also present within the above-mentioned axis. The gills surface is optimally exposed to incoming water flow to maximize nutrients intake and gas exchanges, and each gill is composed of numerous W-shaped filaments, each of which is reinforced by an internal rod rich in collagen (Figure 5).

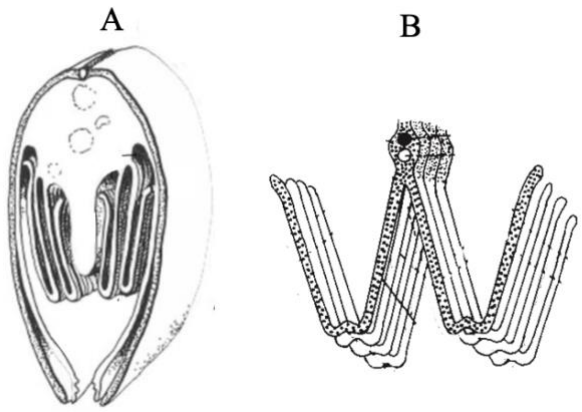

Figure 5 - Transversal vision of lamellibranchs gill anatomy (A); Section of lamellibranch gill showing the ctenidial axis and four W-shaped filaments (B)

The branchial arms thus formed are called lamellae, and it is possible to distinguish the inner descending lamellae from the outer ascending ones, among which is the exhalating chamber. This peculiar conformation is typical in bivalves belonging to both Pteriomorphia and Heterodonta subclasses, also known as “Filibranchs” and “Eulamellibranchs” respectively. However, only in the latter the gills are connected by several interfilamentous junctions, showing a more advanced branchial structure. The less evolved bivalves (Protobranchia subclass), have pennate gills and simple filaments, while the more evolved ones, belonging to Poromyoidea superfamily, are also called “Septibranchs”, having two perforated muscular septa instead of the usual gills shape. As mentioned before, vital functions such as feeding and breathing mainly depend on the movement of branchial cilia that is under nervous control. When the incoming water flow generated by currents hits the gills surface, the lateral cilia trap the particles aggregated in mucus and convey them to the frontal cilia, where particles sorting occurs. The sets of larger frontal cilia collect particles to be periodically ejected as pseudo-faeces trough the exhalant siphon, while the thinner ones convey the particulate organic matter towards the labial palps located in the mouth, whose main function is to constantly remove materials from the food tract to prevent gills saturation. Regarding the breathing function, the rich haemolymph supply and the wide surface make the gills suitable for gas exchanges, even if the latter also occur through the mantle surface. A system of afferent veins connects the kidneys to the branchial filaments, where the gas exchanges take place. Once oxygenated, the haemolymph flows towards the heart and the kidney through efferent veins. Relying on the above-mentioned vital functions, the gills can be considered as the first interface between bivalve molluscs and the surrounding water. As consequence, these organs mainly suffer from environmental stress, along with the digestive

gland that can be compared to the liver from a functional point of view. For these reasons, gills and digestive gland represent valuable sentinel tissues for the determination of inflammatory response after exposure to different contaminants that leads to morpho-functional alterations and haemocytes infiltrations in most cases (Tresnakova, Famulari, et al., 2023; Tresnakova, Impellitteri, et al., 2023).

2.1.5 *The digestive system*

The digestive system of bivalve molluscs consists of a mouth, oesophagus, stomach, digestive gland, intestine, and anus. As already mentioned, the triangular shaped palps are located on both sides of the mouth, acting as a sorter of particles from the environment. The selected food flow towards the stomach through a narrow ciliated oesophagus. This transport mechanism based on the movement of cilia is essential to propel materials throughout the alimentary channel, compensating for the absence of muscular walls. The large stomach of these invertebrates has an oval shape, situated within the digestive gland, and connected to it through multiple ducts. A semi-transparent, gelatinous rod called the crystalline style extends from the posterior end of the stomach and projects forward, resting against the gastric shield. The rotating style, driven by cilia in the style sac, releases carbohydrate-splitting enzymes as it abrades and dissolves. In intertidal bivalves, the style is not a permanent structure and dissolves during low tide when the mollusc is not feeding, reforming when the tide returns (Langton & Gabbott, 1974). The style plays additional roles in digestion, as it wraps the food-laden mucous string around its head, facilitating particle dislodgement. The style rotation aids in mixing the contents of the stomach, while ciliary tracts in the stomach, excluding the gastric shield, act as sorting areas. Finer particles and digested matter are kept suspended by cilia, sweeping them towards the digestive gland duct openings, while larger particles separate and enter the intestine through a deep groove on the stomach floor. The digestive gland, characterized by its brown or black colour, is composed of blind-ending tubules that connect to the stomach through ciliated ducts. It serves as the primary site of intracellular digestion, where materials are taken up by digestive cells through pinocytosis and digested within vacuoles. The end products of digestion are released into the system, while waste is retained in membrane-bound residual bodies and later released into the tubules. The released waste, enclosed in excretory spheres, is swept towards the stomach and eventually the intestine. The tubules consist of two cell types: digestive cells and basophil cells. The first ones are

responsible for material uptake and intracellular digestion, while the latter are involved in protein synthesis. The digestive gland also produces various digestive enzymes, including carbohydrate-splitting enzymes, fat-digesting enzymes, and proteolytic enzymes (Reid, 1968; Langdon, 1996). Moreover, the storage of metabolic reserves in the digestive gland provides an energy source during gametogenesis and periods of physiological stress (Bayne, Thompson, et al., 1976). Rejected particles from the stomach and waste material from the digestive gland pass into the coiled intestine, where they are formed into faecal pellets and expelled through the anus.

2.1.6 The circulatory system

The heart of bivalve molluscs is situated in the mid-dorsal region near the hinge line of the shell, enclosed within the pericardium that surrounds it dorsally and a portion of the intestine ventrally. Comprised of a single muscular ventricle and two thin-walled auricles, the heart drives haemolymph flow from the auricles into the ventricle, propelling it into the anterior aorta. Pseudo- and Eulamellibranch bivalves also have a posterior aorta. The anterior aorta branches into several arteries, notably the pallial arteries that supply the mantle, and the visceral arteries (gastro-intestinal, hepatic, and terminal) that provide haemolymph to the stomach, intestine, shell muscles, and foot. The arteries form a network of vessels throughout the tissues, which then join to create veins emptying into the extensive pallial, pedal, and median ventral sinuses. This open circulatory system enables haemolymph in the sinuses to directly interact with tissues. In mussels, some haemolymph from the kidney network enters the gills and returns to the heart via the kidneys. In other bivalves, haemolymph from the gills flows directly to the heart. The mantle plays a prominent role in oxygenation, since it is permeable to the gases dissolved in the water and it transfers the dissolved oxygen to the circulating liquid through diffusion. For these reasons, the mantle hosts well-developed circulatory pathways in all bivalves. Haemolymph has essential roles in the physiology of these animals, encompassing gas exchange, osmoregulation, nutrient distribution, waste elimination, and internal defence (Bayne, Widdows, et al., 1976). Additionally, it acts as a fluid skeleton, temporarily providing rigidity to organs like the labial palps, foot, and mantle edges. The haemolymph contains numerous cells called haemocytes that float in colourless plasma, playing significant roles in various physiological processes, including nutrient digestion, excretion, tissue repair, and internal defence. Haemocytes can move freely out of the

sinuses into surrounding connective tissues, the mantle cavity, and gut lumen, further contributing to these processes.

2.1.7 The nervous system

The nervous system of bivalves is relatively simple and bilaterally symmetrical, comprising three pairs of ganglia and several pairs of nerves. The cerebral ganglia are connected by a short commissure above the oesophagus, and two pairs of nerve cords extend from each cerebral ganglion towards the posterior of the animal. One pair leads back to the visceral ganglion located on the surface of the posterior adductor muscle, while the second pair extends posteriorly and ventrally to the pedal ganglia in the foot. The cerebral ganglia innervate various parts of mollusc body, including the palps, anterior adductor muscle, mantle, statocysts, and osphradia. The pedal ganglia control the foot, while the visceral ganglia oversee a wide range of organs, such as gills, heart, kidney, digestive tract, mantle, siphons, and pallial sense organs. In scallops, the paired visceral ganglia merge to form an elementary brain with optic lobes for the eyes on the mantle edge, making it the most complex nervous structure in Bivalvia (P. G. Beninger & Le Pennec, 1991). The ganglia also serve a neurosecretory role, producing peptides released into the circulatory system. These peptides play crucial roles in regulating growth, gametogenesis, and glycogen metabolism (Zwann & Mathieu, 1992). Sensory organs in bivalves have shifted from the anterior end to the mantle edge, with most sensory receptors concentrated on the middle fold of the mantle. Pallial tentacles covered in epithelial sensory cells are sensitive to touch, eliciting reflex actions such as local mantle or siphon muscle contractions. More profound stimuli cause coordinated retraction of the entire animal into its shell, controlled by the visceral ganglion. Ocelli, detecting sudden changes in light intensity, may also be present on the mantle or siphons of some species. Sensory receptors called osphradia, known in gastropods, are difficult to detect in bivalves and their exact function remains unclear. A pair of statoreceptors near the pedal ganglia plays a role in orientation during swimming (V. C. Barber, 1968), though its function in other bivalves is yet to be fully understood.

2.1.8 The excretory organs

Bivalve molluscs have two types of excretory organs: the pericardial glands and the paired kidneys. In mussels, the U-shaped kidneys are reddish-brown and located ventral to the pericardial cavity and dorsal to the gill axis, extending the entire length of the gill axis from labial palps to the posterior adductor muscle. In scallops, the paired kidneys attach to the anterior margin of the central adductor muscle, partially concealed by the gonad. One arm of each kidney is glandular and opens into the pericardium, while the other end is a thin-walled bladder that connects to the mantle cavity through a nephridiopore. Pericardial glands, also known as Keber's organs, develop from the epithelial lining of the pericardium and cover the auricular walls of the heart. Certain cells of the pericardial glands accumulate waste, which is periodically discharged into the pericardial cavity and eliminated through the kidneys. Other cells in the pericardial glands are involved in filtering the haemolymph as the first step in urine formation. The filtrate then flows to the glandular part of the kidney, where the processes of ion secretion and re-absorption occur. This results in urine with a high concentration of ammonia, along with smaller amounts of amino acids and creatine. Most aquatic invertebrates excrete ammonia as the final product of protein metabolism. Although kidneys and pericardial glands are the primary excretory organs, waste products may also be lost across the general body surface and particularly across the gills. In mussels and scallops, the kidney plays a vital role in storing and eliminating hydrocarbons and heavy metals like zinc and cadmium. This metal sequestration can lead to an increased incidence of renal cysts (Wakashin et al., 2018). Additionally, the kidney serves as the site of infection for several parasites and bacteria in bivalves (Azevedo, 1989; Ngo & Choi, 2004; Le et al., 2015; Brian & Aldridge, 2020; Cho et al., 2020).

2.1.9 The reproductive system

The reproductive system of these invertebrates is quite simple, with gonads that exist as paired structures composed of branching tubules (canaliculi and acini) whose epithelial lining produces gametes. This system is supported by connective tissue, and nutritional cells are located mainly against the walls of the acinus in females. This type of cells surrounding the oocyte make up the follicle. The tubules merge to form ducts that lead into larger ones, eventually culminating in a short gonoduct. In more primitive bivalves, the gonoduct opens into the kidneys, and eggs and sperm are released through the kidney opening (nephridiopore) into the mantle cavity. However,

in most bivalves the gonoducts are separated from the kidneys and open through independent pores near the nephridiopore into the mantle cavity. Fertilization takes place externally, with the gametes being released through the exhalant opening of the mantle. Just some species of oyster brood the eggs within the mantle cavity. Most species of bivalve molluscs are dioecious, meaning that they have separate sexes, with no obvious sexual dimorphisms. Thus, the standard approach for the determination of sex requires histological assessment of fixed gonadal tissues and the subsequent examination with a light microscope. Although not applicable to all species, several authors proposed alternative methods for sex determination, based on the difference in energy reserves between eggs and sperm (Jabbar & Davies, 1987) or on the presence of a male-associated polypeptide (Mikhailov et al., 2002). The hermaphroditism is commonly found in scallops. These synchronous hermaphrodites produce male and female gametes simultaneously either within the same tubules or in distinct zones. In most cases, the protandry prevents the self-fertilization releasing the male gametes first. On the other hand, some species of oyster or clam exhibit asynchronous hermaphroditism, alternating male periods to female periods interspersed by the change of sex. Clams are mainly dioecious, despite two other sexual patterns have been observed: asynchronous and simultaneous hermaphroditism. In the first case, the mollusc first develops as a male and then a subsequent transition with an equal sex ratio occurs, while in the second case the specimens are both male and female at the same time, releasing sperm first, followed by eggs. In clams, gonads are generally found at the base of the foot, while in oysters, they cover the external surface of the digestive gland. Mussels are also mainly dioecious, and the gonadal development occurs within the mantle tissue that appear orange in females and creamy-white in males when ripe. Bivalve molluscs follow an annual reproductive cycle, comprising gametogenesis, one or more spawning events, and subsequent gonad reconstitution. During spermatogenesis, primary spermatogonia undergo multiple mitotic divisions to produce secondary spermatogonia, which then go through meiosis to become spermatocytes. The latter first develop into spermatids that later differentiate into flagellated spermatozoa. Oogenesis proceeds similarly, where primary oogonia undergo repeated mitosis to form secondary oogonia, which enter meiosis. After that, the oogonia development pauses at the prophase stage of meiosis I, and the rest of meiotic stages are completed at the fertilisation. The oocytes then undergo the vitellogenesis phase, accumulating lipid globules and small amounts of glycogen that cause an increase in oocyte size. Oocyte lysis occurs throughout the gonadal cycle, particularly during the onset of spawning and at the end of the breeding season. The age at the first sexual

maturity is variable, depending on the species of bivalves. As mentioned before, the most reliable approach for assessing the reproductive cycle involve either histological or squash preparations of the gonads. However, these methods may be insufficient or too subjective, providing only a rough estimation of the overall gonadal development in some species (Barber & Blake, 2006). For these reasons, complementary methods based on the observation of spawning in natural or laboratory conditions, the appearance of larvae in the plankton or their settlement, serve as valuable supplements to information obtained from gonad preparations. Nevertheless, histological assessment of gonadal tissues can provide valuable information about the stages of development, the attainment of sexual maturity, and the spawning periods throughout the year. A mean gonad index (GI) can be calculated by multiplying the number of individuals at each development stage by the corresponding numerical ranking and dividing the result by the total number of individuals in the sample. This index tends to increase during the gametogenesis and decreases during the spawning period. Several patterns of gonadal development have been proposed by many authors (Devauchelle, 1990; Lango-Reynoso et al., 2000; Delgado & Pérez-Camacho, 2005, 2007; Smaoui-Damak et al., 2007). According to Thorarinsdóttir (1993), it is possible to recognize six different stages:

I. *Maturing (recovering).* The initial signs of recovery after spawning are observed at this stage. The gonad starts to grow and appears flabby, containing a significant amount of free water. The follicles within the gonad increase in size and become denser, with connective tissue forming between them. The lumina of the gonad begin to fill with growing oocytes that measure 20–30 µm in diameter. The genital ducts undergo a conformational change, losing their circular shape during this stage.

II. *Maturing (filling).* The gonad continues to grow and becomes even larger and thicker, showing a brighter colour. Although still flabby, it contains less free water. The follicles within the gonad increase in size, becoming closer to each other. In male follicles, spermatozoa are arranged radially, while in female ones, the lumen contains half-grown oocytes, with most of them attached to the follicle wall. There is a reduced presence of connective tissue at this stage.

III. *Maturing (half-full).* The dimensions of gonads continue to increase, while the free water content is reduced significantly. The follicles appear tightly packed together. The lumina of the follicles are now filled with either spermatozoa or fully-grown oocytes, measuring 50–60 µm in diameter, and the connective tissue regresses further.

IV. *Mature (full).* At this stage, the gonad has reached its maximum size and no longer contains free water. The follicles are tightly packed together, showing well-defined colours, with cream-colored testicles and the ovary showing the typical shades from orange to brick-red. Moreover, male follicles appear densely packed with spermatozoa, whose heads measure about 3 µm, and the follicle walls become extremely thin. Female follicles are filled with polygonal or hexagonal oocytes that are closely packed together. The presence of connective tissue is limited to the alimentary canal and gonoducts, which appear flattened.

V. *Spawning.* The gonads are completely differentiated, showing dull and flabby tissue with a significant amount of free water that depends on the number of emptied follicles. Areas with un-spawned follicles can be present, exhibiting ripe germ cells at Stage IV of development. In some sections, ova or sperm can be observed in ciliated ducts.

VI. *Spent.* The gonad has significantly reduced in volume, appearing dull, flaccid, and fawn-coloured, and containing a considerable amount of free water. The follicles are empty, with only a few residual germ cells remaining. Amoebocytes are observed attacking un-spawned gametes, occasionally visible as cellular debris. In later stages, some reorganization of follicles and early gametogenic stages becomes evident.

Other methods for determining gonadal developmental stages include stereological techniques that quantify changes in volume of different components within the gonad. A reliable assessment of reproductive stage can also be obtained by measuring the mean gonad weight as a proportion of total body weight. Moreover, approaches based on image analysis of histological sections (Barber & Blake, 2006), changing in DNA content of male gonad (Thompson, 1984), and changes in density and size of oocytes (Lango-Reynoso et al., 2000) have been proposed. Considering the limitations of each of the known methods, the best strategy to assess the gametogenesis involves the joint use of histological procedures and the above techniques.

2.1.10 The larval development

As mentioned earlier, in most marine bivalves the fertilization is external. For this reason, eggs and sperm are released directly from the genital ducts into the water column. Sperm penetration is enabled by the release of substances that can dissolve the vitelline membrane surrounding the egg. Once fertilization has occurred, meiosis is completed in the egg which subsequently undergo

rapid cell division, resulting in a spherical mass of cells. Cilia begin to appear around 4-5 hours after fertilization, allowing the swimming of the mass. Approximately 24 hours after fertilization, the larva reaches the ciliated trochophore stage (Figure 6).

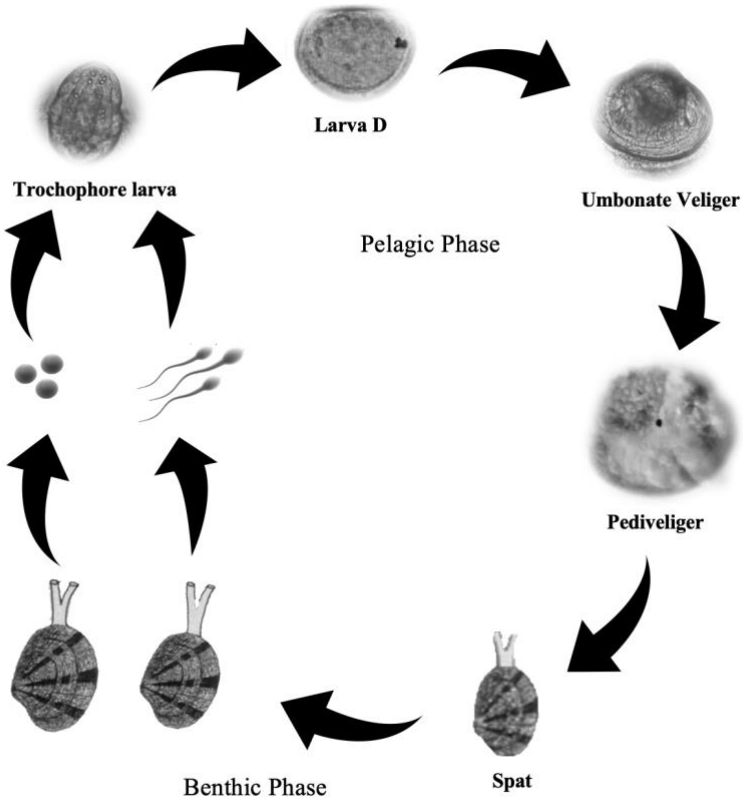

Figure 6 - Life cycle of Ruditapes spp.

At this point the secretion of the first larval shell, also known as prodissoconch I, begins. Once this process is completed, the larva, now called veliger with a shell length of about 100-120 µm, immediately starts to produce the second larval shell (prodissoconch II). This second shell is formed by the mantle and shows growth lines. The main characteristic of veliger larvae is the presence of the velum, a circular tissue lobe with a ring of cilia, primarily involved in vital activities such as feeding and swimming. The cilia capture small food particles (1-2 µm diameter) and sweep them towards the mouth and into a simple gut. The development of pigmented eyespots and extensible ciliated foot takes place as metamorphosis approaches. The larva at this stage is called pediveliger and measure between 210 and 300 µm, now exhibiting most of the characteristics of adult bivalves, such as ciliated palps for food sorting, a thin mantle secreting the shell, a foot used in crawling and byssus secretion, a few pairs of gill filaments, functioning

digestive and nervous systems. Larvae show various responses to environmental factors. The veligers show positive phototropism and a marked sensitivity to pressure, keeping them in shallow waters, while pediveliger show positive geotropism and are less responsive to pressure, leading them to descend to the bottom for settlement. A series of swimming and crawling behaviours ultimately lead to attachment when a suitable substrate is found. This transition marks the end of the pelagic larval phase and the beginning of benthic life, which requires major morphological changes. Larvae of bivalves generally become competent to settle at a shell length of about 250-300 µm, although some species may delay this process until they reach a larger size. Before attaching, bivalve larvae demonstrate the ability to discriminate between different substrates. This behaviour was observed in pediveligers, which are capable to actively explore the substratum using the foot, performing various tests for the evaluation of different factors before the final settlement (Pascual & Zampatti, 1995). This cycle of activity may be repeated over several days, and it is particularly necessary in bivalve molluscs for which the settlement is an irreversible process, such as oysters. Depending on the life stage, mussels, scallops, and clams settle on various substrates, such as algae, hydroids, stones, coral reefs, and shells. They use byssal threads or cementing mechanisms for attachment. Most larvae of bivalves experience an epifaunal post-larval stage and a subsequent planktonic post-larval stage. The release of attractant pheromones by adults and juveniles is likely to be very important during these phases of pre-settlement. In addition, relationships with the species that make up the associated microbiota are believed to play a crucial role in the survival of newly attached bivalves (Milan et al., 2019; Gerpe et al., 2021). Moreover, several factors like density of adult populations and the presence of other species can influence larval settlement. Once a suitable substrate is found, the larva ceases crawling and starts the attachment process, cementing itself in place or using byssal threads depending on the species. Metamorphosis is always a critical phase in the life cycle of bivalve molluscs, involving a significant reorganization of the body structure necessary for the adaptation to sedentary life. Some bivalve larvae can delay metamorphosis for weeks. This is the case of mussel larvae, which can delay this process for up to five or six weeks in cool temperate waters by drifting with a long thread secreted from special glands in the foot. This behaviour allows them to remain in the water column for an extended period, adding to their pelagic dispersal time. During metamorphosis, rapid morphological changes occur in the attached larva, now referred to as a plantigrade. The extent of reorganization varies among species. In oysters (Walne, 1974), after the attachment, the velum, foot, eyespot, and anterior adductor muscle

disappear, while the mouth moves through an angle of 90°, and the posterior muscle moves centrally. Connections between gill filaments form gradually, following the Eulamellibranchs pattern. The attached left shell valve begins to form the characteristic cup shape of the adult shell. This process takes approximately three to four days, during which the larva cannot feed but relies on stored nutrients as an energy source. The result is the formation of the adult shell called dissoconch, which is distinct from the larval prodissoconch II shell in pigmentation, ornamentation, and mineral content. Moreover, there is a noticeable change in shape, making the dissoconch shell more like the later adult form. It is known that the prodissoconch-dissoconch boundary provides a clear morphological trait useful for differentiating true juveniles from post-larvae in metamorphosis. In addition, the shape, hinge, and ligament structure of the larval shell are valuable features for species identification, providing data on ecology, biogeography, and developmental history at the population level (Lutz & Kennish, 1992).

2.2 Description of the species Ruditapes decussatus (Linnaeus, 1758)

The grooved carpet shell clam is a bivalve mollusc of high ecological and commercial interest, belonging to the family Veneridae. The currently accepted taxonomic classification is given below, according to the World Register of Marine Species (WoRMS):

- Class BIVALVIA (Linnaeus, 1758)
- Subclass AUTOBRANCHIA (Grobben, 1894)
- Infraclass HETEROCONCHIA (J. E. Gray, 1854)
- Subterclass EUHETERODONTA (Giribet & Distel, 2003)
- Superorder IMPARIDENTIA (Bieler, P. M. Mikkelsen & Giribet, 2014)
- Order VENERIDA (Gray, 1854)
- Superfamily VENEROIDEA (Rafinesque, 1815)
- Family VENERIDAE (Rafinesque, 1815)
- Subfamily TAPETINAE (Gray, 1851)
- Genus RUDITAPES (Chiamenti, 1900)
- Species RUDITAPES DECUSSATUS (Linnaeus, 1758)

The name Euheterodonta, meaning “variables teeth”, is derived from one of the main characteristics of molluscs belonging to this taxon, which bear three cardinal teeth on at least one

valve. Moreover, in the superfamily Veneroidea, the shell is generally composed of two equal and symmetrical valves. About 3500 species spread around the world belong to the family Veneridae, and they are globally known as edible molluscs. The species most valuated for human consumption are commonly called “Venus clams”, and 43 of them are reported in the Mediterranean and Black Sea (including introduced species) (Sealife Base). The shell shape of these molluscs is highly variable, and the common character that allows their identification at morphological level is the hinge, consisting of three divergent cardinal teeth on both valves. The species of clams found in Italian seas are listed below, with those of commercial interest highlighted in bold:

- Subfamily CALLOCARDIINAE (Dall, 1895)

  Callista chione **(Linnaeus, 1758)**

  Pitar rudis (Poli, 1795)

- Subfamily VENERINAE (Rafinesque, 1815)

  Chamelea gallina **(Linnaeus, 1758)**

  Mercenaria mercenaria (Linnaeus, 1758)

  Venus casina (Linnaeus, 1758)

  Venus nux (Gmelin, 1791)

  Venus verrucosa **(Linnaeus, 1758)**

- Subfamily DOSINIINAE (Deshayes, 1853)

  Dosinia exoleta **(Linnaeus, 1758)**

  Dosinia lupinus **(Linnaeus, 1758)**

- Subfamily PETRICOLINAE (d'Orbigny, 1840)

  Mysia undata (Pennant, 1777)

- Subfamily TAPETINAE (Gray, 1851)

  Polititapes aureus **(Gmelin, 1791)**

  Polititapes rhomboides **(Pennant, 1777)**

***Ruditapes decussatus* (Linnaeus, 1758)**

***Ruditapes philippinarum* (A. Adams & Reeve, 1850)**

***Venerupis corrugata* (Gmelin, 1791)**

Other Mediterranean species belonging to the family Veneridae are not commercialised because of their rarity or small size. Due to high intraspecific variability, the identification of these molluscs based on shell morphology can be difficult and not always possible. Although comparison of specimens from different stocks can sometimes facilitate the assessment of specific divergence, taxonomic uncertainties persist. Morphology of soft parts is, in some cases, a relevant and decisive discriminatory element, as for the two most important species belonging to the genus *Ruditapes* (Chiamenti, 1900) found in the Mediterranean: *R. decussatus* (Linnaeus, 1758) and *R. philippinarum* (A. Adams & Reeve, 1850). The first one is an Atlantic Mediterranean species, showing a distribution along the Euro-African coast from British Islands to Senegal, being found throughout the *Mare Nostrum* to the Red Sea via the Suez Canal. The second one is of Japanese origin with a wide Indo-Pacific distribution from Pakistan to the former Soviet Union, and later introduced to the North American Pacific coast and Euro-Mediterranean coasts (Figure 7).

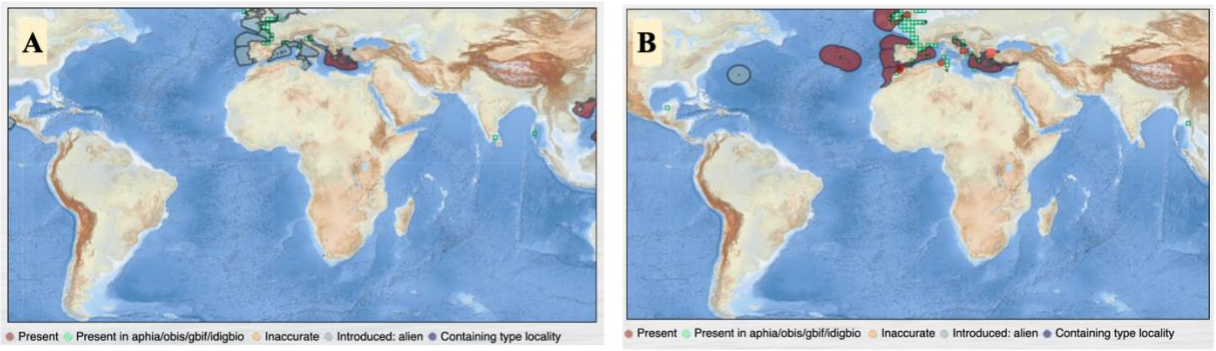

Figure 7 - Spatial distribution of R. philippinarum (A) and R. decussatus (B) - Source: "World Register of Marine Species" (WoRMS)

The introduction of the Manila clam (*R. philippinarum*) in Italy occurred in March 1983 in the Venice Lagoon, as part of the shellfish research program of the Consortium for the Development of Fisheries and Aquaculture in Veneto (Pellizzato, 1990), showing promising results from the first experimental trials. Since then, the alien species has spread rapidly, supplanting the native species in the Mediterranean shellfish culture landscape, mainly due to greater strength and

adaptability (Rossi R. & Paesanti F., 1992; Rossi R., 1996), as well as faster growth rates and longer reproductive period (Breber P., 1980; Breber P, 1985a, 1985b). The genus *Ruditapes* currently includes another species, *R. bruguieri* (Hanley, 1845), whose presence is not documented in Mediterranean (WoRMS). Due to taxonomic proximity, the description of the cryptic species under study undoubtedly requires comparison with the related species of Indo-Pacific origin. These bivalve molluscs have a foot that is clearly axis-shaped, showing a wide, enlarged neck especially when the animal is retracted inside the shell. The inner and middle folds of mantle have two posterior welds that allow communication between the pallial cavity and the surrounding environment by means of three openings: the posterior-dorsal, the posterior-ventral, and the wide ventral openings. The mantle extends into two siphons at the rear openings: the dorsal exhalant and the ventral inhalant syphons (Figure 8).

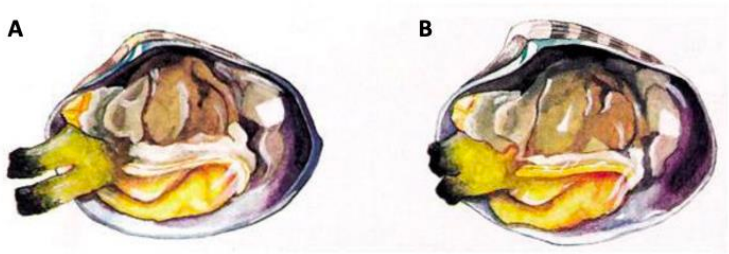

Figure 8 - Anatomical differences between R. decussatus (A) and R. philippinarum (B) - Saba, S. (2012)

The apex of the latter is surrounded by a series of tiny inward-facing tentacles whose main function is to prevent too large, suspended particles from entering. Moreover, as mentioned before, the mantle edges are usually characterised by dark pigmentation which is helpful in protecting tissues from potentially harmful effects of solar radiation (Seed, 1976). Inside the inhalant siphon, the mantle forms a membrane that serves to channel the water to be ejected. The wide gills are those typical of the Eulamellibranchs described in the previous paragraphs. Although not too obvious, discriminating characters of shell shape and structure can be observed among species belonging to the genus *Ruditapes* (Figure 9).

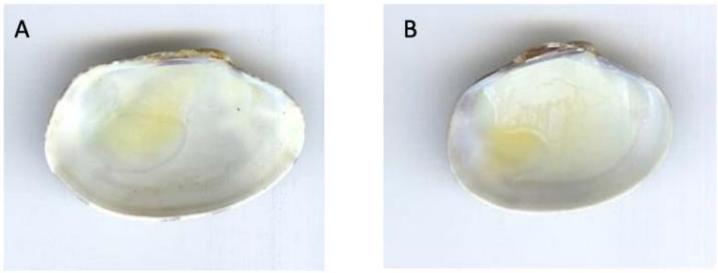

Figure 9 - Ventral view of the shells of R. decussatus (A) and R. philippinarum (B), showing the main morphological differences

The two valves of *R. decussatus* are generally less convex in shape than those of *R. philippinarum,* which shows markedly recessed edges in the front part of the shell and a more regular rounding at the end of the rear portion. In addition, specimens of Manila clam show a more obvious shell sculpture, which appears more pronounced in the posterior region. Here the radial structure prevails, forming a series of small tubercles by crossing the transverse one. The sculpture just described does not differ so sharply in the grooved carpet shell clams. The shell of both species shows the lunular surface finely striated and well demarcated, with the central area more coarsely furrowed in *R. decussatus*. Each valve has three cardinal teeth, two of which are stockier and markedly bifid in *R. philippinarum* than in *R. decussatus*. In addition, both species exhibit high colour polymorphism of the outer surface, generally more pronounced in the shell of the alien species (Cannas, 2010). Regarding the inner surface of the shell, the shape of the palleal sinus can be considered a discriminating characteristic: in the native species it is asymmetrical, deeper and approaches the dorsal/ventral midline sometimes exceeding it, while in the alien species it is symmetrical, shorter, and never exceeds the midline of the shell (Cannas, 2010) (Figure 10).

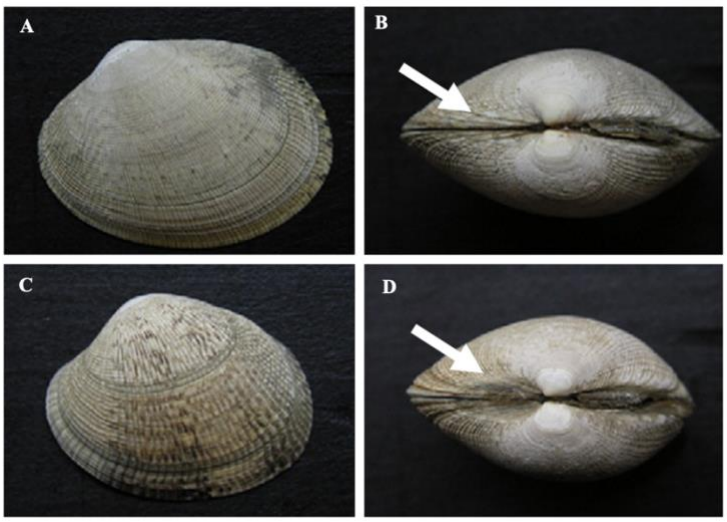

Figure 10 - Comparison of external shell morphology of R. decussatus (A,B) and R. philippinarum (C,D). Evident differences can be noted in the striation patterns (A,C), as well as in the morphology of the lunula (B,D) indicated by the white arrows

Another significant difference is the absence of stains, a typical character of the grooved carpet shell clam and a rare condition in Manila clam. However, the most striking of the interspecific differences concerns the soft parts, particularly the shape and arrangement of the siphons: in the native species they are well separated, while in the Indo-Pacific species they are fused at the base and divided only at the end. The maximum length for both species is about 75 mm Gosling (2015). For the two *Ruditapes* species, sexual maturation occurs as early as in small individuals less than a year old. Several authors claim that *R. decussatus* reaches sexual maturity from 15 mm in shell length (Toba et al., 1993; Mistri M., 2007), whereas in *R. philippinarum* sexual maturation occurs earlier, starting at 5 mm in shell length (Holland D. A., 1974). The deposition may occur at different times, depending on the site and environmental conditions for both species, and gamete release is believed to occur whenever conditions are favourable (Hamida et al., 2004). Among the main triggers of deposition, temperature seems to be of considerable importance, with variable threshold values generally ranging from 14 to 20°C (Drummond et al., 2006). In general, the length of the breeding season for both species increases with proximity to the equator, but there is great variability between sites and even within the same site, and there are often multiple breeding peaks (usually 2 or 3). Relying on data reported in literature about the Mediterranean area, however, it is possible to identify July through October as the main breeding season for *R. decussatus* (Cannas, 2010). Regarding *R. philippinarum*, the duration varies from 1 to 12 months, with the lowest reported breeding temperature of 13°C (Devauchelle, 1990), confirming the better reproductive performances of the alien species compared to the native one. Other

temperature-related environmental parameters, such as salinity, chlorophyll concentration, and photoperiod certainly play a key role as starters for the release of gametes in *Ruditapes spp.* (El-Wazzan et al., 2020). Differences also exist between the two species in the mode of gamete emission: the gonads of the Manila clam mature asynchronously, but these molluscs can retain gametes until the appropriate time for reproduction. The grooved carpet shell clam, on the other hand, emits gametes continuously, but individuals of this species tend to have greater synchrony in maturation (Delgado & Pérez-Camacho, 2007). Hybridization was deemed impossible due to the divergences of the genetic structures of the two species, showing greater variability in the Indo-Pacific clam. However, genetic and cytological evidence has been documented in Spain (Silva S., 2006; Hurtado et al., 2011), and the existence of this phenomenon is nowadays widely recognised.

3. Materials and methods

3.1 Preliminary investigation and sampling

The first phase of the research involved a thorough bibliographic study aimed at characterising the species of interest, focusing on all the biological, ecological, historical, and economic aspects discussed in the previous paragraphs. All data and information collected were useful to identify methods and protocols used during the subsequent experimental phase, as described in detail below. Another key point of the preliminary research concerned the analysis of the context. Visiting the main molluscs distribution centres was essential not only to better understand the functioning of the production chain and marketing of edible lamellibranch bivalves farmed in Capo Peloro areas, but above all to secure the cooperation of those working in the field and to identify the sampling areas, where the greatest number of wild specimens of *R. decussatus* are concentrated. Two sampling points were thus chosen in Lake Faro (38°15'54"N 15°38'35"E - 38°15'55"N 15°38'33"E), shown on the map in Figure 11.

Figure 11 - Satellite view of the sampling area showing the two sampling points (A,B) located in the canal "Faro" of the Capo Peloro Lagoon (38°15'54"N 15°38'35"E - 38°15'55"N 15°38'33"E, respectively)

The survey stations were those where the presence of grooved carpet shell clam has been constant over the years, according to the interviews and field observations carried out during the preliminary stages of the study. Most of the specimens collected were found near the mouth of the canal “Faro” that connects the small marsh to the Strait of Messina, confirming the great positive influence of this stretch of sea on the quality of adjacent waters. Unfortunately, it was not possible to include the large marsh of Ganzirri in the survey, due to the severe death of the native population of *R. decussatus* during the reporting period. The next phase involved the choice of tools and sampling methodologies to be adopted. To avoid affecting the delicate ecosystem balance that governs this area and in full respect for the environment, it was decided to adopt a traditional harvesting method that would be as minimally invasive as possible (Figure 12), using only gloves, thigh-high boots, shovels, and sieves (2 mm mesh size).

Figure 12 - Sampling of R. decussatus specimens (A), sediment sieving (B), isolated clam for morphological identification of the species and faeces collection (C), specimens transferred to the laboratory (D), main tools used for sample processing (E)

At the identified sites, georeferenced by geographical coordinates with a Garmin GPS, periodic samplings were carried out from September 2022 to September 2023, taking no less than 20 individuals of various size each time. A total of 300 specimens were collected. Considering the natural metabolic slowdown due to lower temperatures, samplings were performed every two months during the late autumn/winter periods. From May onwards, as temperatures rose and the breeding season began, individuals were taken every month. The specimens found were immediately separated from the sediment using sieves and transported to the laboratory in special containers, keeping the molluscs alive by immersion in water taken on site. All living specimens were considered, and in some cases even those that were obviously just dead, identifiable by the presence of the flesh inside the shell. Once in the laboratory, each harvested clam was transferred individually into a shallow container and left in the water for the time necessary for the siphons to extrude. This was done before measurements were taken, not only to confirm that the bivalves belonged to the species *R. decussatus* (identified according to Atlas of the Mediterranean Seashells - vol. VII), but also to avoid the weight error due to the loss of water that occurs when these animals stay dry for a long time. In addition, all faeces found in each container were collected to assess the presence of plastic debris excreted by the molluscs.

For each specimen, the following measurements were then taken using a digital caliper with a resolution of 0.01 mm and an analytical balance with 0.01 g accuracy:

- Shell length (mm), the largest dimension in the antero-posterior direction
- Shell height (mm), the largest dimension perpendicular to the length
- Shell width (mm), measured at the maximum convexity of the valves
- Total weight (g)
- Shell weight (g)
- Soft tissues weight (g)

These variables were subsequently used to describe the morphometry of bivalves collected, by calculating the sharpness indices of shell defined as the convexity index (width/height), the compactness index (width/length), and the elongation index (height/length) (Amane et al., 2019). In addition, three different ratios were calculated, based on the shell weight (SW) and the three main measurements of valves: weight ratio 1 (SW/length), weight ratio 2 (SW /height), and weight ratio 3 (SW/width) (Khemissa et al., 2022). Each collected specimen was assigned to three size classes determined through the K-means cluster analysis (see below), according to the shell length (SL):

- Class 1 → 10 ≤ SL ≤ 22.9 (mm)
- Class 2 → 23 ≤ SL ≤ 31.9 (mm)
- Class 3 → 32 ≤ SL ≤ 48 (mm)

All data collected were initially stored in Microsoft Excel and subsequently processed with several software, as described in more detail in the following paragraphs. Samples not intended for further analysis were stored in the freezer.

3.2 Shape analysis of shells

After taking all measurements, the valves of each specimen were separated and photographed individually, dividing them into right and left. All pictures were taken using an iPhone 13 Pro (Apple Inc.) mounted on a special tripod to keep the device perpendicular and at a constant distance from the workbench. First a sheet of graph paper was photographed, which was indispensable for the subsequent calibration of the images. Valves pictures were thus collected, using a black background to increase the contrast during the shooting phase. Each photo was then binarized using ImageJ software (version 1.53k freely available at https://imagej.nih.gov/ij/)

and subsequently classified based on valve side and length class. The shape analysis based on the outlines of the collected shells was performed using shapeR, an open access package that runs on R software (RStudio 2022.07.2 Build 576; RGui 4.1.3 2022.03.10). This package was specially designed to study otolith shape variation among teleost populations or species, but it can prove useful in the study of any two-dimensional object, as pointed out by the authors (Libungan & Pálsson, 2015). Other R packages (i.e., stats, dplyr, ggplot2, ggfortify, vegan) were used to perform the K-means cluster analysis through which the previously mentioned size classes were determined. The outlines were detected through a specific function of shapeR, with the grayscale threshold value set on 0.05 (intensity threshold). The contours thus extracted were linked to the Excel file containing the above-mentioned information on specimens analysed (e.g., shell measurements, body weight, sampling date and site). Wavelet and Fourier coefficients were extracted and adjusted through proper functions of shapeR package to define the allometric relationships between specimen measurements and valve shape. The standardized Wavelet coefficients were also used to obtain comparison plots of mean valve shapes. To estimate the quality of both Wavelet and Fourier reconstruction, a comparison was made between the deviations from the valve outlines, with the value 15 set as maximum number of Fourier harmonics to be shown. Moreover, mean, and standard deviation of calculated coefficients was plotted using the gplots R package, to assess how the variation of coefficients depends on the position along the outline. The outputs returned by the R packages used were loaded into other software for further statistical analysis (*i.e.* Past – version 4.11 freely available at https://www.nhm.uio.no/english/research/infrastructure/past/), as described in the following paragraphs.

3.3 Gonadal development assessment

For each sampling carried out, a portion (n=100) of the collected specimens was allocated to the study of gonadal development, taking care to select individuals of different sizes to assess potential differences. For this purpose, the entire soft body of the selected clams was gently removed from the shell and immediately fixed in 10% buffered formalin solution for no more than 24 hours. Tissue samples thus collected were subsequently washed with distilled water and dehydrated trough an increasing range of alcohol solutions. Xylene was then used to infiltrate the histological samples before embedding in paraffin. Serial sections with a thickness of 5 µm were

obtained from the paraffin blocks using a microtome (EG11504 Leica Biosystems). Haematoxylin and eosin (H&E), xylene and Eukitt (Bio-Optica) were used for staining, clearing, and mounting the sections, respectively. All the necessary observations to assess the gonadal development were performed under a light microscope (Leica DM6 B - Leica Microsystems GmbH Ernst- Leitz-Strasse, Wetzlar, Germany) with a built-in digital camera (Leica DFC 7000 T), using several objectives 10X, 20X, 40X, 63X, 100X. The pictures acquired during this phase were post processed using the integrated Leica Application Suite X (LAS X) software. Each specimen analysed was classified according to its stage of gonadal development, following the scale proposed by Thorarinsdóttir (1993) previously described.

3.4 Age determination

The acetate peel technique was used to estimate the age of the collected specimens, following the protocol proposed by Ropes (1987). As pointed out above, the examination of the dark growth lines within the shell called “annuli”, alternating with light growth-increment deposits, represents a well-preserved record of growth, and the preparation of acetate peels of sectioned shells can better expose these internal depositional features. A representative number of left valves (n=45) were randomly selected for each size class, as they have more prominent teeth in the hinge which make age estimation easier and more reliable. The selected valves were first sectioned using a special saw machine (Struers - Minitom, Champigny sur Marne Cedex, France), making sure to orient the concave inner surface of the shell towards the diamond blade. Special care was taken during this delicate phase, cutting each valve at no more than 300 rpm of the saw blade, and using an appropriate weight (100 grams maximum) on the adjustable arm chosen according to the size of the shell. Sections thus obtained were embedded in a mixture of epoxy resin and hardener (ratio = 15:2 ml), taking care to remove as much as possible any air bubbles that might affect the printing on the acetate sheets. After an overnight hardening period, each resin block was removed from the silicone mould and subjected to a grinding and polishing process through a grinding machine (Struers Labosystem – LaboPol-20, Champigny sur Marne Cedex, France), using four progressively finer grits (220 – 500 – 1200 – 2000) and two solutions containing micro diamond particles (3µ and 1µ), respectively. Once a blemish-free, high gloss valve cutting surface has been achieved, the acetate peels were obtained by soaking the polished face of each resin block in a 2% hydrochloric acid solution for about 30 seconds. The same surface was then flooded

with acetone and covered with a pre-cut acetate sheet, trying to avoid the formation of air bubbles in the middle layer. The acetate was peeled off after drying, and each peel was sandwiched between glass slides for examination under a light microscope (Leica DM6 B - Leica Microsystems GmbH Ernst- Leitz-Strasse, Wetzlar, Germany) with a built-in digital camera (Leica DFC 7000 T).

3.5 Molecular analysis

Following the protocol proposed by Hurtado et al. (2011), 6 specimens of *Ruditapes sp.* were destined for molecular analysis. The selected clams were first identified as three specimens of R. decussatus and three of R. philippinarum (kindly donated by local shellfish farmers), according to the shape and arrangement of the siphons. Total DNA was extracted from portions of the foot and adductor muscle, using DNeasy Blood & Tissue Kit (Qiagen). Nanodrop spectrophotometer (Implen N50 NanoPhotometer, Westlake Village, United States) was used to assess the concentration and purity of DNA samples before storing them at 4°C. The amplification of extracted DNA was performed using GoTaq® G2 Colorless Master Mix (Promega, Madison, WI, United States), with a total solution of 25 µl. The primer used in the amplification reaction was 16S mitochondrial DNA (mtDNA), 16Sar 5' GGCCTGTTTATCAAAAACAT 3' and 16Sbr 5' CCGGTCTGAACTCAGATCACGT 3' (Hurtado et al., 2011). The fragment of mtDNA was amplified under the following thermal cycling conditions: initial denaturation at 95°C for 5 minutes, 35 cycles of denaturation at 95°C for 20 seconds, annealing at 55°C for 20 seconds, extension at 72°C for 20 seconds, and a final extension at 72°C for 7 minutes. All reactions were carried out with QIAamplifier 96 (Qiagen). 5 µl of PCR product were then examined by electrophoresis on 2% (w/v) agarose gel and the amplified samples were purified using QIAquick PCR Purification Kit (Qiagen). The sequencing was carried out by Eurofins Sanger Sequencing Services. The resulting sequences were aligned using the ClustalW algorithm (https://www.genome.jp/tools-bin/clustalw) and analysed using the nucleotide BLAST search (BLAST, http://blast.ncbi.nlm.nih.gov/) against the National Centre for Biotechnology Information (NCBI; https://blast.ncbi.nlm.nih.gov/Blast.cgi) to calculate the statistical significance of the match.

3.6 Occurrence of plastic debris

A total of 60 specimens of *R. decussatus* (20 for each size class) were randomly selected to evaluate the presence of anthropogenic debris. Once in the laboratory, each harvested clam intended for this analysis was washed with deionised water to eliminate any external contamination factor. All samples were then transferred individually in 250 ml glass jars containing about 150 ml of sea water for 24 hours to allow the complete emptying of gut, taking care to cover each container to prevent airborne contamination. The faeces found were thus collected and transferred into a 250 ml glass flask for anthropogenic debris extraction. The chemical digestion was obtained adopting a modified version of the protocol proposed by Savoca, Bottari, et al. (2020), with each sample being processed individually. To remove the organic matter, faeces were digested adding in each 250 ml glass flask a calculated quantity of 10% potassium peroxide (KOH) solution (minimum ratio 1:5 w/v). The conical containers were covered with aluminium foil and placed in a continuously oscillating incubator at 50°C for 48 hours. The supernatant was then collected and filtered through a glass fibre membrane with a pore size of 1.5 – 0.7 mm and 47 mm diameter (Whatman, Grade GF/F, UK), using a vacuum system (Millipore). Analytical blanks were prepared by processing neat filters in the same way. After the filtration phase, each filter was carefully placed in a sterile Petri glass dish for subsequent observations under a stereomicroscope (ZEISS SteREO Discovery.V8). All the plastic particles found were classified according to the shape (fibres and fragments), colour and size, the latter measured using ImageJ software (version 1.53k freely available at https://imagej.nih.gov/ij/). Following the above-mentioned protocol, the samples were processed in a restricted access room to prevent any accidental external contamination. Workspaces and tools were thoroughly cleaned with ethanol and filtered deionised water before each use. Moreover, deionised water and KOH were always pre-filtered (0.45 mm filter). Only sterilised glass items were used during the entire procedure. All assays were performed under a clean air flow cabinet to prevent external contamination. In addition, a paper filter placed in a Petri dish exposed to the laboratory air was used as control blank during the analysis (Giani et al., 2019).

4. Results

4.1 Morphometric measurements and size structure

All 300 specimens of *R. decussatus* sampled during the reporting period were measured and weighed, as summarised in Table 2.

	Min	1st Qu.	Median	Mean ± SD	3rd Qu.	Max	Class
Shell length (mm)	10	17.20	19.00	18.81 ± 2.91	21.25	22.8	1
	23	25.23	27.65	27.47 ± 2.57	29.45	31.8	2
	32.1	34.65	36.40	37.31 ± 3.70	39.15	48	3
Shell height (mm)	8	13.70	14.90	14.67 ± 2.28	16.00	19.5	1
	14.8	18.88	21.50	21.27 ± 3.03	23.80	28.2	2
	22.5	26.25	29.30	29.74 ± 4.46	32.15	41.1	3
Shell width (mm)	3	6.70	7.90	7.70 ± 1.68	9.00	10.5	1
	8.5	11.10	12.15	12.19 ± 1.49	13.22	17	2
	13.1	15.65	16.90	17.31 ± 2.23	18.40	24.2	3
Total weight (g)	0.33	0.74	1.00	1.17 ± 0.65	1.51	4.82	1
	1.46	2.69	3.73	3.82 ± 1.29	4.70	8.2	2
	5.16	7.56	9.60	21.60 ± 81.22	12.03	6.12	3
Soft tissues weight (g)	0.05	0.22	0.30	0.35 ± 0.20	0.45	1.46	1
	0.47	0.80	1.15	1.16 ± 0.44	1.43	2.7	2
	1.34	2.16	2.68	3.15 ± 1.53	3.52	8.2	3
Shell weight (g)	0.2	0.42	0.62	0.70 ± 0.33	0.97	1.57	1
	0.78	1.58	2.04	2.13 ± 0.71	2.64	4.5	2
	2.82	4.40	5.98	5.98 ± 2.51	6.89	15.76	3

Table 2 - Statistical summary of morphometric measurements of R. decussatus specimens from each size class

The graphs obtained via the generic hist() function of R software (Figure 13) show the frequency distribution of the morphometric variables for the entire reporting period.

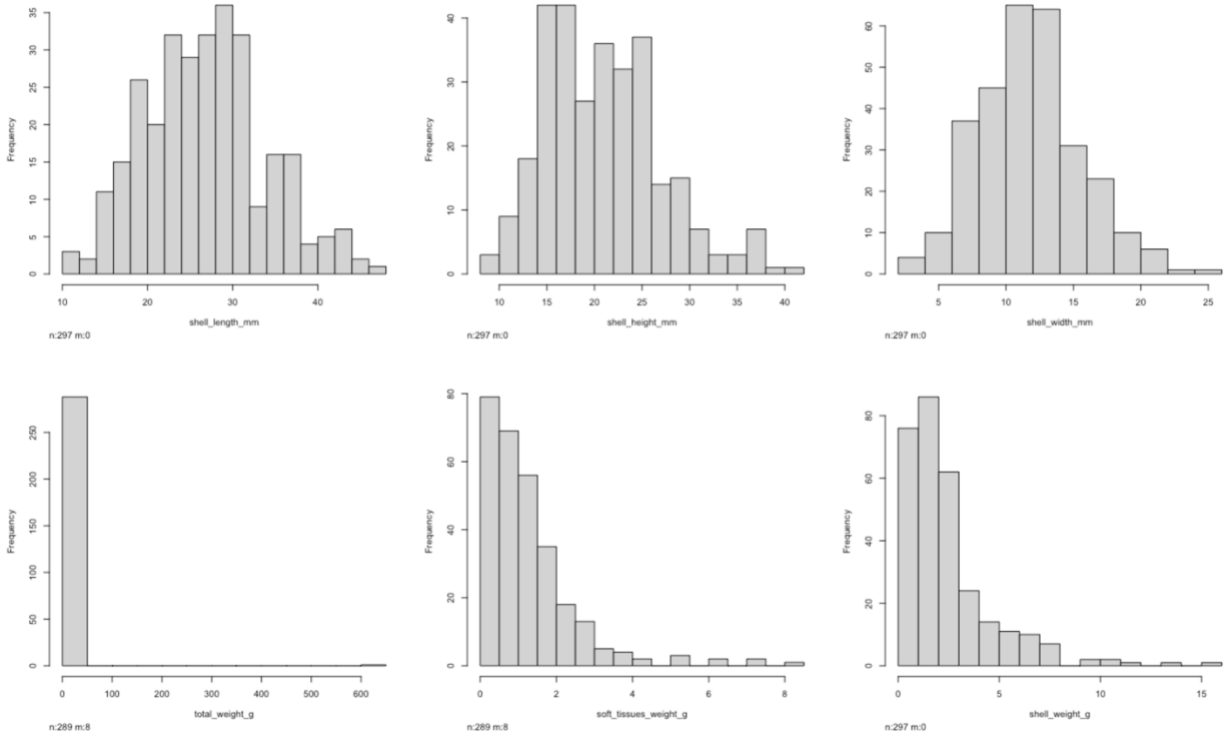

Figure 13 - Frequency distribution of morphometric variables for the entire reporting period

These variables were also used to calculate the sharpness indices of shell defined as the convexity index (width/height), the compactness index (width/length), and the elongation index (height/length), as well as three different ratios based on the shell weight (SW) and the three main measurements of valves (length, height, width). The results are summarised in Table 3.

	Min	1st Qu.	Median	Mean±SD	3rd Qu.	Max	Class
Convexity index	0.31	0.46	0.52	0.52 ± 0.09	0.59	0.69	1
	0.43	0.52	0.57	0.58 ± 0.07	0.64	0.71	2
	0.49	0.55	0.58	0.59 ±0.06	0.63	0.76	3
Compactness index	0.21	0.39	0.42	0.05 ±0.41	0.44	0.51	1
	0.35	0.42	0.44	0.03 ±0.44	0.46	0.54	2
	0.34	0.44	0.46	0.03 ±0.46	0.49	0.51	3
Elongation index	0.58	0.71	0.80	0.08 ±0.78	0.85	0.92	1
	0.63	0.70	0.80	0.07 ±0.77	0.83	0.92	2
	0.66	0.73	0.82	0.07 ± 0.80	0.85	0.92	3
Shell weight/length	0.07	0.025	0.03	0.01 ±0.04	0.04	0.07	1
	0.03	0.06	0.07	0.02 ±0.08	0.09	0.14	2
	0.09	0.13	0.14	0.05 ±0.16	0.18	0.37	3
Shell weight/height	0.02	0.03	0.05	0.02 ±0.05	0.06	0.09	1
	0.04	0.08	0.10	0.03 ± 0.10	0.11	0.18	2

	0.10	0.15	0.18	0.06 ± 0.20	0.24	0.43	3
Shell weight/width	0.04	0.07	0.08	0.04 ±0.09	0.11	0.20	1
	0.09	0.14	0.17	0.04 ± 0.17	0.20	0.30	2
	0.19	0.28	0.34	0.10 ± 0.34	0.37	0.75	3

Table 3 - Statistical summary of the sharpness indices and ratios calculated for R. decussatus specimens from each size class

The K-means cluster analysis (Figure 14) was used to determine three size classes based on shell length (SL), using specific function of different R packages (stats, dplyr, ggplot2, ggfortify, vegan). A total of 92 specimens were assigned to Class 1 (10 mm ≤ SL ≤ 22.9 mm), 148 to Class 2 (23 mm ≤ SL ≤ 31.9 mm), and 60 to Class 3 (32 mm ≤ SL ≤ 48 mm).

Figure 14 - K-means cluster analysis based on shell length

The variance analysis of the above-mentioned morphometric measurements and indices indicated significant differences among size classes and seasons ($p < 0.05$). The results of non-parametric Kruskal-Wallis test performed on the morphometric measurements of specimens collected the four seasons are shown in Table 4 and represented in Figure 15. In addition to a rather regular trend, it is easy to note that the comparison between winter and the other seasons showed greater significance for most of the variables analysed. This could be related to the natural metabolic slowdown due to lower temperatures.

	Comparisons	Mean rank diff.	Significance	Summary	Adjusted P Value
Shell Length (mm)	Winter vs Spring	74.52	Yes	**	0.001
	Winter vs Summer	50.6	Yes	*	0.01
	Winter vs Autumn	78.19	Yes	****	<0.0001
	Spring vs Summer	-23.92	No	ns	0.7511
	Spring vs Autumn	3.67	No	ns	>0.9999
	Summer vs Autumn	27.59	No	ns	0.1183
Shell Height (mm)	Winter vs Spring	25.96	No	ns	>0.9999
	Winter vs Summer	0.7051	No	ns	>0.9999
	Winter vs Autumn	70.04	Yes	***	0.0002
	Spring vs Summer	-25.26	No	ns	0.6325
	Spring vs Autumn	44.08	Yes	*	0.047
	Summer vs Autumn	69.34	Yes	****	<0.0001
Shell Width (mm)	Winter vs Spring	94.61	Yes	****	<0.0001
	Winter vs Summer	58.35	Yes	**	0.0017
	Winter vs Autumn	80.37	Yes	****	<0.0001
	Spring vs Summer	-36.25	No	ns	0.1207
	Spring vs Autumn	-14.24	No	ns	>0.9999
	Summer vs Autumn	22.02	No	ns	0.3766
Total Weight (g)	Winter vs Spring	85.5	Yes	***	0.0001
	Winter vs Summer	66.67	Yes	***	0.0002
	Winter vs Autumn	89.66	Yes	****	<0.0001
	Spring vs Summer	-18.83	No	ns	>0.9999
	Spring vs Autumn	4.156	No	ns	>0.9999
	Summer vs Autumn	22.99	No	ns	0.2808
Soft Tissues Weight (g)	Winter vs Spring	75.83	Yes	***	0.0009
	Winter vs Summer	65.48	Yes	***	0.0002
	Winter vs Autumn	100.4	Yes	****	<0.0001
	Spring vs Summer	-10.35	No	ns	>0.9999
	Spring vs Autumn	24.55	No	ns	0.8573
	Summer vs Autumn	34.9	Yes	*	0.0153
Shell Weight (g)	Winter vs Spring	79.44	Yes	***	0.0004
	Winter vs Summer	70	Yes	****	<0.0001
	Winter vs Autumn	87.93	Yes	****	<0.0001
	Spring vs Summer	-9.449	No	ns	>0.9999
	Spring vs Autumn	8.483	No	ns	>0.9999
	Summer vs Autumn	17.93	No	ns	0.7779

Table 4 - Results of non-parametric Kruskal-Wallis test performed on the morphometric measurements of R. decussatus specimens collected during the four seasons

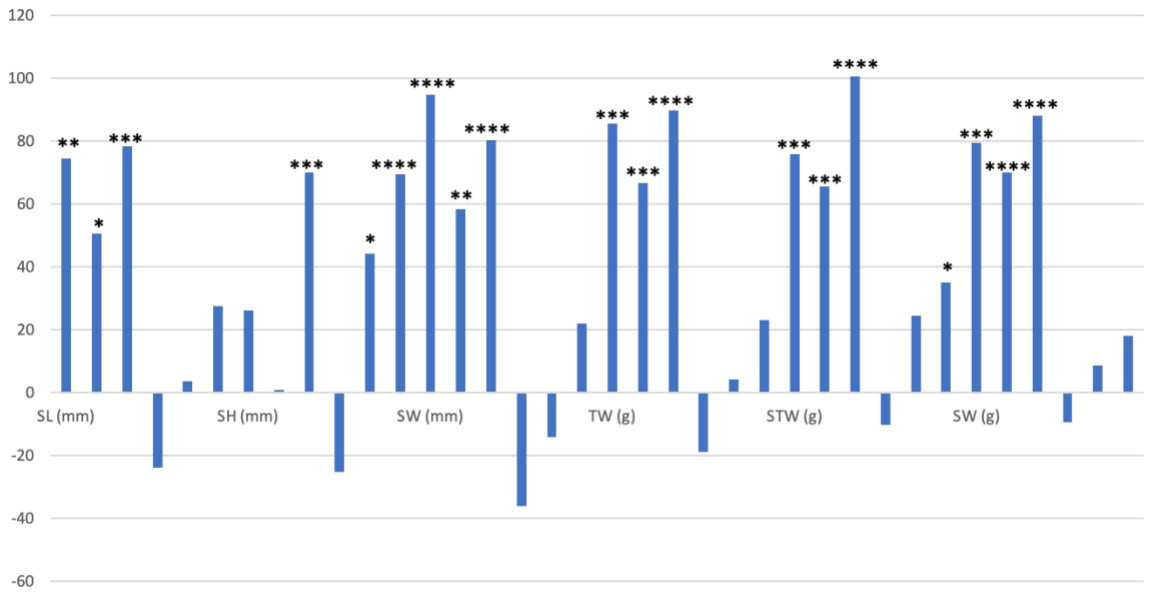

Figure 15 - Plotting the results of Kruskal-Wallis test performed on the morphometric measurements of R. decussatus specimens collected during the four seasons. The asterisk indicates the level of significance; SL = Shell Length; SH = Shell Height; SW = Shell Width; TW = Total Weight; STW = Soft Tissues Weight; SW = Shell Weight

The results of Kruskal-Wallis test performed on the morphometric measurements of specimens belonging to the different size classes showed high level of significance, as expected (Table 5 – Figure 16).

	Comparisons	Mean rank diff.	Significance	Summary	Adjusted P Value
Shell Length (mm)	Class1 vs Class2	-119	Yes	****	<0.0001
	Class1 vs Class3	-222.5	Yes	****	<0.0001
	Class2 vs Class3	-103.5	Yes	****	<0.0001
Shell Height (mm)	Class1 vs Class2	-112.4	Yes	****	<0.0001
	Class1 vs Class3	-211.6	Yes	****	<0.0001
	Class2 vs Class3	-99.18	Yes	****	<0.0001
Shell Width (mm)	Class1 vs Class2	-117.2	Yes	****	<0.0001
	Class1 vs Class3	-218.6	Yes	****	<0.0001
	Class2 vs Class3	-101.4	Yes	****	<0.0001
Total Weight (g)	Class1 vs Class2	-113.2	Yes	****	<0.0001
	Class1 vs Class3	-212.8	Yes	****	<0.0001
	Class2 vs Class3	-99.56	Yes	****	<0.0001
Soft Tissues Weight (g)	Class1 vs Class2	-113.7	Yes	****	<0.0001
	Class1 vs Class3	-209.8	Yes	****	<0.0001
	Class2 vs Class3	-96.11	Yes	****	<0.0001
Shell Weight (g)	Class1 vs Class2	-115.8	Yes	****	<0.0001

	Class1 vs Class3	-218.4	Yes	****	<0.0001
	Class2 vs Class3	-102.6	Yes	****	<0.0001

Table 5 - Results of non-parametric Kruskal-Wallis test performed on the morphometric measurements of R. decussatus specimens belonging to the different size classes

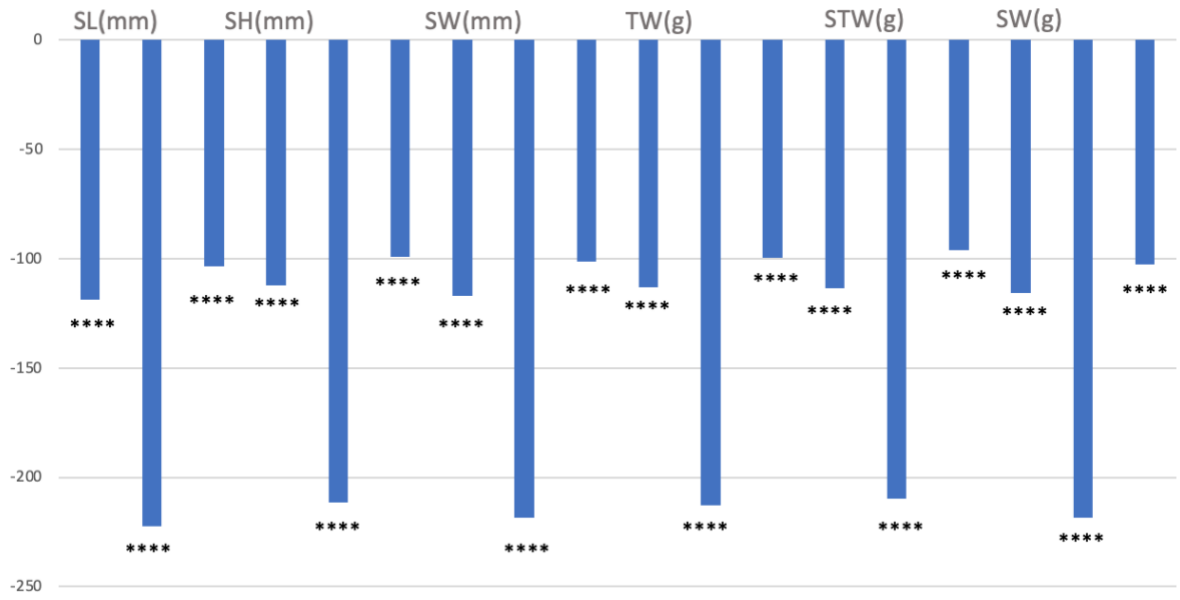

Figure 16 - Plotting the results of Kruskal-Wallis test performed on the morphometric measurements of R. decussatus specimens belonging to the different size classes. The asterisk indicates the level of significance; SL = Shell Length; SH = Shell Height; SW = Shell Width; TW = Total Weight; STW = Soft Tissues Weight; SW = Shell Weight

Similarly, the non-parametric Dunn's test was applied to the sharpness indices and ratios calculated based on morphometric measurements. The results of the comparison between seasons are shown in Table 6 and Figure 17. Even in this case, the comparison between winter and the other seasons showed greater significance for most of the variables analysed. It should also be noted that the results for the compactness index showed significance for all comparisons except for that between summer and autumn.

	Comparisons	**Mean rank diff.**	**Significance**	**Summary**	**Adjusted P Value**
Convexity Index	Winter vs Spring	172.6	Yes	****	<0.0001
	Winter vs Summer	147.4	Yes	****	<0.0001
	Winter vs Autumn	21.79	No	ns	>0.9999
	Spring vs Summer	-25.22	No	ns	0.6356
	Spring vs Autumn	-150.8	Yes	****	<0.0001
	Summer vs Autumn	-125.6	Yes	****	<0.0001
Compactness Index	Winter vs Spring	116.9	Yes	****	<0.0001
	Winter vs Summer	64.04	Yes	***	0.0004

	Winter vs Autumn	54.87	Yes	**	0.0077
	Spring vs Summer	-52.88	Yes	**	0.0042
	Spring vs Autumn	-62.06	Yes	**	0.0011
	Summer vs Autumn	-9.172	No	ns	>0.9999
Elongation Index	Winter vs Spring	-101.1	Yes	****	<0.0001
	Winter vs Summer	-138.2	Yes	****	<0.0001
	Winter vs Autumn	9.859	No	ns	>0.9999
	Spring vs Summer	-37.08	No	ns	0.1047
	Spring vs Autumn	111	Yes	****	<0.0001
	Summer vs Autumn	148.1	Yes	****	<0.0001
Shell weight/length	Winter vs Spring	76.99	Yes	***	0.0006
	Winter vs Summer	77.35	Yes	****	<0.0001
	Winter vs Autumn	91.13	Yes	****	<0.0001
	Spring vs Summer	0.3569	No	ns	>0.9999
	Spring vs Autumn	14.13	No	ns	>0.9999
	Summer vs Autumn	13.78	No	ns	>0.9999
Shell weight/height	Winter vs Spring	95.82	Yes	****	<0.0001
	Winter vs Summer	96.59	Yes	****	<0.0001
	Winter vs Autumn	86.6	Yes	****	<0.0001
	Spring vs Summer	0.7626	No	ns	>0.9999
	Spring vs Autumn	-9.221	No	ns	>0.9999
	Summer vs Autumn	-9.983	No	ns	>0.9999
Shell weight/width	Winter vs Spring	56.51	Yes	*	0.0265
	Winter vs Summer	75.52	Yes	****	<0.0001
	Winter vs Autumn	91.32	Yes	****	<0.0001
	Spring vs Summer	19.01	No	ns	>0.9999
	Spring vs Autumn	34.81	No	ns	0.2147
	Summer vs Autumn	15.79	No	ns	>0.9999

Table 6 - Results of non-parametric Dunn's test performed on the sharpness indices and ratios calculated for R. decussatus specimens collected during the four seasons

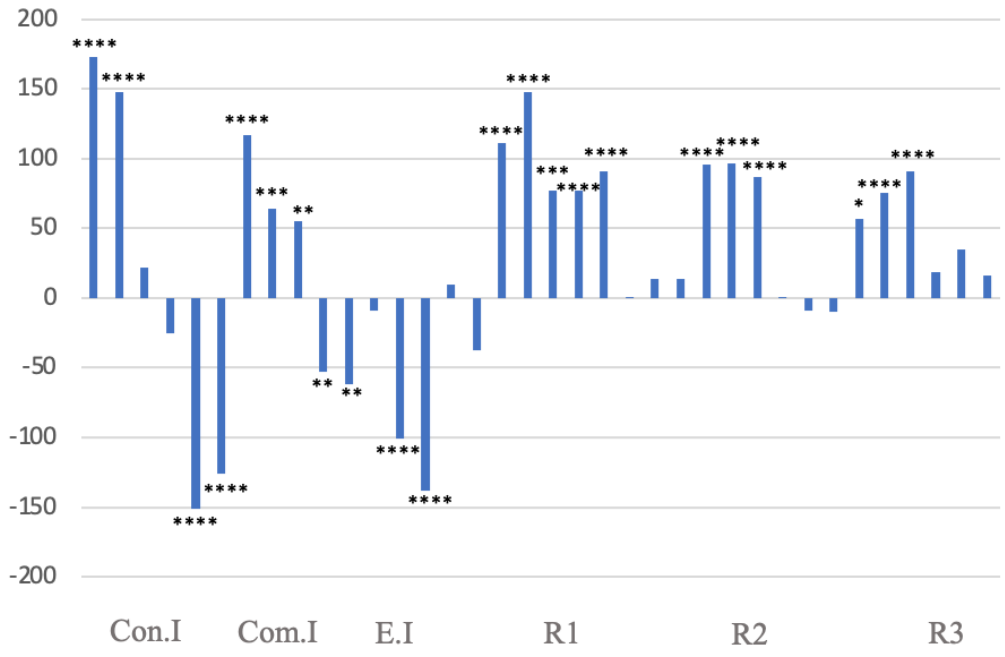

Figure 17 - Plotting the results of Dunn's test performed on the sharpness indices and ratios calculated for R. decussatus specimens collected during the four seasons. The asterisk indicates the level of significance; Con. I = Convexity Index; Com. I = Compactness Index; E. I = Elongation Index; R1 = Ratio 1 (Shell weight/length); R2 = Ratio 2 (Shell weight/height); R3 = Ratio 3 (Shell weight/width)

The results of Dunns' test performed on the sharpness indices and ratios calculated for specimens belonging to the different size classes showed high level of significance, as shown in Table 7 and Figure 18. More specifically, the comparison of the mean value convexity indices calculated showed that specimens belonging to Class 3 had a more convex shell (0.59 ±0.06) from a frontal view than individuals from other classes (Class 1 = 0.52 ± 0.09; Class 2 = 0.58 ± 0.07). Regarding the compactness, clams from Class 1 exhibited the highest mean value of the corresponding index (0.05 ±0.41), suggesting that specimens belonging to this class had a more curved valve dome from a ventral view. The lowest mean values of elongation index were detected among *R. decussatus* from Class 2 and 3 (0.07 ±0.77 and 0.07 ± 0.80, respectively), which suggested that the shells were slender from a lateral view than those of Class 1 (0.08 ±0.78). An increasing trend of the mean weight ratios was noted, as expected, among size classes. The mean values of ratios of weight to linear shell variables ranged from 0.01 ±0.04 to 0.10 ± 0.34, with the highest mean value found among Class 3 specimens.

	Comparisons	Mean rank diff.	Significance	Summary	Adjusted P Value
Convexity Index	Class 1 vs Class 2	-53.51	Yes	****	<0.0001
	Class 1 vs Class 3	-63.15	Yes	****	<0.0001
	Class 2 vs Class 3	-9.64	No	ns	>0.9999
Compactness Index	Class 1 vs Class 2	-67.23	Yes	****	<0.0001
	Class 1 vs Class 3	-123.4	Yes	****	<0.0001
	Class 2 vs Class 3	-56.14	Yes	****	<0.0001
Elongation Index	Class 1 vs Class 2	14.13	No	ns	0.6549
	Class 1 vs Class 3	-13.83	No	ns	>0.9999
	Class 2 vs Class 3	-27.96	No	ns	0.1033
Shell weight/length	Class 1 vs Class 2	-112.3	Yes	****	<0.0001
	Class 1 vs Class 3	-212.8	Yes	****	<0.0001
	Class 2 vs Class 3	-100.5	Yes	****	<0.0001
Shell weight/height	Class 1 vs Class 2	-111.3	Yes	****	<0.0001
	Class 1 vs Class 3	-210.4	Yes	****	<0.0001
	Class 2 vs Class 3	-99.15	Yes	****	<0.0001
Shell weight/width	Class 1 vs Class 2	-105.5	Yes	****	<0.0001
	Class 1 vs Class 3	-210.5	Yes	****	<0.0001
	Class 2 vs Class 3	-105	Yes	****	<0.0001

Table 7 - Results of non-parametric Dunn's test performed on the sharpness indices and ratios calculated for R. decussatus specimens belonging to the different size classes

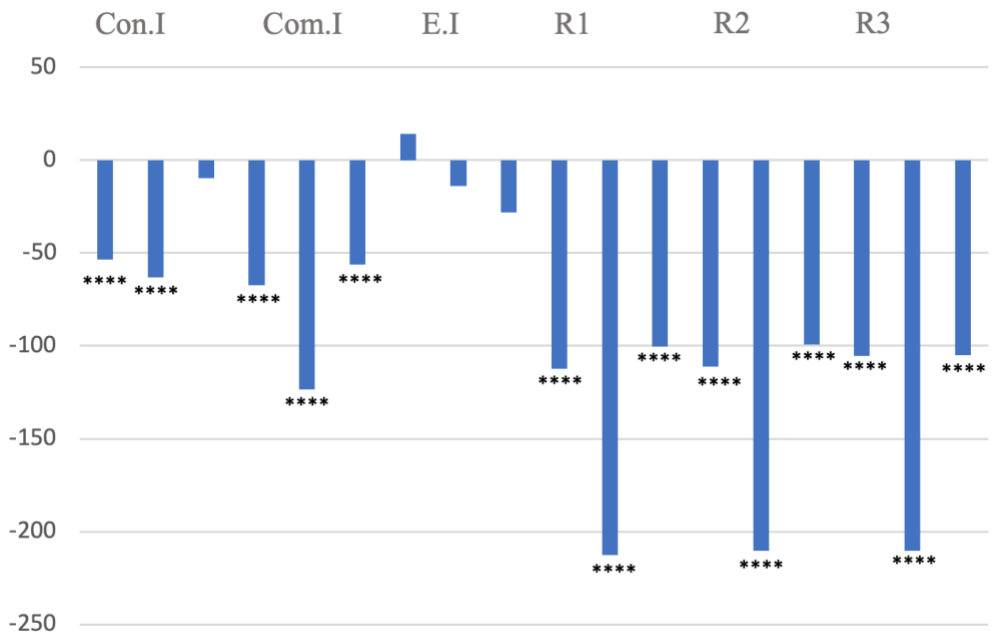

Figure 18 - Plotting the results of Dunn's test performed on the sharpness indices and ratios calculated for R. decussatus specimens belonging to the different size classes. The asterisk indicates the level of significance; Con. I = Convexity Index; Com. I = Compactness Index; E. I = Elongation Index; R1 = Ratio 1 (Shell weight/length); R2 = Ratio 2 (Shell weight/height); R3 = Ratio 3 (Shell weight/width)

The percentage of *R. decussatus* of each size class per season is shown in Figure 19. It is easy to deduce from the graph that Class 2 has always been the most abundant in all seasons. The specimens belonging to this class accounted for about 61% of the clams collected in winter, followed by 56% during spring, 51% in autumn and 44% during summer. Regarding Class 1, it showed a similar trend in all seasons (36% in both autumn and spring, about 32% in summer) except in winter (about 6%). The largest size class (Class 3) was most abundant in winter (about 33% of specimens collected during this season), followed by 24% in summer, 13% during autumn and 8% in spring.

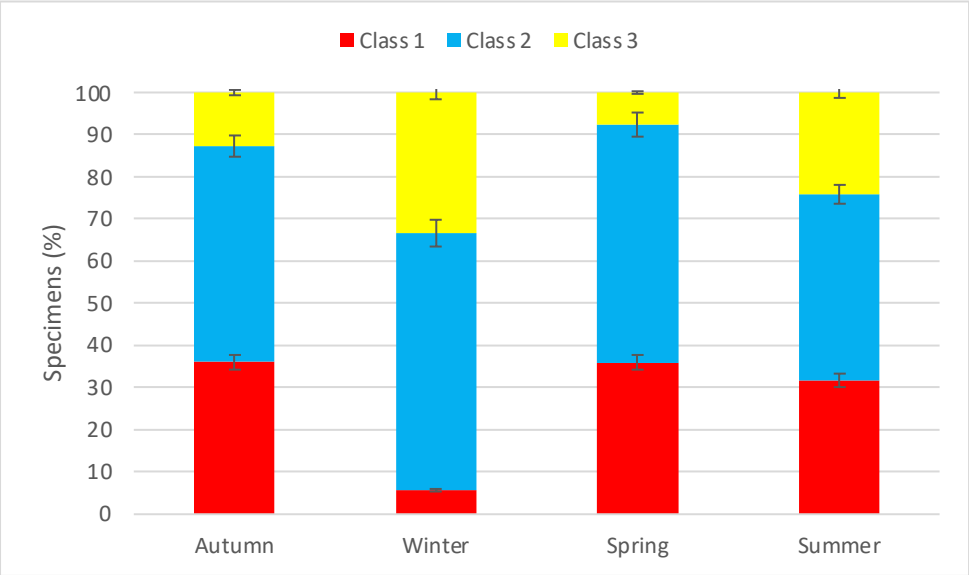

Figure 19 - Percentage of R. decussatus of each size class per season

The histograms in Figure 20 show the shell length frequency distribution of specimens caught in the study area during different seasons, obtained via the generic hist() function of R software. The peak in the spring sample is probably related to the emergence of recruits, while in the summer the asymmetry of the curve could be caused by the increase in the first length classes resulting from recruitment. The confidence intervals analysis revealed significant differences in shell length between seasons (Table 8). The smallest individual of all those sampled was found in spring, with a shell length of 10 mm, while the largest was found in summer (48 mm). The minimum mean value of shell length was recorded in spring (25.03 mm), the season in which, as pointed out before, the distribution of shell lengths seems to be influenced by recruitment.

	Min.	1st Qu.	Median	Mean ± SD	3rd Qu.	Max.
Autumn	15.00	21.75	24.25	25.14 ± 5.36	27.68	38.30
Winter	21.90	28.57	30.15	30.88 ± 5.12	35.20	42.30
Spring	10.00	21.25	25.60	25.03 ± 6.76	28.40	43.00
Summer	13.40	19.40	27.90	27.27 ± 8.05	31.62	48.00

Table 8 - Statistical summary of shell length measurements per season

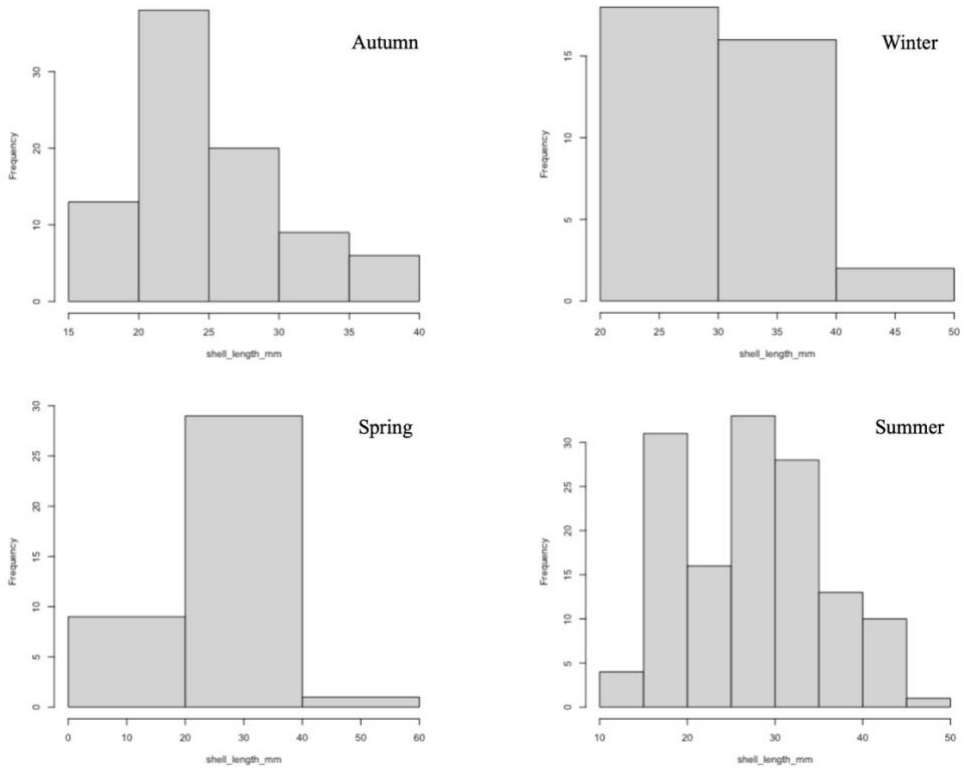

Figure 20 - Shell length frequency distribution of R. decussatus specimens caught in the study area during different seasons

4.2 Analysis of the shell shape

Once the three size classes has been determined as previously described, a shape analysis based on the outlines of the shell was performed for each of them. To assess the existence of any asymmetries and/or interclass differences, the contours were detected for both right and left valve of each specimen, using the shapeR function detect.outline() on RStudio. The boundaries thus extracted were linked to the Excel file containing the above-mentioned information on specimens analysed (e.g., shell measurements, body weight, sampling date and site). Both Wavelet and Fourier coefficients were calculated and adjusted through proper functions of shapeR package to define the allometric relationships between specimen measurements and valve shape. The graphs in Figure 21 represent a comparison between the mean shape of right

and left valve of individuals in the three size classes, obtained through standardised Wavelet coefficients. As also demonstrated by the results of the ANOVA performed on the extrapolated coefficients ($p < 0.05$), significant differences were detected in all the classes analysed (Table 9).

Class	Valve comparison	p value	Df	F	Sum of Sqs.
1	Left vs Right	0.001	1	34.481	6.0106
2	Left vs Right	0.001	1	53.113	8.289
3	Left vs Right	0.001	1	19.621	2.9297

Table 9 - Results of the ANOVA analysis performed to compare the outlines of left and right valves ($p < 0.05$)

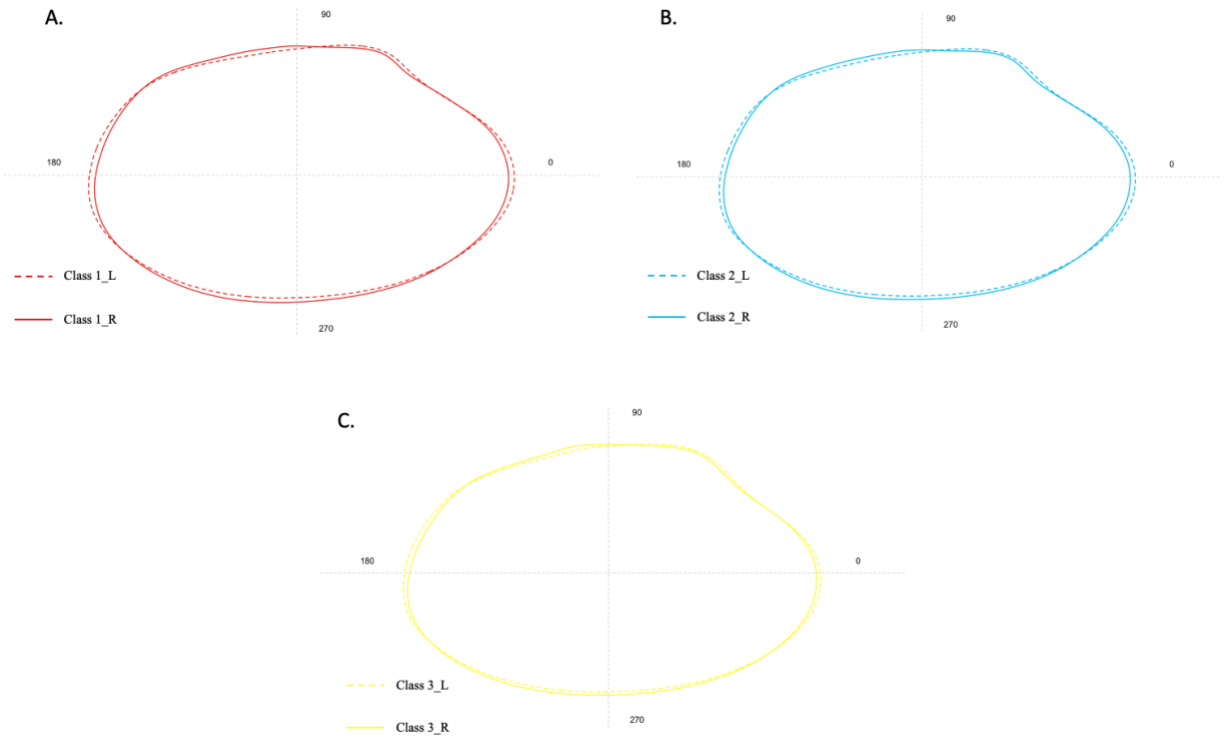

Figure 21 - Comparisons of the mean shell shape of left and right valves from Class 1 (A), Class 2 (B), and Class 3 (C). All the reconstructions were based on standardised Wavelet coefficients

Similarly, an interclass comparison of mean shape was performed for both left and right valve (Figure 22). The quality of reconstructions based on Wavelet and Fourier coefficients was estimated by comparing the deviations from the outlines detected, with the value 15 set as the maximum number of Fourier harmonics to be shown. In addition, the mean and standard deviation of the coefficients were plotted together to evaluate how their variation depends on the position along the contour, using proper functions of the gplot R package (Figure 23 A-D). The

expected significant differences between the size classes analysed were again confirmed by the results of the ANOVA (p = 0.001 for both left and right valves).

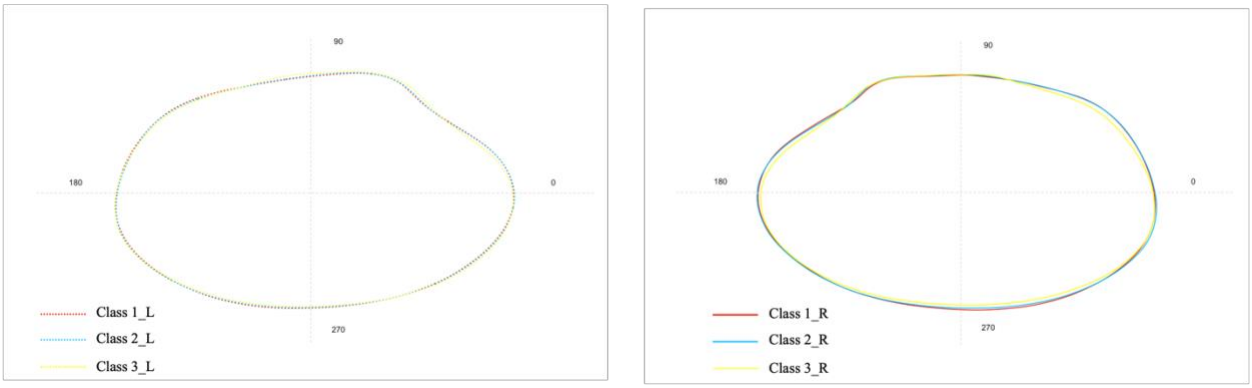

Figure 22 - Comparisons of the mean shell shape of left (on the left) and right (on the right) valves from the three size classes. All the reconstructions were based on standardised Wavelet coefficients

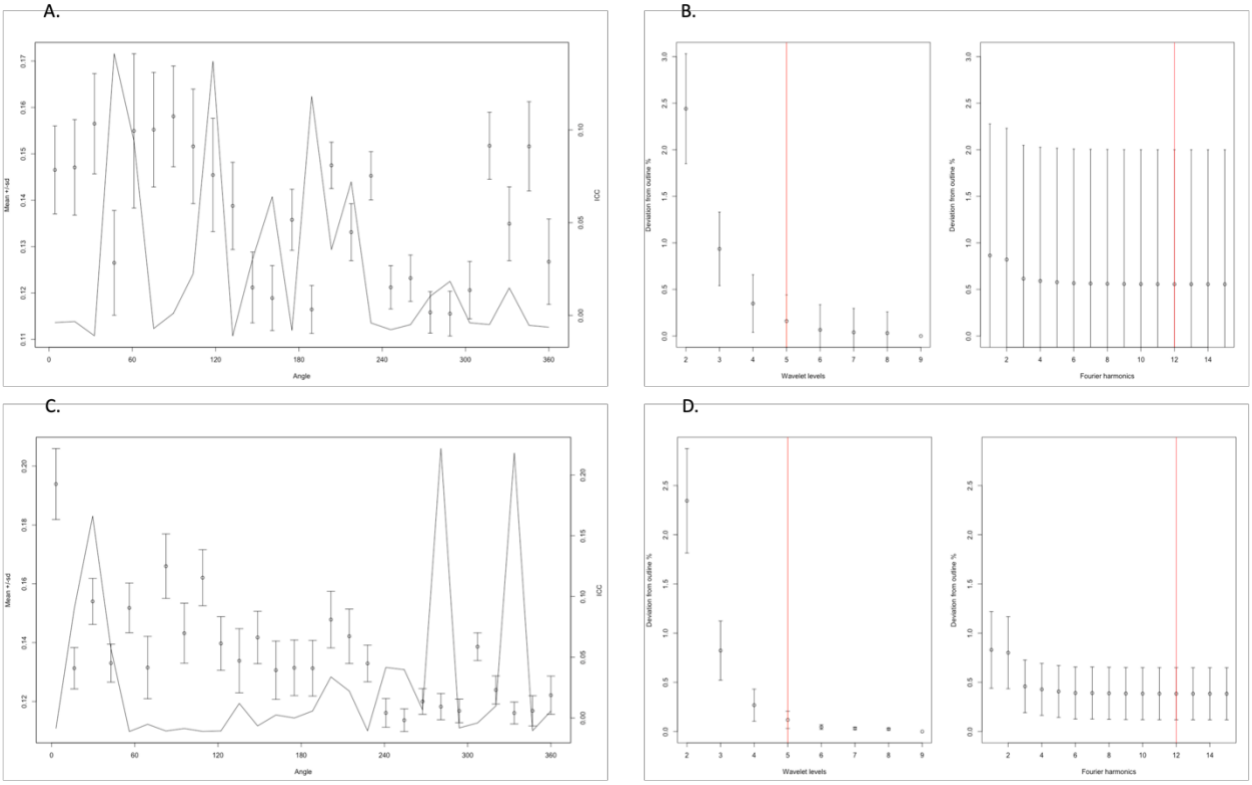

Figure 23 - Plotting the mean and standard deviation of the coefficients calculated for right (A) and left valves (C) to evaluate how their variation depends on the position along the contour; Quality reconstruction plot based on standardised coefficients of right (B) and left valves (D) with the value 15 set as the maximum number of Fourier harmonics to be shown.

The outputs returned by the R packages used for the shape analysis were loaded into Past software for statistical data analysis (version 4.11 freely available at https://www.nhm.uio.no/english/research/infrastructure/past/). A Linear Discriminant Analysis

(LDA) was then performed on the standardised Fourier coefficients of each class for both left and right valve, with ellipses including the 95% confidence intervals. The LDA results showed that the outlines of the right valves of specimens from Class 1 were moderately separated from those extrapolated for the other two classes (Figure 24 A). Similarly, the contours of the left valves of Class 3 individuals appeared more distinctly separated from those of the other size classes (Figure 24 B).

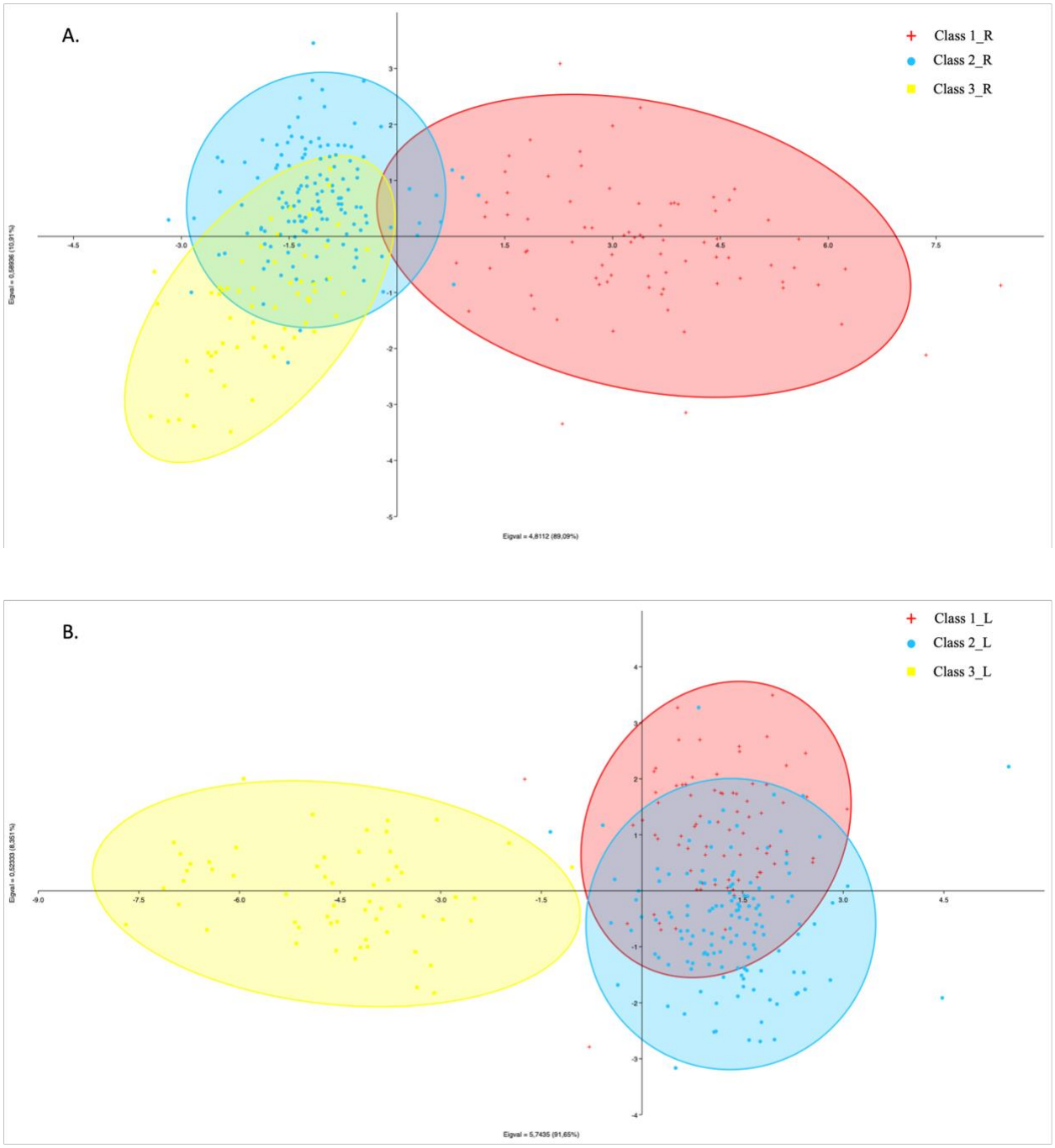

Figure 24 - Linear Discriminant Analysis (LDA) performed on the standardised Fourier coefficients of each size class for both right (A) and left valve (B), with ellipses including the 95% confidence intervals.

4.3 Sex ratio and gonadal development

Out of a total of 300 specimens of *R. decussatus* collected, 100 were allocated for histological examination, aimed at sex determination and assessment of gonadal development. The sex ratio (male/female = 1.17) calculated according to the presence of spermatozoa and oocytes did not deviate significantly from the expected proportion of 1:1 (Herrmann et al., 2009). Among all clams analysed, 54% were identified as males, and 46% as females. No cases of hermaphroditism were documented. Figure 25 shows the sex ratio expressed as percentage of individual belonging to a gender on the total number of bivalves sampled in the four seasons.

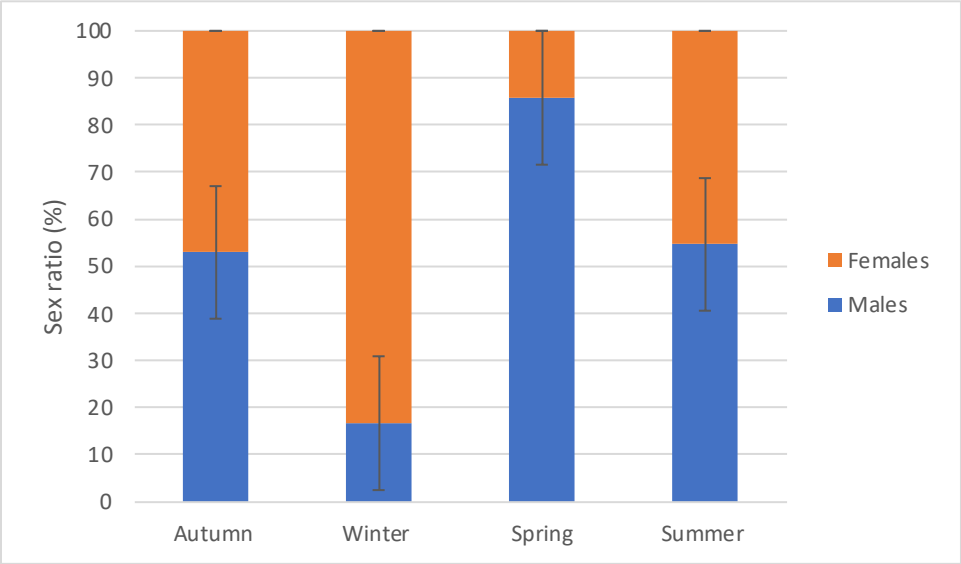

Figure 25 - Sex ratio expressed as percentage of individual belonging to a gender on the total number of bivalves sampled in the four seasons. The black segments indicate the standard error

During the autumn period, males represented about 53% and females about 47%. A similar trend was observed in summer (about 55% males and 45% females). On the other hand, opposite sex ratios were documented during winter and spring, with 17% males and 83% females and 86% of males and 14% of female, respectively. The histological analysis of gonadal tissues also allowed to determine the stage of sexual maturation of each *R. decussatus* specimen captured in the study area. All the previously described stages (Thorarinsdóttir, 1993) were documented during the reporting period, as shown in Figure 26.

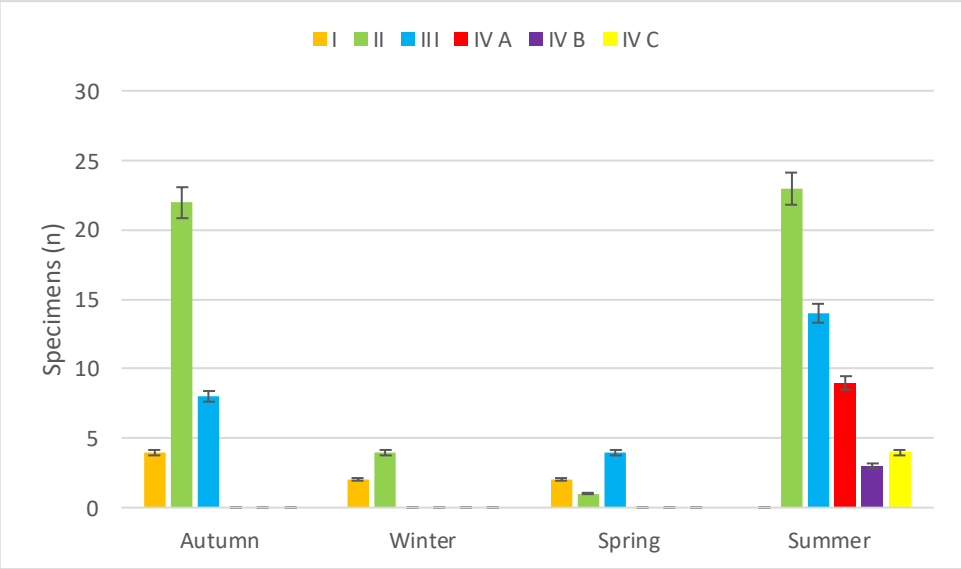

Figure 26 - Distribution of the different gonadal development stages documented per season. The black segments indicate the standard error

More specifically, 34 of the specimens analysed were caught during the autumn season, showing the first three stages of gonadal development (stage I - *n=4*; stage II – *n=22*; stage III – *n=8*). The 6 specimens collected in winter were assigned to the stage I and II (*n=2* and *n=4* respectively). The same stages documented in autumn were found also in spring, with different ratio (stage I – *n=2*; stage II – *n=1*; stage III – *n=4*). Summer was the season that showed the greatest variability in gonad development, probably due to higher temperatures and the beginning of the breeding season. Specimens collected from June to August were classified as belonging to all stages except the first (stage II – *n=23*; stage III – *n=14*; stage IV A – *n=9*; stage IV B – *n=3*; stage IV C – *n=4*). Data collected were also expressed as percentage of individual belonging to each stage of gonadal development on the total number of bivalves sampled in the four seasons (Figure 27).

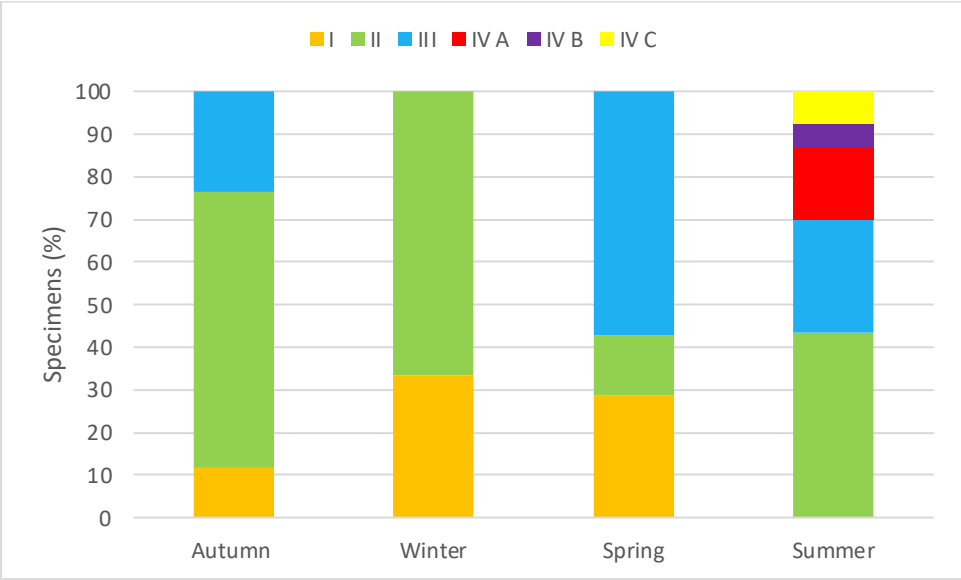

Figure 27 - Percentage of individual belonging to each stage of gonadal development on the total number of bivalves sampled in the four seasons

Approximately 12% of the clams harvested during the autumn period were assigned to stage I, about 65% to stage II, and 23% to stage III. In winter, only the initial stages of gonadal development were documented, with 33% of *R. decussatus* belonging to stage I and 67% to stage II. As pointed out before, specimens collected in autumn and spring showed the same stages of sexual maturation with different percentages, being about 29% individuals classified as stage I, 14% as stage II, and 57% as stage III. During the summer months, which coincide with the peak of breeding season of this species, all bivalves collected were found to be in the ripening, releasing and resting phase. About 43% clams analysed were assigned to stage II, 27% to stage III, 17% to stage IV A, 6% to stage IVB, and 7% to stage IV C. Figures 28 and 29 show a comparison of the first three stages of gonadal development documented in males and females during the reporting periods. It is very difficult or often impossible to determine the sex of specimens at stage I, during which the main component of the gonad is connective tissue and a significant amount of free water, with no distinguishable gametes. Most clams classified as belonging to this stage were found during winter and early spring, probably due to the cold temperature and the resulting metabolic slowdown. First signs of gonadal tissue proliferation can be observed from stage II onwards. Although still flabby, the gonad appears significantly increased in size, with a reduced free water content. The half-grown oocytes are now visible within the lumen of female follicle, with most of them attached to the wall. Spermatogonia and spermatocytes are arranged radially in male follicle, and even spermatids can be noted when the bivalve is more developed. This was the only documented stage in all four seasons, mainly in winter and autumn, followed

by the late summer period. A larger gonad size and a significantly reduced free water content characterise the stage III, also known as “half-full maturing”. The follicles appear tightly packed together and connective tissue in further reduce. Free oocytes appear in the lumen of female follicle, and new generations of oocytes of different sizes are visible along the wall. Inside the male follicle, spermatogonia, spermatocytes, spermatids and spermatozoa are now evident, with a predominance of the latter two in more developed specimens. This stage of gonadal development was mainly documented during the late spring, as temperatures rose and the breeding season began. Sexually mature individuals were only found during the summer sampling season. The three documented stages of gonadal development (IV A, IV B, IV C) are shown in Figures 30 and 31. Among the male specimens analysed, it was possible to recognise all three stages, whereas among the females only stage IV A was reported. At this latter stage, the gonad has reached its maximum size and no longer contains free water. The female follicle is mostly filled with free oocytes of polygonal or hexagonal shape which appear closely packed together. The main gonadic components of male follicle are mature spermatozoa whose heads measure about 3 µm, forming elongated or centric bands. During the subsequent spawning phase (stage IV B), gonads show a significant amount of free water that depends on the number of emptied follicles. Areas with un-spawned follicles can be present, exhibiting ripe germ cells at stage IV of development. The spent stage (IV C) is characterised by mostly empty follicles significantly reduced in volume, with broken walls. Un-spawned gametes are occasionally visible as cellular debris, together with the amoebocytes that attack them. Some reorganization of follicles and early gametogenic stages becomes evident in later stages.

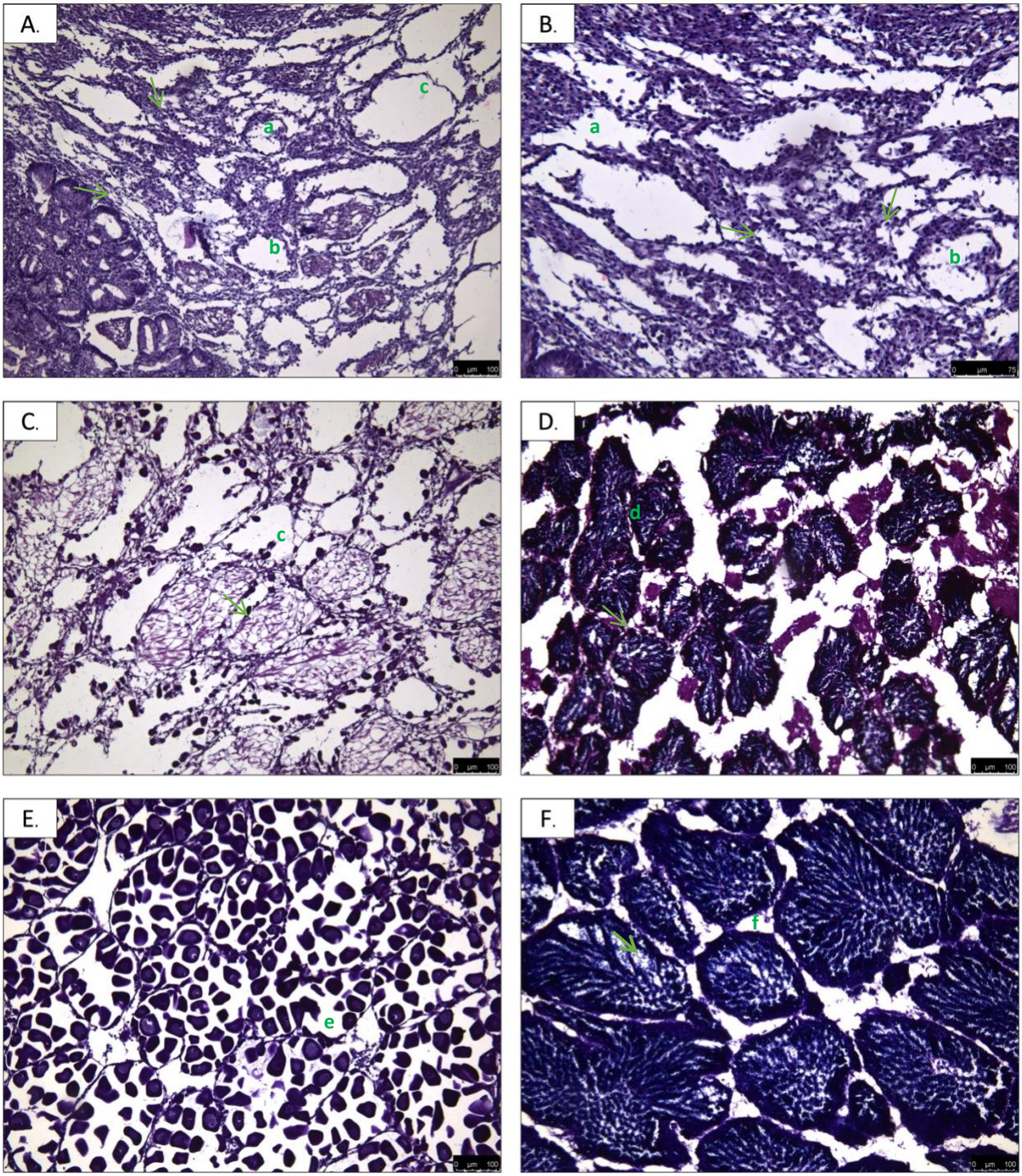

Figure 28 - Representative histological sections of male and female gonads of Ruditapes decussatus stained with haematoxylin and eosin. Stage I Maturing (recovering): 10x (A) 20x (B) (a) gonad growing and flabby, (b) genital ducts loosing circular configuration. Stage II Maturing (filling): 10x (C) female and (D) male (c) Lumen of females contains half-grown oocytes, many of them attached to the follicle wall (d) radially arranged spermatozoa. Stage III Maturing (half full): 10x (E) female and (F) male. Follicles becoming packed together, (e) lumina becoming packed with fully grown oocytes 50-60 µm in diameter and (f) lumina becoming packed with spermatozoa. Arrows indicate free water – Scale bars: 100 µm (A, C, D, E, F) and 75 µm (B)

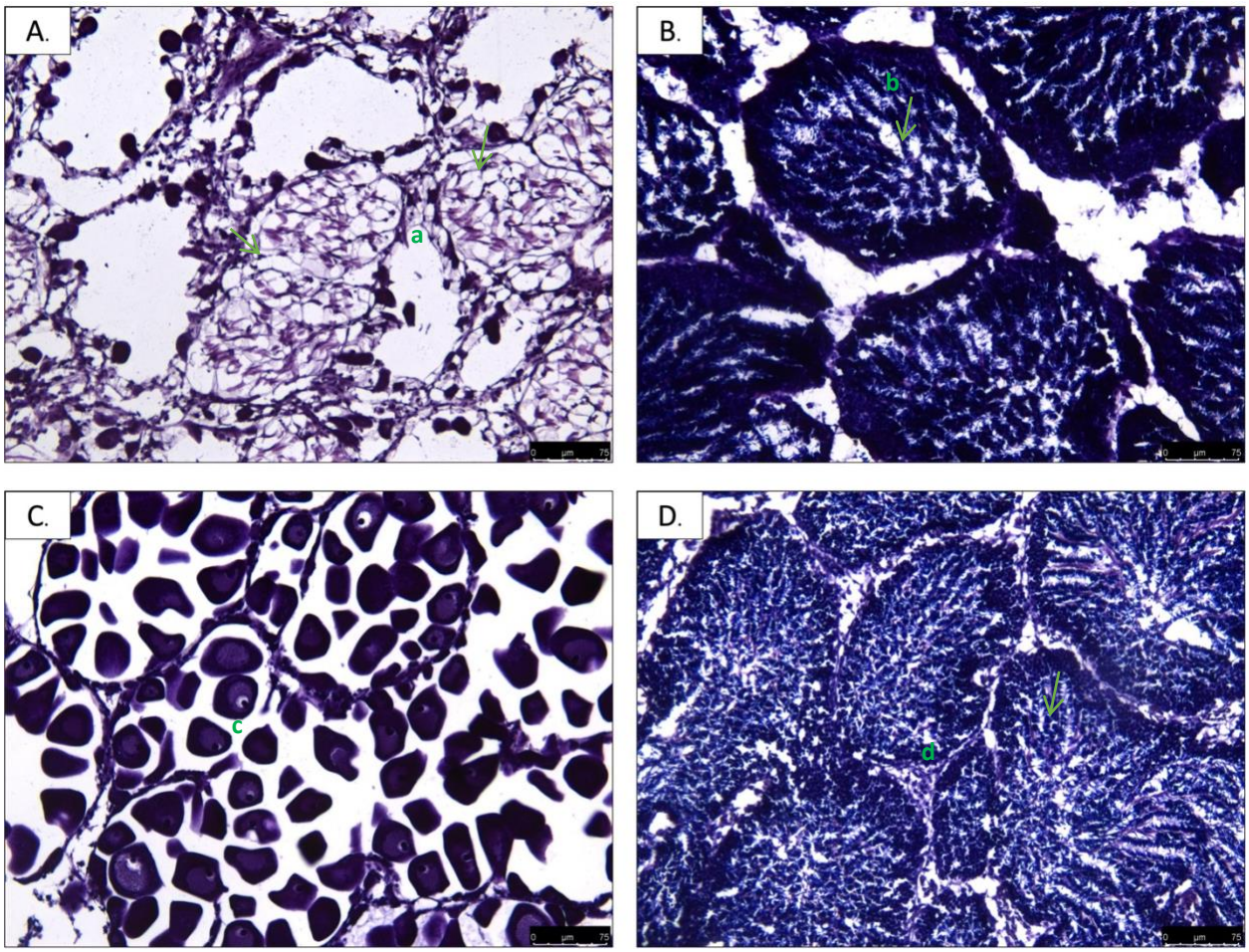

Figure 29 - Representative histological sections of male and female gonads of Ruditapes decussatus stained with haematoxylin and eosin. Stage II Maturing (filling): 20x (A) female and (B) male. (a) Lumen of females contains half-grown oocytes, many of them attached to the follicle wall, (b) radially arranged spermatozoa. Stage III Maturing (half full): 20x (C) female and (D) male. Follicles becoming packed together, (c) lumina becoming packed with fully grown oocytes 50-60µm in diameter and (d) lumina becoming packed with spermatozoa. Arrows indicate free water – Scale bars: 75 µm

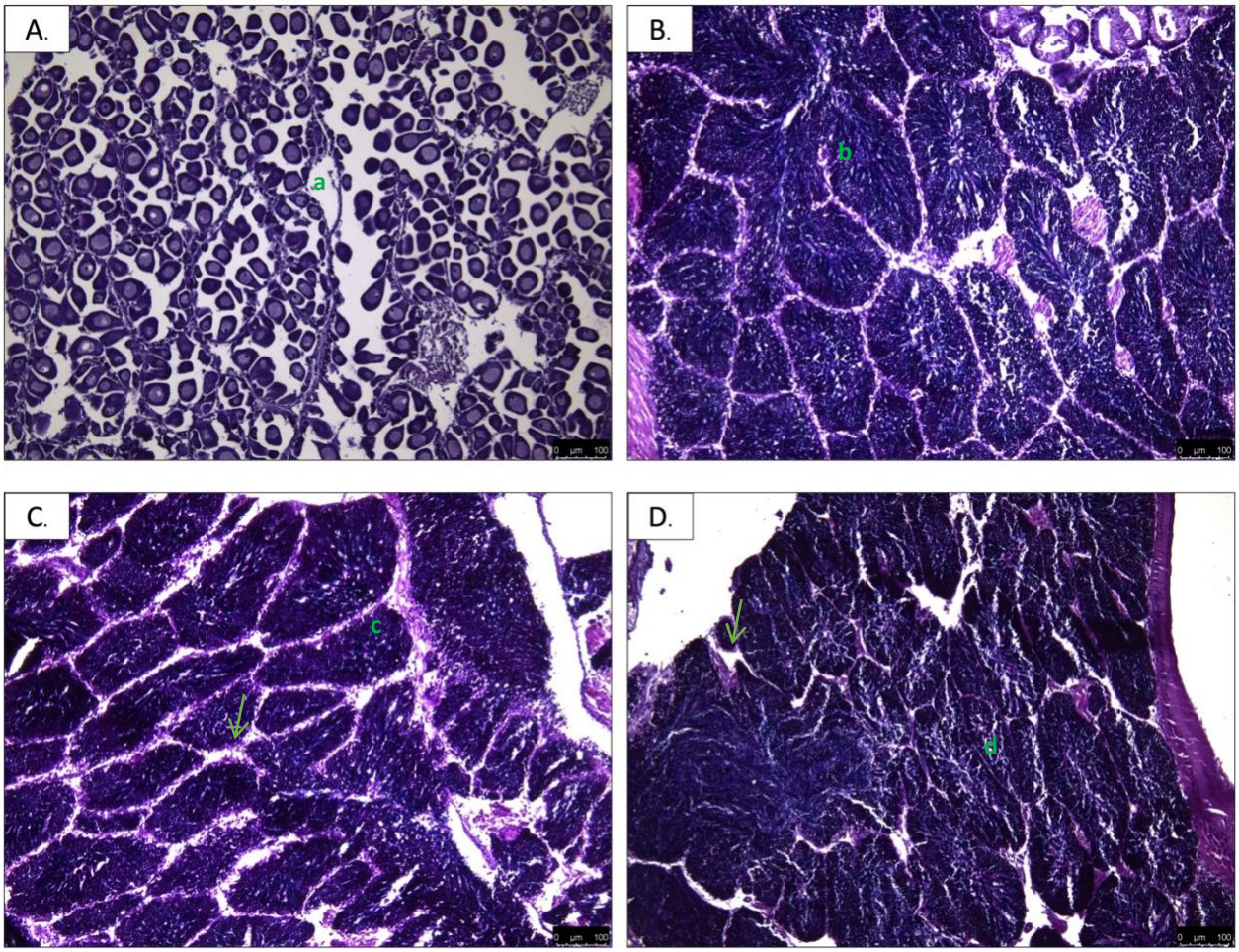

Figure 30 - Representative histological sections of male and female gonads of Ruditapes decussatus stained with haematoxylin and eosin. Stage IVA, Mature (full): 10x (A) female and (B) male. Gonad has gained maximum size. Follicle walls are extremely thin with highly coloured. ***(a)*** *Female follicles crowded with polygonal or hexagonal oocytes.* ***(b)*** *Male follicles packed to the periphery with spermatozoa. Stage IVB, Spawning: 10x (C) male.* ***(c)*** *Follicles of varying degrees of spawning are crowded by phagocytes. Stage IVC Spent: 10x (D) male* ***(d)*** *Follicles empty, retaining few residual germ cells. Arrows indicate free water - Scale bars: 100 µm*

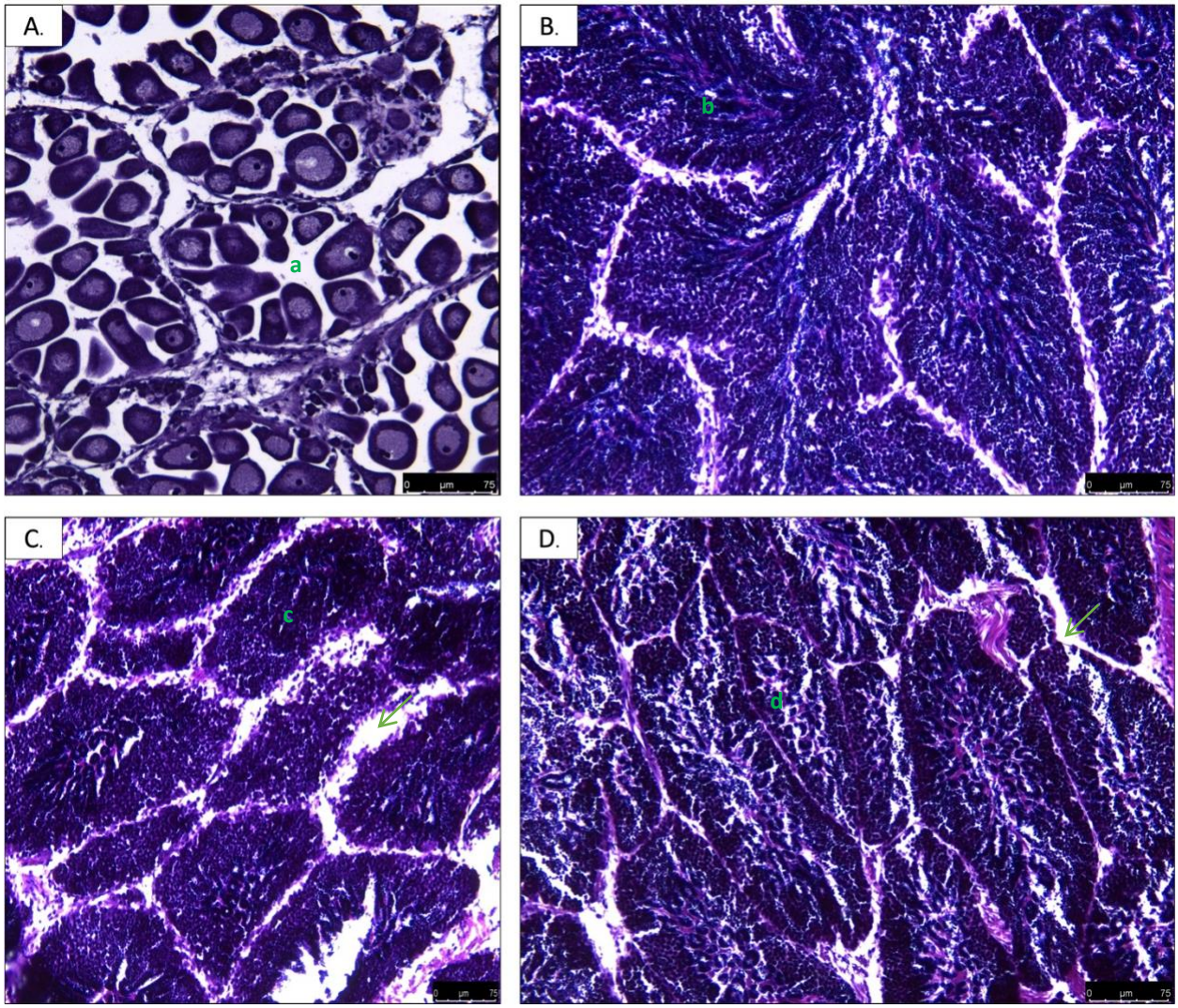

Figure 31 - Representative histological sections of male and female gonads of Ruditapes decussatus stained with haematoxylin and eosin. Stage IVA, Mature (full): 20x (A) female and (B) male. Gonad has gained maximum size. Follicle walls are extremely thin with highly coloured. ***(a)*** *Female follicles crowded with polygonal or hexagonal oocytes.* ***(b)*** *Male follicles packed to the periphery with spermatozoa. Stage IVB, Spawning: 20x (C) male.* ***(c)*** *Follicles of varying degrees of spawning are crowded by phagocytes. Stage IVC Spent: 20x (D) male* ***(d)*** *Follicles empty, retaining few residual germ cells. Arrows indicate free water - Scale bars: 75 µm.*

4.4 Age estimation

The left valves of 45 *R. decussatus* specimens (15 for each size class) were intended for age estimation analyses using the acetate peels technique described in materials and methods section. The age of many bivalve species can be determined by counting the growth rings on the shell surface that form as annual periodic event. However, this method may lead to discordant or incomplete age determination, as pointed out before. Therefore, the estimation of the age of the selected specimens was based on the examination of the internal dark growth lines (annuli), alternating with light growth-increment deposits. The results are summarised in Table 10, showing an estimated age ranging from 1 to 8 years out of the total number of samples tested.

	Min	Max	Mean ± SD	Class
AGE	1	4	3 ± 0,85	1
	3	7	4,53 ± 1	2
	4	8	5,7 ± 1,18	3

Table 10 - Estimated ages for each size class

The youngest specimens (estimated age = 1) belonged to Class 1, with a shell length of 17.5 mm, while the oldest was from Class 3 (estimated age = 8), with a shell length of 48 mm. Although an exponential trend line can be seen between shell length and estimated ages (Figure 32), it should be noted that in some cases smaller clams were found to be older than larger ones.

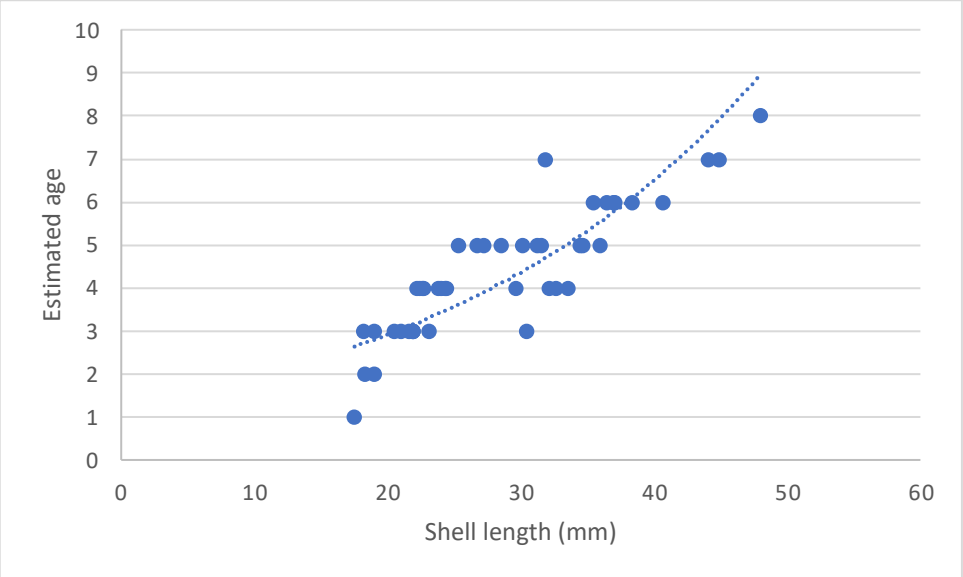

Figure 32 - Plotting the ratio between shell length and estimated age of the 45 specimens of R. decussatus analysed

The Figure 33 shows alternating annuli and clear growth bands on which the age determination was based. The images obtained using a light microscope equipped with a digital camera were taken in binary format and neutral colour to increase the contrast. The acetate peel replicas make the sequences of narrow and wide growth lines more clearly visible. The narrow lines correspond to the slow shell deposition that usually takes place during the winter, while the wider lines are formed during the summer months.

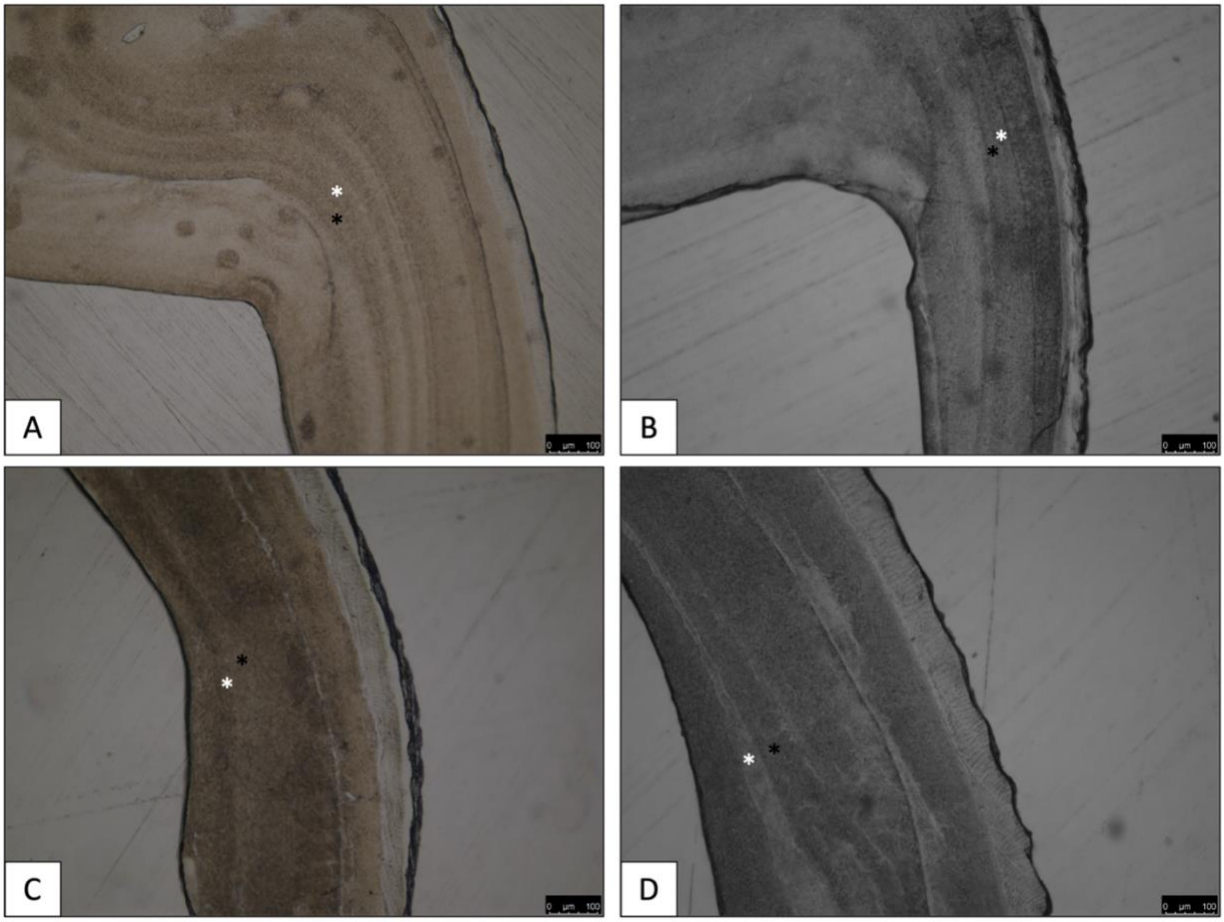

Figure 33- Acetate peel replicas used to estimate the age of R. decussatus specimens analysed. Pictures were taken in neutral colour (A,C) and in binary format (B,D) to increase the contrast between the dark annuli (black asterisk) and the light growth-increment deposits (white asterisk). Scale bars: 100 µm

4.5 DNA sequence amplification

The whole genomic DNA extracted from muscle tissues of specimens morphologically identified as *R. philippinarum* and *R. decussatus* was analysed by 2% agarose gel electrophoresis, and the results are shown in Figure 34.

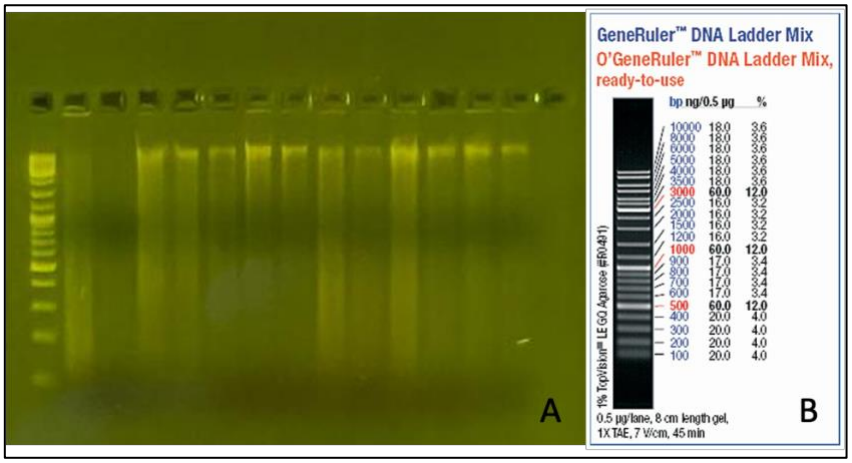

Figure 34 - Agarose gel electrophoresis of genomic DNA extracted from muscle tissue by Qiagen Blood and Tissue Kit. The whole genomic DNA obtained was analysed by 2% agarose gel electrophoresis (A); Nucleic acid molecular weight marker, GeneRuler DNA Ladder Mix (Thermo Fisher Scientific) (B

The PCR products obtained through the amplification of 16S mitochondrial DNA (mtDNA) region extracted were of 553 (*R. philippinarum*) and 522 bp (*R. decussatus*). Due to a difference of only 31 bp between these sequences, they were hardly discernible on the 2% agarose gel. The comparison between the extracts of the two species in shown in (Figure 35).

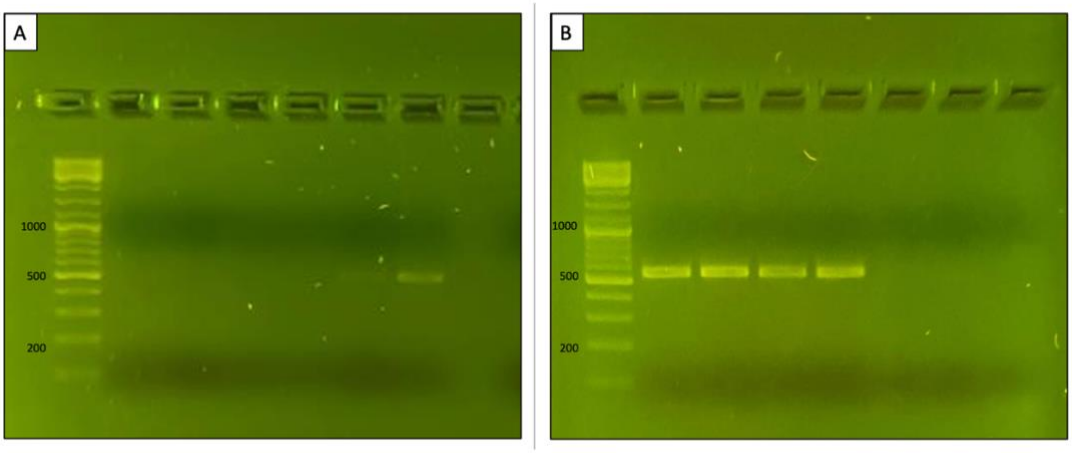

Figure 35 - Agarose gels (2%) showing the amplified PCR products of the 16S mitochondrial rDNA of R. decussatus (522 bp) (A) and R. philippinarum (553 bp) (B); Nucleic acid molecular weight marker, GeneRuler DNA Ladder Mix (Thermo Fisher Scientific)

After being purified, the PCR products were sent for sequencing. The results were first aligned and then analysed using the nucleotide BLAST search against the National Centre for Biotechnology Information (NCBI) to calculate the statistical significance of the match (Figure 36). As summarised in Table 11, the resulting sequences of DNA extracted from 3 specimens showed identities higher than 98% with the *R. philippinarum* 16S mtDNA sequences present in the NCBI database (accession code: HQ634142.1). The other 3 samples showed identities higher than 96% with the *R. decussatus* 16S mtDNA sequences in the same database (accession code: HQ634141.1), confirming the results of species determination based on the shape and arrangement of the siphons.

Specimen	Description	Species	Query cover	Identity	Accession
8	16S rRNA gene; mtDNA	*R. philippinarum*	93%	100%	HQ634142.1
60	16S rRNA gene; mtDNA	*R. philippinarum*	97%	98.98%	HQ634142.1
3	16S rRNA gene; mtDNA	*R. philippinarum*	100%	100%	HQ634142.1
21	16S rRNA gene; mtDNA	*R. decussatus*	95%	100%	HQ634141.1
28	16S rRNA gene; mtDNA	*R. decussatus*	90%	96.77%	HQ634141.1
32	16S rRNA gene; mtDNA	*R. decussatus*	92%	97.63%	HQ634141.1

Table 11 - Results of the aligned sequences analysed using the nucleotide BLAST search against the National Centre for Biotechnology Information (NCBI), showing high percentages of identity that confirmed the determination of species on a morphological basis

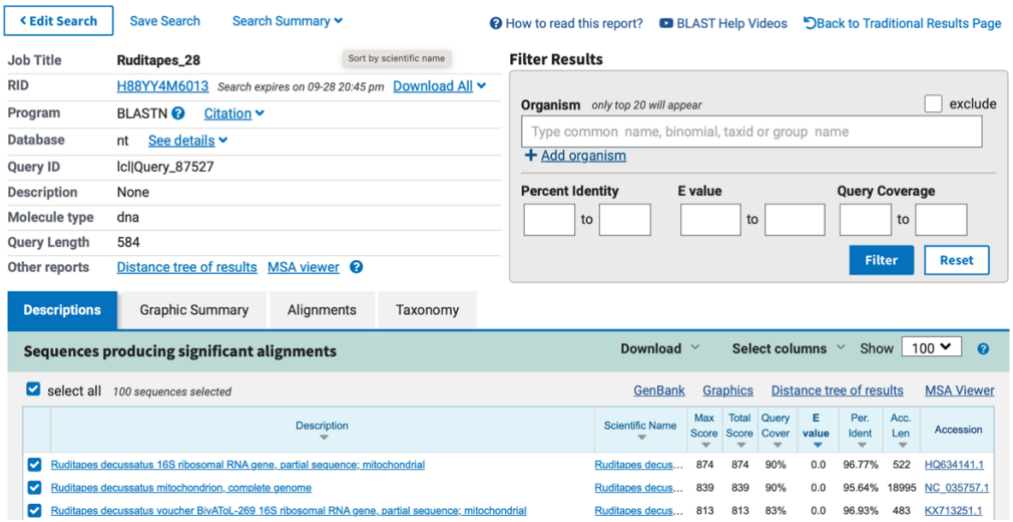

Figure 36 - Example of screen for displaying the results of the nucleotide BLAST search against the National Centre for Biotechnology Information (NCBI; https://blast.ncbi.nlm.nih.gov/Blast.cgi)

4.6 Description of plastic debris found in faeces

A total of 170 anthropogenic particles were detected in the faeces of 60 analysed specimens. In the Table 12 is reported the summary of items analysed for each size class, together with the mean weight of individuals who apparently had ingested plastics.

Classes	N. of specimens	Weight (g) Mean ± SD	N. of items found	Items/Individual Mean ± SD
1	20	0.76 ± 0.3	47	2.35 ± 1.92
2	20	3.6 ± 0.9	53	2.30 ± 1.87
3	20	8.3 ± 3.0	57	2.85 ± 2.80

Table 12 - Summary of items analysed for each size class

The airborne contamination was low, with 0.47 ± 0.66 items/filter (mean ± SD) detected in the analytical blanks compared with 2.47 ± 1.76 items/filter (mean ± SD) found in the collected clams' faeces. Significant differences of the abundance of anthropogenic debris were detected among the three size classes based on shell length. Specimens belonging to Class 3 showed the highest levels of contamination, with 2.85 ± 2.80 items/individual (mean ± SD). Bivalve molluscs from the other two size class showed similar abundance of plastic particles, with 2.30 ± 1.87 items/individual (mean ± SD) for Class 2 and 2.35 ± 1.92 items/individual (mean ± SD) for Class 1. All the plastic debris found in each size class were in the form of fibers and fragments. However, fibre was the predominant form, being about 84% of the total number of anthropogenic particles found in clam faeces. More specifically, the specimens from Class 1 were contaminated by 97.8% of fibers and 2.2% of fragments, while clams from Class 2 showed 82.7% of fibers and 17.3% of fragments. Regarding *R. decussatus* from Class 3, 94.7% of plastic debris found was in form of fibre and 5.3% in form of fragments (Figure 37).

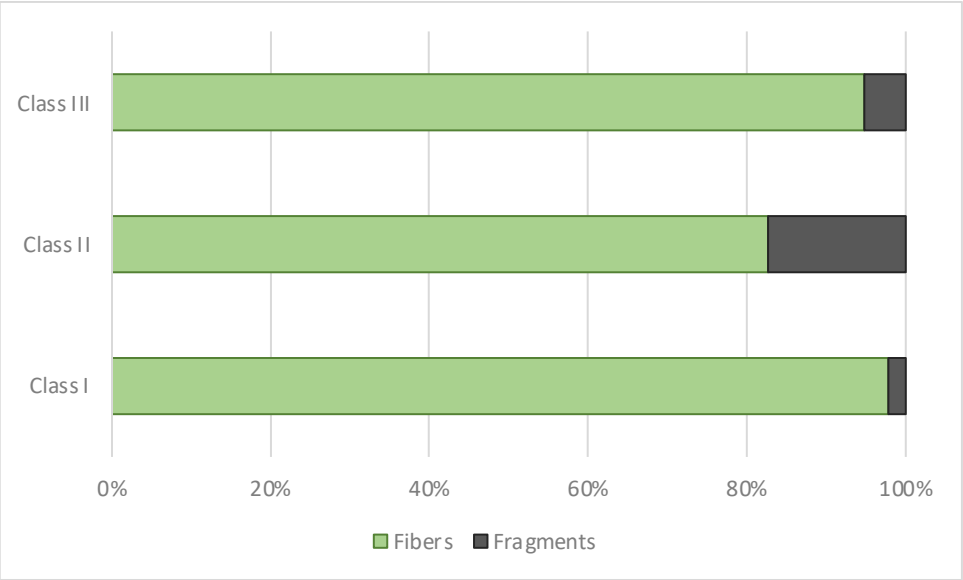

Figure 37 - Percentage of plastic debris in form of fibre and fragment found in the three size classes

The size of the fibers ranged from 0.1 to 5 mm, with the smallest mean size found in Class 3 (1.0 ± 1.0 mm; mean ± SD), followed by Class 2 (1.2 ± 1.0 mm; mean ± SD) and Class 1 (1.7 ± 1.3 mm; mean ± SD), as shown in Figure 38.

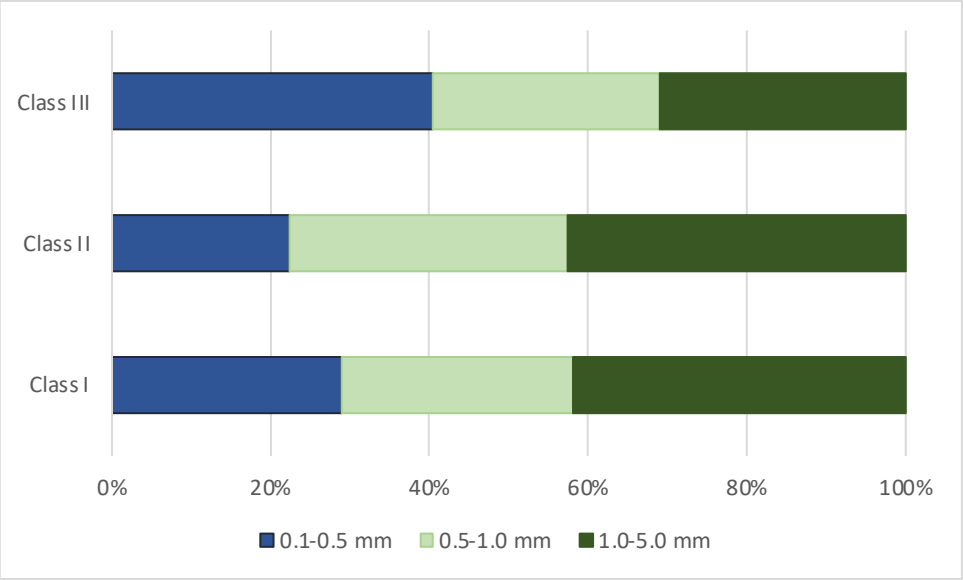

Figure 38 - Percentage of plastic debris found in the three size classes, classified according to size range

On the other hand, the mean size of fragments was smaller in Class 2 (0.135 ± 0.085 mm; mean ± SD) than in Class 3 (0.363 ± 0.195 mm; mean ± SD), while only one fragments was found among Class 1 specimens analysed, with size of 0.341 mm. All the anthropogenic debris collected were also classified according to colours. The most frequently documented in the three size classes

were white (35.26%) and blue (34.6%), followed by black (16%), transparent (10.9%), and purple (3.24 %) (Figure 39). Only blue, transparent, and white plastic particles were found among specimens belonging to Class 1. Some representative pictures of plastic debris of different size and colour found in clams faeces analysed are shown in Figure 40.

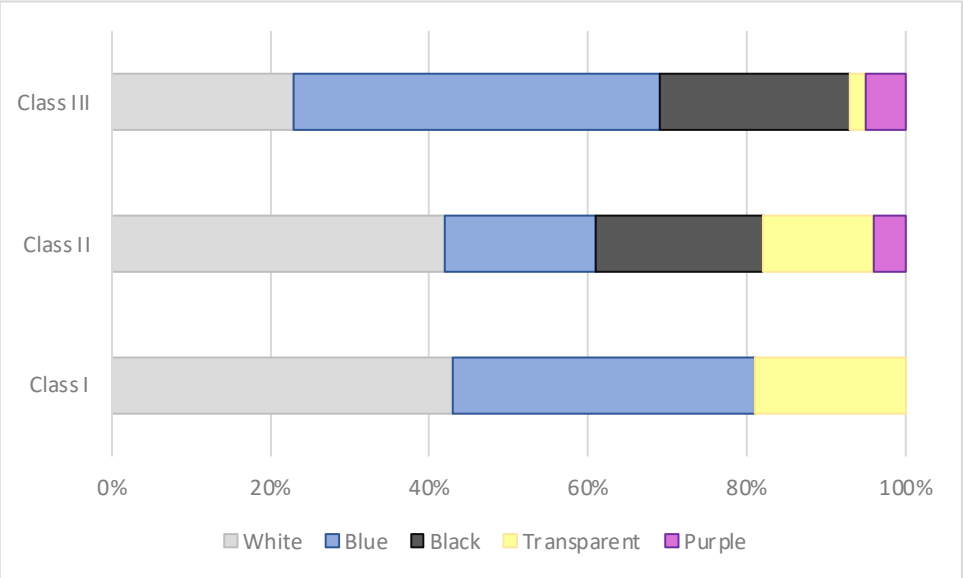

Figure 39 - Percentage of plastic debris found in the three size classes, classified according to colour

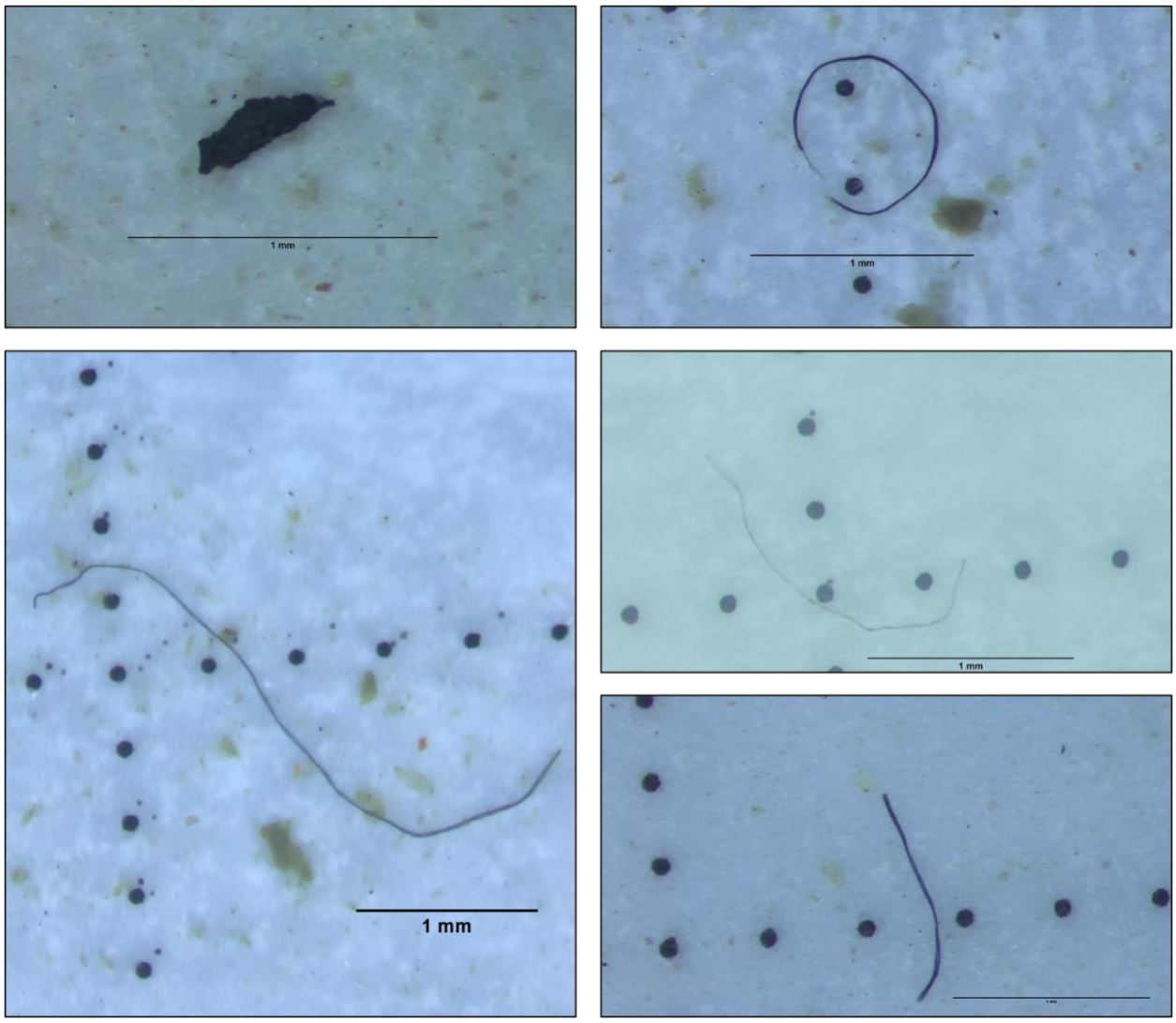

Figure 40 - Representative pictures of plastic debris of different form, size and colour found in clams faeces analysed. Scale bars: 1 mm

5. Discussion

5.1 The population of Ruditapes decussatus from Lake Faro (Messina – Italy)

In view of the ecological role and the high commercial interest, special attention has been paid to Veneridae in recent decades. It is now well known that bivalve molluscs belonging to this family can exhibit a wide morphological variation, which is usually closely related to their life cycle and several ecological aspects (Ghozzi et al., 2022). This phenotypic plasticity relatable to different environmental conditions has been widely reported for *Ruditapes spp.* (Watanabe, 2010; Caill-Milly et al., 2012; Arranz et al., 2023). In particular, many studies based on morphometric analysis have been conducted on natural population of *R. philippinarum* in their native environments such as Japan, as well as in several countries around the world where this species was introduced, including the Atlantic coast of Africa, the eastern Pacific, and the European shores (Fan et al., 2007; Huo et al., 2010; Caill-Milly et al., 2012; Nerlović et al., 2016). In contrast, there is limited literature available on the native European species *R. decussatus* (Amane et al., 2019; Ghozzi et al., 2022). Although some studies on the grooved carpet shell have been carried out with different approaches in Europe (Borsa & Millet, 1992; Delgado & Pérez-Camacho, 2005, 2007; Matias et al., 2013; Ghiselli et al., 2017; Machado et al., 2018), the research performed on the Italian coasts are still scarce. Moreover, to the best of our knowledge, no investigations of different biological and ecological aspects of this species has so far focused on a natural population living in Lake Faro of Messina (Italy). From this perspective, the results of this study constitute a solid data base for future research, undoubtedly needed to fully understand the dynamics and structure of the local population of *R. decussatus*. As previously pointed out, the main factor that appears to have a high influence on the population structure is recruitment. During the four seasons studied, this event occurred in a generalised way, although it showed greater influence in spring. This was the season during which the smallest individual of all those sampled was found (shell length = 10 mm), as well as the lowest mean shell length value recorded (25.03 mm). Moreover, the specimens belonging to Class 1 (shell length between 10 and 22.9 mm) showed a similar distribution pattern in all seasons (36% in both autumn and spring, about 32% in summer) except in winter (about 6%), suggesting that recruitment may extend into the autumn and summer seasons, probably depending on different environmental factors as temperature and salinity. The fact that individuals with a shell length of less than 23 mm accounted for approximately 30% of the total number of samples collected could be partially attributable to the sampling bias

favouring larger sizes. The most common fishing method of using a rake and/or a shovel to disturb the sediment, combined with the tendency of to target larger specimens, likely accounts for this distortion (Juanes et al., 2012). This circumstance rules out the chance of encountering recently settled recruits, which would typically lead to bimodal size frequency distribution in clam populations (Sejr et al., 2002; Dang et al., 2010). On the other hand, considering that the sampling methodologies adopted during the survey are very similar to the harvesting technique used by local shell fishermen, the strategy pursued may provide a more realistic overview of the native *R. decussatus* population living in the Faro Canal of the Capo Peloro Lagoon. The most abundant size class in all seasons ranged from 23 to 31.9 mm of shell length (Class 2), suggesting that the studied population of *R. decussatus* is relatively young. The dominance of this size class, which showed abundance rates of 61% in winter, 56% in spring, 51% in autumn and 44% in summer, could be related to the uncontrolled artisanal harvesting of larger specimens by locals. Specimens belonging to Class 3 (shell length between 32 and 48 mm) were in fact the least numerous, constituting only 20% of the total number of clams collected during the reporting period. However, natural limiting factors such as the presence of predators, low growth rates and massive mortality events related to environmental parameters might also be affecting to this lack of large individuals. The comparison of the main morphometric descriptors revealed significant differences in shell shape between specimens of different size classes, as well as between clams collected in different seasons. In the latter case, the comparison between winter and the other seasons showed greater significance for most of the variables analysed. Considering that temperature and food availability seems to be the main factors affecting growth rates and reproduction of bivalve molluscs (Urrutia et al., 1999), the significant differences found could be related to the natural metabolic slowdown due to lower temperatures. In general, bivalves are poikilothermic organisms, meaning they have limited ability to generate internal heat through metabolic processes (Huo et al., 2018). They manage to survive with relatively low energy expenditure compared to warm-blooded animals of similar size. When stressed, these molluscs employ valve closure as a strategy, conserving metabolic energy, which is effective under brief stressful situations (Verdelhos et al., 2015). However, considering the high thermal conductivity due to the chemical composition of the shell (calcium carbonate mainly in the form of aragonite), the extreme temperatures cannot be mitigated through valve closure (Gómez-Martínez et al., 2002). Temperatures out of the optimal range may thus seriously compromise the health status of these molluscs. The data here presented are in line with those reported by Urrutia et al. (1999),

concerning similar metabolism rates among different seasons. According to the morphometric measurements of specimens belonging to the different size classes, larger individuals had a more convex shell from a frontal view than individuals from other classes. Clams from Class 1 had a more curved valve dome form a ventral view, while *R. decussatus* specimens from Class 2 and 3 had a slender shell form a lateral view than those of Class 1. As many authors pointed out, the differences in shell shape could be related to the above-mentioned phenotypic plasticity affected by environmental conditions and ecological pressure (Watanabe, 2010). This aspect should be also considered for individuals of different sizes belonging to the same population, which may live buried in the sediment at different depths. In addition, the great positive influence of the Strait of Messina on the quality of adjacent transitional waters is another factor that must be considered in terms of temperature, salinity, and food availability. Laudien et al. (2003) studied this morphological variability among four population of the surf clam *Donax serra* in South Africa. The comparison of the main morphometric descriptors revealed that clams living in cold water were significantly flatter, rounder and less wedge-shaped to increased stability in the subtidal habitats while specimens from warm water were more elongated and wedge shaped, allowing a faster burrowing. Moreover, a thicker, rounder, and denser shell may ensure a more effective retention of water, as well as a faster and deeper burrowing. Such characteristics can be a valuable defence tool against potential predators, definitely present in the study area (Sanfilippo et al., 2022).

5.2 Shape analysis of shells from different size classes

The extensive literature study conducted for this investigation revealed that there are not many studies focusing on the analysis of the shell shape of bivalves. Most of them are not very recent and are based on the elliptic Fourier analysis of shell outlines coordinates from digital images (Dommergues et al., 2003; Haines & Crampton, 2003). In recent decades, this method applied to the morphometric approach has mainly been used to discriminate between geographical groups of the same commercial clam species (Palmer et al., 2004), as well as for the evaluation of interspecific differences between congeneric bivalves (Rufino et al., 2006), and for the identification of ecophenotypic trends within different freshwater mussel species (Zieritz & Aldridge, 2009). Regarding the genus *Ruditapes*, the elliptic Fourier analysis has been performed in some studies focused on the comparison between sympatric populations of *R. decussatus* and *R. philippinarum* located in Adriatic lagoons in the north-eastern part of Italy (Costa, Menesatti,

et al., 2008), as well as in studies aimed to evaluate the overall shape differences in Manila clams and grooved carpet shell clams from different populations, related to the geographical and genetic distances (Costa, Aguzzi, et al., 2008). The success of this analytical method is due to its numerous advantages over other methods of Fourier shape analysis, which include data points on the outline that do not have to be equidistant, the outline centroid that do not have to be biologically homologous or mathematically determined, and the potential application of the method to very complex curves (Crampton, 2007). Despite its validity and widespread use, the elliptic Fourier analysis has always been performed so far using different dedicated software for each step. Hence the idea of using shapeR, an open access package that runs on R software, to perform the shape analysis based on the outlines of the collected shells previously photographed and converted in binary format. To the best of our knowledge, this was the first time a similar approach and methodology was adopted for this type of analysis on bivalve molluscs. Although the above-mentioned package was specially designed to study otolith shape variation among teleost populations or species, it can prove useful in the study of any two-dimensional object, as pointed out by the authors (Libungan & Pálsson, 2015). Once the outlines of each valve have been detected through specific functions, both Wavelet and Fourier coefficients can be extracted and adjusted using the same package to define the allometric relationships between specimen measurements and valve shape, linking them to an Excel file containing information on samples. All these steps are aimed at obtaining comparison plots of mean valve shapes, as well as the estimation of the quality of Wavelet and Fourier reconstruction. As an additional check, mean and standard deviation of calculated coefficients can be plotted to assess how the variation of coefficients depends on the position along the outline. In addition, several statistical analyses can be performed using shapeR package. In this study, the shape analysis was performed on both right and left valve of each collected specimen, to evaluate the existence of any asymmetries and/or interclass differences. The results revealed significant differences in all the size class analysed, confirmed by the analyses of variance performed on the calculated coefficients ($p < 0.05$). Further statistical analyses on the outputs returned by the R packages were carried out using other specific software (*i.e.* Past). More specifically, the Linear Discriminant Analysis (LDA) performed on the standardised Fourier coefficients confirmed the differences previously detected, showing that the outlines of the right valves of specimens from Class 1 were moderately separated from those extrapolated for the other two classes. Similarly, the contours of the left valves of Class 3 individuals appeared more distinctly separated from those of the other size

classes. Apart from the predictable differences in shell shape between individuals of the three size classes, attributable to the growth patterns discussed above, the slight differences found between the right and left valve certainly deserve special attention. As already reported by other authors on the shape of the scallop shell (Sherratt et al., 2017), this could be related to an ecomorph undergoing a different selective pressure from the environment. It is believed that the two valves of bivalve molluscs originated from a single-valved ancestral condition (S. Smith et al., 2013), wherein the shell field elongated dorso-ventrally and later folded along the mid-dorsal region (Stanley, 1970). This implies that the two valves are closely linked in development and follow the same gene regulatory pathways (Jacobs et al., 2000). However, based on the previously mentioned findings about scallops, the slight asymmetry detected between left and right valve of *R. decussatus* specimens could be closely related to their ecomorph type. This pattern can be seen as a representation of how various ecomorphs move, considering that the more sedentary bivalve molluscs are generally characterised by a greater asymmetry in shell shape (Sherratt et al., 2017).

5.3 Gonadal development, ageing and sex ratio

While several studies have explored the gametogenic cycle of *R. decussatus* in their natural habitat (Camacho et al., 2003; Delgado & Pérez-Camacho, 2005, 2007; Ketata et al., 2007), many of them are based on experimental trials conducted in laboratory settings. This approach allows for a faster and more controllable conditioning of molluscs, regardless of the natural fluctuations in biotic and abiotic environmental variables that can affect the species' biological characteristics. As already pointed out above, the reproductive cycle of bivalves is significantly affected by both internal and external factors, with temperature being regarded as one of the main factors regulating the emission processes of gametes (Urrutia et al., 1999). According to the results of various laboratory investigations, even slight rises in water temperature can trigger factors for spawning Gosling (2015). Concurrently, other environmental factors like salinity, nutrients concentration and chlorophyll-a must be considered, as they govern the entire life cycle of these molluscs and can substantially influence the consumption processes and energy acquisition (Rodríguez-Moscoso & Arnaiz, 1998; Ojea et al., 2004). The biotope in the Capo Peloro lagoon where the survey was carried out shows all the typical characteristics of a transitional environment, with widely varying water temperature and salinity. This is mainly due to the

presence of several canals that allows the communication with the surrounding sea, being essential for small exchanges of water that occur daily, following the tidal pattern (Manganaro et al., 2011). For that reason, this transitional environment is particularly relevant from an ecological point of view, especially because of the strong correlation with the Strait of Messina, globally known for its peculiar habitats (Butman & Raymond, 2011; Capillo et al., 2018; Savoca et al., 2020; D'Iglio et al., 2023). However, the salinity of lakes waters does not exclusively depend on the connections with the sea, being the result of the interaction between rainwater conveyed in underground aquifers mainly fed by the hills, and marine waters (Manganaro et al., 2011). In our latitudes, both water temperature and salinity follow the usual seasonal pattern, with higher values in summer and lower levels in winter. However, during autumn and spring, the temperature undergoes gradual changes in response to the typical climate shifts of these seasons, whereas salinity levels fluctuate rapidly due to the above-described environmental characteristics. It is widely known that water nutrient concentrations are linked to the growth of phytoplankton, thereby increasing the food supply for filter-feeding organisms (Brown & Hartwick, 1988). However, in cases of significant and constant water exchange between a lagoon and the adjacent sea, daily nutrient fluctuations can arise, affecting the local Bivalve population (Saxby et al., 2002). Regarding the sex ratio of the studied *R. decussatus* population from Capo Peloro Lagoon, the males/females proportion calculated according to the presence of spermatozoa and oocytes did not deviate significantly from the expected proportion of 1:1 (Herrmann et al., 2009). Among all clams analysed, 54% were identified as males, and 46% as females. In addition, no cases of hermaphroditism were documented. Considering the different seasons during the reporting period, males represented about 53% and females about 47% in autumn. A similar trend was observed in summer (about 55% males and 45% females). On the other hand, opposite sex ratios were documented during winter and spring, with 17% males and 83% females and 86% of males and 14% of female, respectively. These different sex ratios could be due to the higher proportion of indeterminate specimens during the spring and especially winter months (Delgado & Pérez-Camacho, 2007). Concerning gonadal development, approximately 12% of the clams harvested during the autumn period were assigned to stage I, about 65% to stage II, and 23% to stage III. In winter, only the initial stages of gonadal development were documented, with 33% of *R. decussatus* belonging to stage I and 67% to stage II. Specimens collected in autumn and spring showed the same stages of sexual maturation with different percentages, being about 29% individuals classified as stage I, 14% as stage II, and 57%

as stage III. During the summer months, which coincide with the peak of breeding season of this species, all bivalves collected were found to be in the ripening, releasing and resting phase. About 43% clams analysed were assigned to stage II, 27% to stage III, 17% to stage IV A, 6% to stage IVB, and 7% to stage IV C. Once again, according to the results here presented, the water temperature seems to play an essential role in gametogenesis and spawning. Most clams classified as belonging to stage I (with no distinguishable gametes) were found during winter and early spring, probably due to the cold temperature and the resulting metabolic slowdown (Huo et al., 2018). From the late spring onwards, as temperatures rose and the breeding season began, maturing stages were mainly documented, while sexually mature individuals were only found during the summer sampling season. In fact, consistent with previous studies on *R. decussatus* in temperate regions (Breber, 1980; P. Beninger & Lucas, 1984), spawning was observed during late summer when temperature values were higher. On the other hand, early stages of gonadal development were mainly documented during late autumn and winter, coinciding with a gradual decrease in water temperature. As environmental conditions improved during the spring, gametogenesis began, reaching the mature gonadal stage the following summer. The reproductive pattern described here is in line with what has been reported in several studies on bivalve molluscs in the wild (Rodríguez-Moscoso & Arnaiz, 1998; Ojea et al., 2004; Saba, 2011), with most clams belonging to Veneridae family appearing to spawn in summer (Shafee & Daoudi, 2008). Furthermore, the influence of temperature on the reproductive behaviour of the grooved carpet shell clam has been confirmed by laboratory experiments that clearly indicate a direct relationship between gonadal development rate and temperature increase (Delgado & Pérez-Camacho, 2007). Age estimation is an extremely important component of all the studies focused on population dynamics, with no exception for bivalve molluscs. This biological aspect is essential for proper management of clam breeding, avoiding the depletion of a stock or any damage to the population (Bargione et al., 2020). In this study, the acetate peel technique was used for shell growth analysis of *R. decussatus,* following the protocol proposed by Ropes (1987). The examination of the dark growth lines within the shell called “annuli”, alternating with light growth-increment deposits, represents a well-preserved record of growth, and the preparation of acetate peels of sectioned shells can better expose these internal depositional features. The validity of this method has been confirmed by several authors who have used it to determine the age of various bivalve species (Ramón & Richardson, 1992; Moura et al., 2013), including *Ruditapes sp.* (Moura et al., 2017). Considering that juvenile shells required treatments which

involved a more delicate grinding and polishing phases, only specimens with a shell length of less than 17 mm were selected for age estimation of *R. decussatus* from the Capo Peloro Lagoon. A representative number of left valves (*n=45*) were randomly selected for each size class, as they have more prominent teeth in the hinge which make age estimation easier and more reliable. The results showed an estimated age ranging from 1 to 8 years out of the total number of samples tested. The youngest specimens (estimated age = 1) belonged to Class 1, with a shell length of 17.5 mm, while the oldest was from Class 3 (estimated age = 8), with a shell length of 48 mm. Although an exponential trend line can be seen between shell length and estimated ages, it should be noted that in some cases smaller clams were found to be older than larger ones. The acetate sheets were again confirmed as a valuable tool for bivalve age estimation, detecting both the external composite prismatic layer and the internal nacreous layer. Notably, the outer prismatic layer exhibited clear growth patterns. In all the samples analysed, areas of rapid growth were evident as broad transparent sections, while slow growth was identifiable by narrow dark lines, sometimes accompanied by a crevice on the shell surface. Anomalies in growth, such as false rings, were noticeable as abrupt disruptions in the natural growth pattern and could also feature a surface crevice (Moura et al., 2017). It should be noted that, although the light microscope with a built-in digital camera can be used effectively to analyse the shell sections, the phase-contrast microscope could provide better resolution, thus facilitating the identification of the growth increment. Moreover, the use of specific dyes for carbonate structures such as the Alizarin Red S (Bernar et al., 2022), could certainly make age reading easier.

6. Conclusions

Whereas, to the best of our knowledge, this is the first study with a multidisciplinary approach focusing on an autochthonous population of *Ruditapes decussatus* located in the lagoon of Capo Peloro, the aim was to provide a solid baseline useful for future investigations, undoubtedly necessary to better understand several biological and ecological aspect of this historically important fishery resource. Relying on the results achieved so far, it is possible to state that the native grooved carpet shell clams showed robust reproductive capabilities in the studied area. The indigenous population seems to be well adapted to the environmental conditions prevalent in this transitional habitat, particularly the abrupt fluctuations in key external factors like temperature and salinity due to the seasons and constant communication with the Strait of Messina. Consequently, these bivalves can consistently undergo their gametogenic cycle, leading to a steady recruitment of young individuals. Based on the findings presented, the relatively young population analysed is in an overall good physiological condition, especially in terms of its resilience to environmental variations and regularity in gonadal maturation periods. On the other hand, the scarce presence of individuals of commercial size suggests a lack of control over artisanal and illegal harvesting practiced by locals in this area. In this light, greater awareness, and consciousness on the part of the entire community would be desirable, being indispensables for the proper management of this important resource for the territory. Although clam farming is a traditional activity that is fully part of the heritage of the city of Messina, today all efforts are mainly focused on the distribution of imported products. It appears that there is currently no effective policy for the management of local resources, probably because they are not considered profitable enough. The general tendency seems to be to consider core operations, such as sowing or seed transfer, site cleaning, monitoring and surveillance, as ancillary activities of little importance to the economy of the sector. It is believed that a closer cooperation between local shellfish farmers, the region of Sicily and the world of scientific research could lead to the development of the expertise needed to preserve and fully reintroduce the native grooved carpet shell clam into the national shellfish farming scene.

References

Abruzzese, D., & Genovese, S. (1952). Osservazioni geomorfologiche e fisico-chimiche sui laghi di Ganzirri e Faro. *Bollettino Pesca, Piscicoltura e Idrobiologia 7*, 3–20.

Addadi, L., Joester, D., Nudelman, F., & Weiner, S. (2006). Mollusk shell formation: a source of new concepts for understanding biomineralization processes. *Chemistry–A European Journal*, *12*(4), 980–987.

Albano, M., Panarello, G., di Paola, D., D'Angelo, G., Granata, A., Savoca, S., & Capillo, G. (2021). The mauve stinger Pelagia noctiluca (Cnidaria, Scyphozoa) plastics contamination, the Strait of Messina case. *International Journal of Environmental Studies*, *78*(6), 977–982. https://doi.org/10.1080/00207233.2021.1893489

Alonzo, V., Bruni, V., Lo Curto, R., & Maugeri, T. (1979). Occurrence of Vibrio parahaemolyticus and Vibrio alginolyticus in the brackish lake of Ganzirri. *Rapp. Comm. Int. Mer Médit., 25/26(6).*

Alonzo, V., Bruni, V., Lo Curto, R., Maugeri, T. L., Russo, D. I., & Scoglio, M. E. (1981). Occurrence of halophilic vibrios in mussels in a brackish lake. *Revue Internationale d'Oceanographie Medicale 63/64*, 1–9.

Amane, Z., Tazi, L., Idhalla, M., & Chlaida, M. (2019). Morphometric analysis of European clam Ruditapes decussatus in Morocco. *AACL Bioflux*, *12*, 1623–1634.

Antonini, C., Donadelli, V., Finocchiaro, G., Giovanardi, O., Marino, G., Raicevich, S., & Tomassetti, P. (n.d.). *Coordinatore statistico: Luca SEGAZZI 1 ISPRA*. www.registro.asa.it.

Antonioli, F., Pra, G., Segre, A. G., & Labini, S. (2004). New data on Late Holocene uplift rates in the Messina Strait area, Italy. *Quaternaria Nova*, *8*, 45–67.

Aricò, N. (1999). *Illimite Peloro. Interpretazioni del confine terracqueo* (Mesogea).

Arranz, K., Urrutxurtu, I., Martínez-Patiño, D., & Navarro, E. (2023). Growth and Physiological Performance in Growth Phenotypes of the Carpet Shell Clam (Ruditapes decussatus) Fed Diets of Variable Lipid/Carbohydrate Ratios. *Aquaculture Nutrition*, *2023*, 1–13. https://doi.org/10.1155/2023/3622475

Azevedo, C. (1989). Fine structure of Perkinsus atlanticus n. sp.(Apicomplexa, Perkinsea) parasite of the clam Ruditapes decussatus from Portugal. *The Journal of Parasitology*, 627–635.

Bald, Borja, Murua, & Muxica. (2003). Ensayo del effecto de la alteracion del substrato en la explotacion de ricursos bivalvos. In *Inf téc. Gov Vasco* (Vol. 98, pp. 1–59).

Barber, B. J., & Blake, N. J. (2006). Reproductive physiology. *Developments in Aquaculture and Fisheries Science*, *35*, 357–416.

Barber, V. C. (1968). The structure of mollusc statocysts, with particular reference to cephalopods. *Symp. Zool. Soc. Lond.*, 37–62.

Bargione, G., Vasapollo, C., Donato, F., Virgili, M., Petetta, A., & Lucchetti, A. (2020). Age and Growth of Striped Venus Clam Chamelea gallina (Linnaeus, 1758) in the Mid-Western Adriatic Sea: A Comparison of Three Laboratory Techniques. *Frontiers in Marine Science*, *7*, 582703. https://doi.org/10.3389/fmars.2020.582703

Barrier P. (1995). *The Straits of Messina during Pliocene and Pleistocene times (Italy)*. 71–81.

Bayne, B. L. (1971). Some morphological changes that occur at the metamorphosis of the larvae of Mytilus edulis. *The Fourth European Marine Biology Symposium*, 259–280.

Bayne, B. L., Thompson, R. J., & Widdows, J. (1976). Physiology I. In B. L. Bayne (Ed.), *Marine Mussels: Their Ecology and Physiology* (pp. 121–206). Cambridge University Press.

Bayne, B. L., Widdows, J., & Thompson, R. J. (1976). Physiology II. In B. L. Bayne (Ed.), *Marine Mussels: Their Ecology and Physiology* (pp. 207–260). Cambridge University Press.

Beninger, P. G., & Le Pennec, M. (1991). Functional anatomy of scallops. *Scallop: Biology, Ecology and Aquaculture*, 133–223.

Beninger, P., & Lucas, A. (1984). Seasonal variations in condition, reproductive activity, and gross biochemical composition of two species of adult clam reared in a common habitat: Tapes decussatus L. (Jeffreys) and Tapes philippinarum (Adams & Reeve). *Journal of Experimental Marine Biology and Ecology*, *79*, 19–37. https://doi.org/10.1016/0022-0981(84)90028-5

Bergamasco, A., Azzaro di Rosamarina, M., Giuseppa, P., Giuseppa, C., Sanfilippo, M., & Maugeri, T. (2005). Ganzirri Lake, north-eastern Sicily. *Loicz Report and Studies*, 103–110.

Bernar, A., Gebetsberger, J., Bauer, M., Streif, W., & Schirmer, M. (2022). Optimization of the Alizarin Red S Assay by Enhancing Mineralization of Osteoblasts. *International Journal of Molecular Sciences*, *24*, 723. https://doi.org/10.3390/ijms24010723

Bevelander, G., & Nakahara, H. (1969). An electron microscope study of the formation of the nacreous layer in the shell of certain bivalve molluscs. *Calcified Tissue Research*, *3*, 84–92.

Biddittu, I., Laura, B., & Riccobono, F. (1979). Eneolitico di facies Piano Conte a Ganzirri (Messina). *Sicilia Archeologica*, *12*, 40–87.

Boldina-Cosqueric, I., Amiard, J.-C., Amiard-Triquet, C., Dedourge-Geffard, O., Métais, I., Mouneyrac, C., Moutel, B., & Berthet, B. (2010). Biochemical, physiological and behavioural markers in the endobenthic bivalve Scrobicularia plana as tools for the assessment of estuarine sediment quality. *Ecotoxicology and Environmental Safety*, *73*(7), 1733–1741.

Bonnard, M., Romeo, M., & Amiard-Triquet, C. (2009). Effects of copper on the burrowing behavior of estuarine and coastal invertebrates, the polychaete Nereis diversicolor and the bivalve Scrobicularia plana. *Human and Ecological Risk Assessment*, *15*(1), 11–26.

Borja, Bald, & Rodríguez. (2007). Proyecto piloto de ensayo de siembra de almeja fina (Ruditapes Decussatus) en el estuario de Plentzia. In *Inf téc. Gov. Vasco* (Vol. 109, pp. 1–72).

Borsa, P., & Millet, B. (1992). Recruitment of the clam Ruditapes decussatus in the Lagoon of Thau, mediterranean. *Estuarine, Coastal and Shelf Science*, *35*(3), 289–300. https://doi.org/https://doi.org/10.1016/S0272-7714(05)80049-6

Bottari, A., Bottari, C., Carveni, P., Giacobbe, S., & Spanò, N. (2005). Genesis and geomorphologic and ecological evolution of the Ganzirri salt marsh (Messina, Italy). *Quaternary International*, *140–141*, 150–158. https://doi.org/10.1016/j.quaint.2005.07.001

Bottari, C., & Carveni, P. (2009). Archaeological and historiographical implications of recent uplift of the Peloro Peninsula, NE Sicily. *Quaternary Research*, *72*(1), 38–46. https://doi.org/10.1016/j.yqres.2009.03.004

Breber P. (1980). Annual gonadal cycle in the carpet shell clam Venerupis decussata in Venice lagoon, Italy. *Proceedings of the National Shellfisheries Association, 70(1)*, 31–35.

Breber, P. (1980). Annual gonadal cycle in the carpet-shell clam Venerupis decussata in Venice Lagoon, Italy. *Proceedings of the National Shellfisheries Association*, *70*, 31–35.

Breber P. (1985a). L'introduzione e l'allevamento in Italia dell'arsella del Pacifico Tapes semidecussatus Reeve (Bivalvia; Veneridae). *Oebalia*, *11(2)*, 675–680.

Breber P. (1985b). On growing of the carpet-shell clam (Tapes decussatus L.): two years experiencein Venice lagoon. *Aquacolture*, *44*, 51–56.

Brian, J. I., & Aldridge, D. C. (2020). An efficient photograph-based quantitative method for assessing castrating trematode parasites in bivalve molluscs. *Parasitology*, *147*(12), 1375–1380.

Brown, J. R., & Hartwick, E. B. (1988). Influences of temperature, salinity and available food upon suspended culture of the Pacific oyster, Crassostrea gigas: II. Condition index and survival. *Aquaculture*, *70*(3), 253–267. https://doi.org/https://doi.org/10.1016/0044-8486(88)90100-7

Buceti, G. (2004). *Gialò. I misteri del Peloro* (A. Sfameni, Ed.).

Butman, D., & Raymond, P. A. (2011). Significant efflux of carbon dioxide from streams and rivers in the United States. *Nature Geoscience*, *4*(12), 839–842. https://doi.org/10.1038/ngeo1294

Caill-Milly, N., Bru, N., Mahé, K., Borie, C., & D'Amico, F. (2012). Shell Shape Analysis and Spatial Allometry Patterns of Manila Clam (*Ruditapes philippinarum*) in a Mesotidal Coastal Lagoon. *Journal of Marine Biology*, *2012*, 281206. https://doi.org/10.1155/2012/281206

Camacho, A., Delgado, M., Fernández-Reiriz, M.-J., & Labarta, U. (2003). Energy balance, gonad development and biochemical composition in the clam Ruditapes decussatus. *Marine Ecology-Progress Series - MAR ECOL-PROGR SER*, *258*, 133–145. https://doi.org/10.3354/meps258133

Cannas, A. (2010). *Dinamica di popolazione di Ruditapes decussatus (L) e insediamento di Ruditapes philippinarum (Adams & Reeve) in Sardegna (Italia)* [Doctoral thesis]. Università degli Studi di Cagliari.

Capillo, G., Panarello, G., Savoca, S., Sanfilippo, M., Albano, M., Volsi, R. L., Consolo, G., & Spanò, N. (2018). Intertidal ponds of messina's beachrock faunal assemblage, evaluation of ecosystem dynamics and communities' interactions. *AAPP Atti Della Accademia Peloritana Dei Pericolanti, Classe Di Scienze Fisiche, Matematiche e Naturali*, *96*, A41–A416. https://doi.org/10.1478/AAPP.96S3A4

Carazzi, D. (1897). *L'ostricoltura e la mitilicoltura nello stagno di Faro* (Hoepli Ulrico, Ed.). Libraio della Real Casa Milano.

Caselli, L., & Borzì, L. (1901). Note e proposte per il miglioramento igienico ed agricolo industriale nei laghi del Faro (Messina). *Ufficio Tecnico Municipio Di Messina. Tip. De Francesco, Messina*.

Cavaliere, A. (1963). Biologia ed ecologia della flora dei laghi di Ganzirri e Faro, sua sistematica e distribuzione stagionale. *Bollettino Pesca, Piscicoltura e Idrobiologia, 18*, 171–186.

Cesari, P., & Pellizzato, M. (1990). Biologia di Tapes philippinarum. In *Tapes philippinarum Biologia e Sperimentazione* (pp. 21–46). Ente Sviluppo Agricolo Veneto (E.S.A.V.).

Chi, H., Pan, X., & Zhang, G. (2023). Structure and function of the periostracum in the bivalve Perna viridis. *Micron*, *169*, 103458. https://doi.org/https://doi.org/10.1016/j.micron.2023.103458

Chillemi, F. (1995). Capo Peloro e la spiaggia di Tono. In In Edas (Ed.), *I Casali di Messina. Strutture urbane e patrimonio artistico* (pp. 63–68).

Cho, Y.-G., Kang, H.-S., Le, C. T., Kwon, M. G., Jang, M.-S., & Choi, K.-S. (2020). Molecular characterization of Urosporidium tapetis sp. nov., a haplosporidian hyperparasite infecting metacercariae of Parvatrema duboisi (Dollfus 1923), a trematode parasite of Manila clam Ruditapes philippinarum on the west coast of Korea. *Journal of Invertebrate Pathology*, *175*, 107454.

Ciaccio, C. (1983). La salvaguardia dei laghi di Ganzirri e Faro. *Atti Del Convegno Sul Tema: La Protezione Dei Laghi e Delle Zone Umide in Italia. Vol. XXXIII*, 395–403.

Cortese, G., Pulicanò, G., Manganaro, A., Potoschi, A., Giacobbe, S., Giacobbe, M. G., Gangemi, E., Sanfilippo, M., & Spanò, N. (2000). Fluttuazioni ed anomalie abiotiche e biotiche nei Pantani di Capo Peloro. *Atti 2° Congresso Nazionale Delle Scienze Del Mare (CoNISMa)*, 167–168.

Costa, C., Aguzzi, J., Menesatti, P., Antonucci, F., Rimatori, V., & Mattoccia, M. (2008). Shape analysis of different populations of clams in relation to their geographical structure. *Journal of Zoology*, *276*, 71–80. https://doi.org/10.1111/j.1469-7998.2008.00469.x

Costa, C., Menesatti, P., Aguzzi, J., D'Andrea, S., Antonucci, F., Rimatori, V., Pallottino, F., & Mattoccia, M. (2008). External Shape Differences between Sympatric Populations of Commercial Clams Tapes decussatus and T. philippinarum. *Food and Bioprocess Technology*, *3*, 43–48. https://doi.org/10.1007/s11947-008-0068-8

CRAMPTON, J. (2007). Elliptic Fourier shape analysis of fossil bivalves: Some practical considerations. *Lethaia*, *28*, 179–186. https://doi.org/10.1111/j.1502-3931.1995.tb01611.x

Crisafi, P. (1954). Un anno di ricerche fisico-chimiche continuative sui pantani di Ganzirri e Faro. *Bollettino Pesca, Piscicoltura e Idrobiologia, 9*, 5–31.

Dang, C., Xavier, D., Meriame, G., Paroissin, C., Bru, N., & Caill-Milly, N. (2010). The Manila clam population in Arcachon Bay (SW France): Can it be kept sustainable? *Journal Of Sea Research (1385-1101) (Elsevier Science Bv), 2010-02 , Vol. 63 , N. 2 , P. 108-118*, *63*. https://doi.org/10.1016/j.seares.2009.11.003

De Vico, G., & Carella, F. (2012). *Argomenti di Patologia Comparata dei Molluschi-Aspetti ecologoci e sanitari.* LOFFREDO EDITORE.

Delgado, M., & Pérez-Camacho, A. (2005). Histological study of the gonadal development of Ruditapes decussatus (L.)(Mollusca: Bivalvia) and its relationship with available food. *Scientia Marina*, *69*, 87–97.

Delgado, M., & Pérez-Camacho, A. (2007). *Comparative study of gonadal development of Ruditapes philippinarum (Adams and Revé) and Ruditapes decussatus (L.)(Mollusca, Bivalvia): Influence of temperature*.

Delia, S., Grillo, O. C., Mauro, A., & Donia, D. (1984). Indagine sulle condizioni igieniche dei laghi di Ganzirri e Faro. *IV Conv. Pat. Clin. Igien. Amb.*, 347–360.

Devauchelle, N. (1990). Sviluppo sessuale e maturità di Tapes philippinarum. In *Tapes philippinarum: biologia e sperimentazione* (pp. 49–62). Ente Sviluppo Agricolo Veneto (E.S.A.V.).

D'Iglio, C., Albano, M., Famulari, S., Savoca, S., Panarello, G., Di Paola, D., Perdichizzi, A., Rinelli, P., Lanteri, G., Spanò, N., & Capillo, G. (2021). Intra- and interspecific variability among congeneric Pagellus otoliths. *Scientific Reports*, *11*(1). https://doi.org/10.1038/s41598-021-95814-w

D'iglio, C., Natale, S., Albano, M., Savoca, S., Famulari, S., Gervasi, C., Lanteri, G., Panarello, G., Spanò, N., & Capillo, G. (2022). Otolith Analyses Highlight Morpho-Functional Differences of Three Species of Mullet (Mugilidae) from Transitional Water. *Sustainability (Switzerland)*, *14*(1). https://doi.org/10.3390/su14010398

Dommergues, E., Dommergues, J.-L., Magniez, F., Neige, P., & Verrecchia, E. (2003). Geometric Measurement Analysis Versus Fourier Series Analysis for Shape Characterization Using the Gastropod Shell (Trivia) as an Example. *Mathematical Geology*, *35*. https://doi.org/10.1023/B:MATG.0000007785.96748.62

Donn, T. E., & Els, S. F. (1990). BURROWING TIMES OF DONAX-SERRA FROM THE SOUTH AND WEST COASTS OF SOUTH-AFRICA. *The Veliger*, *33*, 355–358. https://www.biodiversitylibrary.org/part/94243

Drummond, L., Mulcahy, M., & Culloty, S. (2006). The reproductive biology of the Manila clam, Ruditapes philippinarum, from the North-West of Ireland. *Aquaculture*, *254*, 326–340. https://doi.org/10.1016/j.aquaculture.2005.10.052

Dulzetto, F. (1942). Sui caratteri dell'"Engraulis" del lago di Ganzirri. *Boll. Acc. Gioenia Sc. Nat., Catania: Serie III, Fasc. XIX*, 1–8.

El-Wazzan, E., Khafage, A., Kamal, M., & Abbas, A. (2020). Reproductive cycle of the grooved carpet shell clam, Ruditapes decussatus (Linnaeus, 1758), from three Egyptian fisheries. *Cahiers de Biologie Marine*, *61*, 181–194.

Fan, D., Zhang, A., Yang, Z., & Sun, X. (2007). Observations on shell growth and morphology of the bivalve Ruditapes philippinarum. *Chinese Journal of Oceanology and Limnology*, *25*(3), 322–329. https://doi.org/10.1007/s00343-007-0322-3

Ficalbi, E. (1898). Cenni sopra la molluschicoltura nei laghi di Ganzirri e del Faro (Messina) e sopra le cause e i rimedi dell'odierno deperimento. *Giorn. It. Di Pesca e Acquac. Anno III, 3* .

Gamberini. (1920). Circa i diritti della pesca e d'uso nei laghi di Ganzirri e Faro. *Monografia Marittima*, 359–375.

Gerpe, D., Lasa, A., Lema, A., & Romalde, J. L. (2021). Metataxonomic analysis of tissue-associated microbiota in grooved carpet-shell (Ruditapes decussatus) and Manila (Ruditapes philippinarum) clams. *International Microbiology*, *24*(4), 607–618. https://doi.org/10.1007/s10123-021-00214-9

Ghiselli, F., Milani, L., Iannello, M., Procopio, E., Chang, P., Nuzhdin, S., & Passamonti, M. (2017). The complete mitochondrial genome of the grooved carpet shell, Ruditapes decussatus (Bivalvia, Veneridae). *PeerJ*, *5*, e3692. https://doi.org/10.7717/peerj.3692

Ghozzi, K., Dhiab, R. Ben, Challouf, R., & Bradai, M. N. (2022). Morphometric Variation among Four Local Ruditapes decussatus Populations in Monastir Bay (Eastern Coast, Tunisia). *Brazilian Archives of Biology and Technology*, *65*. https://doi.org/10.1590/1678-4324-2022210235

Giani, D., Baini, M., Galli, M., Casini, S., & Fossi, M. C. (2019). Microplastics occurrence in edible fish species (Mullus barbatus and Merluccius merluccius) collected in three different geographical sub-areas of the Mediterranean Sea. *Marine Pollution Bulletin*, *140*, 129–137. https://doi.org/https://doi.org/10.1016/j.marpolbul.2019.01.005

Gómez-Martínez, O., Aranda, D., Quintana, P., Pichardo, J., & Alvarado-Gil, J. (2002). Photoacoustic determination of the thermal properties of bivalve mollusk shells. *Marine Biology*, *141*, 911–914. https://doi.org/10.1007/s00227-002-0880-z

Gosling, E. (2015). *Marine Bivalve Molluscs - Second Edition* (Wiley Blackwell).

Goulletquer P., & Bacher C. (1988). Empirical modelling of the growth of Ruditapes philippinarum by means of non linear regression on factorial coordinates. *Aquat. Living Resour.*, *1*, 141–154.

Haines, A., & Crampton, J. (2003). Improvements To The Method Of Fourier Shape Analysis As Applied In Morphometric Studies. *Palaeontology*, *43*, 765–783. https://doi.org/10.1111/1475-4983.00148

Hamida, L., Medhiouband, M.-N., Cochard, J. C., Romdhane, M.-S., & Le Pennec, M. (2004). Etude comparative du cycle de reproduction de la palourde Ruditapes decussatus en milieu naturel (sud Tunisie) et contrôlé (écloserie). In *Cah. Biol. Mar* (Vol. 45).

Helm M.M., & Pellizzato M. (1990). Riproduzione ed allevamento in schiuditoio della specie Tapes philippinarum. In *Tapes philippinarum biologia e sperimentazione* (pp. 117–140). Ente Sviluppo Agricolo Veneto (E.S.A.V.).

Hernawan, U. E. K. O. (2008). Symbiosis between the giant clams (Bivalvia: Cardiidae) and zooxanthellae (Dinophyceae). *Biodiversitas Journal of Biological Diversity*, *9*(1).

Herrmann, M., Alfaya, J., Lepore, M., Penchaszadeh, P., & Laudien, J. (2009). Reproductive cycle and gonad development of the Northern Argentinean (Bivalvia: Mesodesmatidae). *Helgoland Marine Research*, *63*, 207–218. https://doi.org/10.1007/s10152-009-0150-2

Holland D. A., C. K. K. (1974). Reproductive cycle of the Manila clam (Venerupis japonica) from Hood Canal, Washington. *Proceedings of the National Shellfisheries Association (64)*, 53–58.

Huo, Z., Li, Y., Rbbani, G., Wu, Q., & Yan, X. (2018). Temperature challenge on larvae and juveniles of the Manila clam Ruditapes philippinarum. *Aquaculture Research*, *49*. https://doi.org/10.1111/are.13600

Huo, Z., Yan, X., Zhao, L., Zhang, Y., Yang, F., & Zhang, G. (2010). Effects of shell morphological traits on the weight traits of Manila clam (Ruditapes philippinarum). *Acta Ecologica Sinica*, *30*(5), 251–256. https://doi.org/https://doi.org/10.1016/j.chnaes.2010.08.004

Hurtado, N., Pérez-García, C., Morán, P., & Pasantes, J. (2011). Genetic and cytological evidence of hybridization between native Ruditapes decussatus and introduced Ruditapes philippinarum (Mollusca, Bivalvia, Veneridae) in NW Spain. *Aquaculture*, *311*, 123–128. https://doi.org/10.1016/j.aquaculture.2010.12.015

Inoue, N., Ishibashi, R., Ishikawa, T., Atsumi, T., Aoki, H., & Komaru, A. (2010). Gene expression patterns and pearl formation in the Japanese pearl oyster (Pinctada fucata): a comparison of gene expression patterns between the pearl sac and mantle tissues. *Aquaculture*, *308*, S68–S74.

D.A. 21/06/01, Pub. L. No. 168, G.U. n. 168 del 21-7-2005 (2001).

Jabbar, A., & Davies, J. I. (1987). A simple and convenient biochemical method for sex identification in the marine mussel, Mytilus edulis L. *Journal of Experimental Marine Biology and Ecology*, *107*(1), 39–44.

Jackson, D. J., McDougall, C., Woodcroft, B., Moase, P., Rose, R. A., Kube, M., Reinhardt, R., Rokhsar, D. S., Montagnani, C., & Joubert, C. (2010). Parallel evolution of nacre building gene sets in molluscs. *Molecular Biology and Evolution*, *27*(3), 591–608.

Jacob, D. E., Soldati, A. L., Wirth, R., Huth, J., Wehrmeister, U., & Hofmeister, W. (2008). Nanostructure, composition and mechanisms of bivalve shell growth. *Geochimica et Cosmochimica Acta*, *72*(22), 5401–5415. https://doi.org/https://doi.org/10.1016/j.gca.2008.08.019

Jacobs, D. K., Wray, C. G., Wedeen, C. J., Kostriken, R., DeSalle, R., Staton, J. L., Gates, R. D., & Lindberg, D. R. (2000). Molluscan engrailed expression, serial organization, and shell evolution. *Evolution & Development*, *2*(6), 340–347. https://doi.org/https://doi.org/10.1046/j.1525-142x.2000.00077.x

Juanes, J. A., Bidegain, G., Echavarri-Erasun, B., Puente, A., García, A., García, A., Bárcena, J. F., Álvarez, C., & García-Castillo, G. (2012). Differential distribution pattern of native Ruditapes decussatus and introduced Ruditapes phillippinarum clam populations in the Bay of Santander (Gulf of Biscay): Considerations for fisheries management. *Ocean & Coastal Management*, *69*, 316–326. https://doi.org/https://doi.org/10.1016/j.ocecoaman.2012.08.007

Ketata, I., Guermazi, F., Rebai, T., & Hamza-Chaffai, A. (2007). Variation of steroid concentrations during the reproductive cycle of the clam Ruditapes decussatus: A one year study in the gulf of Gabès area. *Comparative Biochemistry and Physiology. Part A, Molecular & Integrative Physiology*, *147*, 424–431. https://doi.org/10.1016/j.cbpa.2007.01.017

Khemissa, G., Rym, B. dhiab, Challouf, R., & Bradai, M. (2022). Morphometric Variation among Four Local Ruditapes decussatus Populations in Monastir Bay (Eastern Coast, Tunisia).

Brazilian Archives of Biology and Technology, *65*. https://doi.org/10.1590/1678-4324-2022210235

Kirkendale, L., & Paulay, G. (2017). *Photosymbiosis in Bivalvia* (p. 31).

Kobayashi, I., & Samata, T. (2006). Bivalve shell structure and organic matrix. *Materials Science and Engineering: C*, *26*(4), 692–698. https://doi.org/https://doi.org/10.1016/j.msec.2005.09.101

Lane, D. J. W., & Nott, J. A. (1975). A study of the morphology, fine structure and histochemistry of the foot of the pediveliger of Mytilus edulis L. *Journal of the Marine Biological Association of the United Kingdom*, *55*(2), 477–495.

Langdon, C. J. (1996). Digestion and nutrition in larvae and adults. *Eastern Oyster Crassostrea Virginica*, 231–269.

Lango-Reynoso, F., Chávez-Villalba, J., Cochard, J. C., & Le Pennec, M. (2000). Oocyte size, a means to evaluate the gametogenic development of the Pacific oyster, Crassostrea gigas (Thunberg). *Aquaculture*, *190*(1–2), 183–199.

Langton, R. W., & Gabbott, P. A. (1974). The tidal rhythm of extracellular digestion and the response to feeding in Ostrea edulis. *Marine Biology*, *24*, 181–187.

Laudien, J., Flint, N., van der Bank, H., & Brey, T. (2003). Genetic and morphological variation in four populations of the surf clam Donax serra (R??ding) from southern African sandy beaches. *Biochemical Systematics and Ecology*, *31*, 751–772. https://doi.org/10.1016/S0305-1978(02)00252-1

Le, T. C., Kang, H.-S., Hong, H.-K., Park, K.-J., & Choi, K.-S. (2015). First report of Urosporidium sp., a haplosporidian hyperparasite infecting digenean trematode Parvatrema duboisi in Manila clam, Ruditapes philippinarum on the west coast of Korea. *Journal of Invertebrate Pathology*, *130*, 141–146.

Levi-Kalisman, Y., Falini, G., Addadi, L., & Weiner, S. (2001). Structure of the Nacreous Organic Matrix of a Bivalve Mollusk Shell Examined in the Hydrated State Using Cryo-TEM. *Journal of Structural Biology*, *135*(1), 8–17. https://doi.org/https://doi.org/10.1006/jsbi.2001.4372

Libungan, L. A., & Pálsson, S. (2015). ShapeR: An R Package to Study Otolith Shape Variation among Fish Populations. *PLOS ONE*, *10*(3), e0121102-. https://doi.org/10.1371/journal.pone.0121102

Lo Giudice, P. (1940). I laghi di Faro e Ganzirri dal punto di vista biologico e da quello autarchico. *Atti II Convegno Di Biologia Marina e Le Sue Applicazioni Alla Pesca, V Relazione*, 1–14.

Lovatelli., Alessandro., Farías, Ana., & Uriarte, Iker. (2008). *Estado actual del cultivo y manejo de moluscos bivalvos y su proyección futura : factores que afectan su sustentabilidad en América Latina : Taller técnico regional de la FAO, 20-24 de agosto de 2007, Puerto Montt, Chile*. Organización de las Naciones unidas para la agricultura y la alimentación.

Lutz, R. A., & Kennish, M. J. (1992). Ecology and morphology of larval and early post- larval mussels. In E. M. Gosling (Ed.), *The Mussel Mytilus: Ecology, Physiology, Genetics and Culture* (pp. 53–85). Elsevier Science Publishers B.V.

Maboloc, E. A., Puzon, J. J. M., & Villanueva, R. D. (2015). Stress responses of zooxanthellae in juvenile Tridacna gigas (Bivalvia, Cardiidae) exposed to reduced salinity. *Hydrobiologia*, *762*, 103–112.

Machado, D., Baptista, T., Joaquim, S., Anjos, C., Mendes, S., Matias, A., & Matias, D. (2018). Reproductive cycle of the European clam Ruditapes decussatus from Óbidos Lagoon, Leiria, Portugal. *Invertebrate Reproduction and Development*, *62*. https://doi.org/10.1080/07924259.2018.1472671

Manganaro, A., Pulicanò, G., Reale, A., Sanfilippo, M., & Sarà, G. (2009). Filtration pressure by bivalves affects the trophic conditions in Mediterranean shallow ecosystems. *Chemistry and Ecology*, *25*(6), 467–478. https://doi.org/10.1080/02757540903325120

Manganaro, A., Pulicanò, G., & Sanfilippo, M. (2011). Temporal evolution of the area of Capo Peloro (Sicily, Italy) from pristine site into urbanized area. *Transitional Waters Bulletin*, *5*(1), 23–31. https://doi.org/10.1285/i1825229Xv5n1p23

Marin, F., & Luquet, G. (2004). Molluscan shell proteins. *Comptes Rendus Palevol*, *3*(6), 469–492. https://doi.org/https://doi.org/10.1016/j.crpv.2004.07.009

Marin, F., & Luquet, G. (2005). Molluscan biomineralization: The proteinaceous shell constituents of Pinna nobilis L. *Materials Science and Engineering: C*, *25*(2), 105–111.

Marzano, A. (2013). Oysters and Other Shellfish. In *Harvesting the Sea: The Exploitation of Marine Resources in the Roman Mediterranean*. Oxford Studies on the Roman Economy.

Matias, D., Joaquim, S., Matias, A., Moura, P., De Sousa, J., Sobral, P., & Leitão, A. (2013). The reproductive cycle of the European clam Ruditapes decussatus (L., 1758) in two Portuguese populations: Implications for management and aquaculture programs. *Aquaculture*, *s 406–407*, 52–61. https://doi.org/10.1016/j.aquaculture.2013.04.030

Mazzarelli, G. (1938). L'origine marina dei laghi di Faro e Ganzirri. *Bollettino Pesca, Piscicoltura e Idrobiologia 14*, 31–40.

Mazzola, A., Bergamasco, A., Calvo, S., Caruso, G., Chemello, R., Colombo, F., Giaccone, G., Gianguzza, P., Guglielmo, L., Leonardi, M., Riggio, S., Sarà, G., Signa, G., Tomasello, A., & Vizzini, S. (2010a). Sicilian transitional waters: Current status and future development. In *Chemistry and Ecology* (Vol. 26, Issue SUPPL. 1, pp. 267–283). https://doi.org/10.1080/02757541003627704

Mazzola, A., Bergamasco, A., Calvo, S., Caruso, G., Chemello, R., Colombo, F., Giaccone, G., Gianguzza, P., Guglielmo, L., Leonardi, M., Riggio, S., Sarà, G., Signa, G., Tomasello, A., & Vizzini, S. (2010b). Sicilian transitional waters: Current status and future development. *Chemistry and Ecology*, *26*, 267–283. https://doi.org/10.1080/02757541003627704

Merrill, A. S., Posgay, J. A., & NICHY, F. E. (1966). ANNUAL MARKS ON SHELL AND LIGAMENT OF SEA SCALLOP. *Fishery Bulletin of the Fish and Wildlife Service*, *65*(2), 299.

Mikhailov, A. T., Torrado, M., & Mendez, J. (2002). Sexual differentiation of reproductive tissue in bivalve molluscs: identification of male associated polypeptide in the mantle of Mytilus galloprovincialis Lmk. *International Journal of Developmental Biology*, *39*(3), 545–548.

Milan, M., Smits, M., Dalla Rovere, G., Iori, S., Zampieri, A., Carraro, L., Martino, C., Papetti, C., Ianni, A., Ferri, N., Iannaccone, M., Patarnello, T., Brunetta, R., Ciofi, C., Grotta, L., Arcangeli, G., Bargelloni, L., Cardazzo, B., & Martino, G. (2019). Host-microbiota interactions shed light on mortality events in the striped venus clam Chamelea gallina. *Molecular Ecology*, *28*(19), 4486–4499. https://doi.org/10.1111/mec.15227

Mistri M. (2007). *Valutazione della risorsa Tapes philippinarum in Alto Adriatico: localizzazione e potenzialità produttiva delle aree di nursery naturale*. MIPAF, VI piano triennale.

Moura, P., Garaulet, L., Vasconcelos, P., Chainho, P., Costa, J., & Gaspar, M. (2017). Age and growth of a highly successful invasive species: the Manila clam Ruditapes philippinarum (Adams & Reeve, 1850) in the Tagus Estuary (Portugal). *Aquatic Invasions*, *12*, 133–146. https://doi.org/10.3391/ai.2017.12.2.02

Moura, P., Vasconcelos, P., & Gaspar, M. (2013). Age and growth in three populations of Dosinia exoleta (Bivalvia: Veneridae) from the Portuguese coast. *Helgoland Marine Research*, *67*. https://doi.org/10.1007/s10152-013-0350-7

Nel, R., McLachlan, A., & Winter, D. P. E. (2001). The effect of grain size on the burrowing of two Donax species. *Journal of Experimental Marine Biology and Ecology*, *265*(2), 219–238.

Nerlović, V., Korlević, M., & Mravinac, B. (2016). Morphological and Molecular Differences between the Invasive Bivalve Ruditapes philippinarum (Adams & Reeve, 1850) and the Native Species Ruditapes decussatus (Linnaeus, 1758) from the Northeastern Adriatic Sea. *Journal of Shellfish Research*, *35*(1), 31–39. https://doi.org/10.2983/035.035.0105

Ngo, T. T. T., & Choi, K.-S. (2004). Seasonal changes of Perkinsus and Cercaria infections in the Manila clam Ruditapes philippinarum from Jeju, Korea. *Aquaculture*, *239*(1–4), 57–68.

Nudelman, F., Shimoni, E., Klein, E., Rousseau, M., Bourrat, X., Lopez, E., Addadi, L., & Weiner, S. (2008). Forming nacreous layer of the shells of the bivalves Atrina rigida and Pinctada margaritifera: An environmental- and cryo-scanning electron microscopy study. *Journal of Structural Biology*, *162*(2), 290–300. https://doi.org/https://doi.org/10.1016/j.jsb.2008.01.008

Ojea, J., Pazos, A. J., Martínez, D., Nóvoa, S., Sánchez, J. L., & Abal, M. (2004). Seasonal variation in weight and biochemical composition of the tissues of Ruditapes decussatus in relation to the gametogenic cycle. *Aquaculture*, *238*, 451–468. https://doi.org/10.1016/j.aquaculture.2004.05.022

Palmer, M., Pons, G., & Linde, M. (2004). Discriminating between geographical groups of a Mediterranean commercial clam (Chamelea gallina (L.): Veneridae) by shape analysis. *Fisheries Research*, *67*, 93–98. https://doi.org/10.1016/j.fishres.2003.07.006

Pascual, M. S., & Zampatti, E. A. (1995). Evidence of a chemically mediated adult-larval interaction triggering settlement in Ostrea puelchana: applications in hatchery production. *Aquaculture*, *133*(1), 33–44.

Pellizzato, M. (1990). Acclimazione della specie Tapes philippinarum e primi allevamenti in Italia. In *Tapes philippinarum Biologia e Sperimentazione* (pp. 159–170). Ente Sviluppo Agricolo Veneto (E.S.A.V.).

Pranovi, & Giovanardi. (1995). La pesca di molluschi bivalvi nella Laguna di Venezia: effetti e conseguenze. *Biologia Marina Mediterranea*, *2*(2), 121–122.

PROGRAMMA OPERATIVO NAZIONALE FEAMPA 2021-2027 FONDO EUROPEO PER GLI AFFARI MARITTIMI, LA PESCA E L'ACQUACOLTURA RAPPORTO PRELIMINARE AMBIENTALE. (n.d.).

Ramón, M., & Richardson, C. (1992). Age determination and shell growth of Chamelea gallina (Bivalvia: Veneridae) in the western Mediterranean. *Marine Ecology-Progress Series - MAR ECOL-PROGR SER*, *89*, 15–23. https://doi.org/10.3354/meps089015

Reid, R. G. B. (1968). The distribution of digestive tract enzymes in lamellibranchiate bivalves. *Comparative Biochemistry and Physiology*, *24*(3), 727–744.

Rodríguez-Moscoso, E., & Arnaiz, R. (1998). Gametogenesis and energy storage in a population of the grooved carpet-shell clam, Tapes decussatus (Linné, 1787), in northwest Spain. *Aquaculture*, *162*, 125–139. https://doi.org/10.1016/S0044-8486(98)00170-7

Ropes, J. W. (1987). *Preparation of acetate peels of valves from the ocean quahog, Arctica islandica, for age determinations* (Vol. 50). US Department of Commerce, National Oceanic and Atmospheric Administration ….

Rossi R. (1996). Allevamento di vongola verace filippina (Tapes philippinarum). Gestione della semina e del trasferimento in banco naturale per la ottimizzazione del raccolto. In *Relazione D.M 04/92 del 18.02.1993* (pp. 122–122).

Rossi R., & Paesanti F. (1992). Vongola verace: la situazione europea. *Laguna*, *9*, 24–27.

Rufino, M., Gaspar, M., Pereira, A., & Vasconcelos, P. (2006). Use of shape to distinguish Chamelea gallina and Chamelea striatula (Bivalvia: Veneridae): Linear and geometric morphometric methods. *Journal of Morphology*, *267*, 1433–1440. https://doi.org/10.1002/jmor.10489

Sanfilippo, M., Albano, M., Manganaro, A., Capillo, G., Spanò, N., & Savoca, S. (2022). Spatiotemporal Organic Carbon Distribution in the Capo Peloro Lagoon (Sicily, Italy) in Relation to Environmentally Sustainable Approaches. *Water (Switzerland)*, *14*(1). https://doi.org/10.3390/w14010108

Sanzo, L. (1904). Sulle cause dell'attuale moria dei Molluschi Bivalvi coltivati nei laghi di Ganzirri e Faro (Messina). *Atti Reale Accad. Pel. 19*, 241–259.

Savoca, S., Bottari, T., Fazio, E., Bonsignore, M., Mancuso, M., Luna, G. M., Romeo, T., D'Urso, L., Capillo, G., Panarello, G., Greco, S., Compagnini, G., Lanteri, G., Crupi, R., Neri, F., & Spanò, N. (2020). Plastics occurrence in juveniles of Engraulis encrasicolus and Sardina pilchardus in the Southern Tyrrhenian Sea. *Science of The Total Environment*, *718*, 137457. https://doi.org/https://doi.org/10.1016/j.scitotenv.2020.137457

Savoca, S., Grifó, G., Panarello, G., Albano, M., Giacobbe, S., Capillo, G., Spanó, N., & Consolo, G. (2020). Modelling prey-predator interactions in Messina beachrock pools. *Ecological Modelling*, *434*. https://doi.org/10.1016/j.ecolmodel.2020.109206

Saxby, S. A., Western Australia. Fisheries Research Division., & Western Australia. Department of Fisheries. (2002). *A review of food availability, sea water characteristics and bivalve growth performance at coastal culture sites in temperate and warm temperate regions of the world*. Fisheries Research Division, Dept. of Fisheries.

Seed, R. (1976). Ecology. In B. L. Bayne (Ed.), *Marine mussels: their ecology and physiology* (pp. 13–65). Cambridge University Press .

Sejr, M., Jensen, K., & Rysgaard, S. (2002). Annual growth bands in the bivalve Hiatella arctica validated by a mark-recapture study in NE Greenland. *Polar Biology*, *25*, 794–796. https://doi.org/10.1007/s00300-002-0413-8

Shafee, M., & DAOUDI, M. (2008). Gametogenesis and spawning in the carpet-shell clam, Ruditapes decussatus (L.) (Mollusca: Bivalvia), from the Atlantic coast of Morocco. *Aquaculture Research*, *22*, 203–216. https://doi.org/10.1111/j.1365-2109.1991.tb00510.x

Sherratt, E., Serb, J., & Adams, D. (2017). Rates of morphological evolution, asymmetry and morphological integration of shell shape in scallops. *BMC Evolutionary Biology*, *17*, 248. https://doi.org/10.1186/s12862-017-1098-5

Shirai, K., Takahata, N., Yamamoto, H., Omata, T., Sasaki, T., & Sano, Y. (2008). Novel analytical approach to bivalve shell biogeochemistry: a case study of hydrothermal mussel shell. *Geochemical Journal*, *42*(5), 413–420.

Silva S., M. N. , P. J. J. (2006). Genetic evidence of natural hybridization between Ruditapes decussatus and R. philippinarum. *Org. Divers. Evol.*, *6*(Electr. Suppl. 16, part 1: 71).

Silvestro, S., Capillo, G., Sanfilippo, M., Fiorino, E., Giangrosso, G., Vincenzo, F., Salvatore, D., Vazzana, I., & Faggio, C. (2017). APPRAISAL OF THE ABIOTIC AND BIOTIC FRAMEWORK OF FARO LAKE (MESSINA, SICILY). *Journal of Biological Research*, *90*, 14.

Smaoui-Damak, W., Mathieu, M., Rebai, T., & Hamza-Chaffai, A. (2007). Histology of the reproductive tissue of the clam Ruditapes decussatus from the Gulf of Gabes (Tunisia). *Invertebrate Reproduction & Development*, *50*(3), 117–126.

Smith, N. F., Lepofsky, D., Toniello, G., Holmes, K., Wilson, L., Neudorf, C. M., & Roberts, C. (2019). 3500 years of shellfish mariculture on the Northwest Coast of North America. *PLOS ONE*, *14*(2), e0211194-. https://doi.org/10.1371/journal.pone.0211194

Smith, S., Wilson, N., Goetz, F., Feehery, C., Andrade, S., Rouse, G., Giribet, G., & Dunn, C. (2013). Resolving the evolutionary relationships of molluscs with phylogenomic tools (vol 480, pg 364, 2011). *Nature*, *493*, 708. https://doi.org/10.1038/nature11736

Solino, C. J. (1864). *Collectanea rerum memorabilium: Vol. Cp. II* (John White - Bernolini, Ed.; T.H. Mommsen edition).

Declaratory measure 1342/88, Memorandum predisposto per l'assessorato infrastrutture territoriali del comune di Messina concernente: laghi di Faro e Ganzirri -Declaratoria di interesse etno-antropologico (1988).

Stanley, S. M. (1970). Relation of shell form to life habits of the Bivalvia (Mollusca). *Geological Society of America, Memoir*, *25*, 1–269.

Stevenson, J. A., & Dickie, L. M. (1954). Annual growth rings and rate of growth of the giant scallop, Placopecten magellanicus (Gmelin) in the Digby area of the Bay of Fundy. *Journal of the Fisheries Board of Canada*, *11*(5), 660–671.

Tallqvist, M. (2001). Burrowing behaviour of the Baltic clam Macoma balthica: effects of sediment type, hypoxia and predator presence. *Marine Ecology Progress Series*, *212*, 183–191.

Taylor, J., & Strack, E. (2008). Pearl production. *The Pearl Oyster*, 273–302.

Terni, C. (1901). Notizie del Prof. Terni, Direttore Ufficio d'Igiene Comunale. *Ufficio Tecnico Municipio Di Messina*.

Thompson, R. J. (1984). The reproductive cycle and physiological ecology of the mussel Mytilus edulis in a subarctic, non-estuarine environment. *Marine Biology*, *79*, 277–288.

Thorarinsdóttir, G. G. (1993). The iceland scallop, Chlamys islandica (OF Müller), in Breidafjördur, West Iceland: II. Gamete development and spawning. *Aquaculture*, *110*(1), 87–96.

Toba, M. , Natsume Y., & Yamakawa, H. (1993). Reproductive cycle of Manila clam from Funabashi waters, Tokyo Bay. *Nippon Suisan Gakkaishi*, *59*(1), 15–22.

Tresnakova, N., Famulari, S., Zicarelli, G., Impellitteri, F., Pagano, M., Presti, G., Filice, M., Caferro, A., Gulotta, E., Salvatore, G., Sandova, M., Vazzana, I., Imbrogno, S., Capillo, G., Savoca, S., Velisek, J., & Faggio, C. (2023). Multi-characteristic toxicity of enantioselective chiral fungicide tebuconazole to a model organism Mediterranean mussel Mytilus galloprovincialis Lamarck, 1819 (Bivalve: Mytilidae). *Science of the Total Environment*, *862*. https://doi.org/10.1016/j.scitotenv.2022.160874

Tresnakova, N., Impellitteri, F., Famulari, S., Porretti, M., Filice, M., Caferro, A., Savoca, S., D'Iglio, C., Imbrogno, S., Albergamo, A., Vazzana, I., Stara, A., Di Bella, G., Velisek, J., & Faggio, C. (2023). Fitness assessment of Mytilus galloprovincialis Lamarck, 1819 after exposure to herbicide metabolite propachlor ESA. *Environmental Pollution*, *331*. https://doi.org/10.1016/j.envpol.2023.121878

Trueman, E. R. (1967). The dynamics of burrowing in Ensis (Bivalvia). *Proceedings of the Royal Society of London. Series B. Biological Sciences*, *166*(1005), 459–476.

Urrutia, M. B., Ibarrola, I., Iglesias, J. I. P., & Navarro, E. (1999). Energetics of growth and reproduction in a high-tidal population of the clam Ruditapes decussatus from Urdaibai Estuary (Basque Country, N. Spain). In *Journal of Sea Research* (Vol. 42).

Verdelhos, T., Marques, J., & Anastácio, P. (2015). Behavioral and mortality responses of the bivalves Scrobicularia plana and Cerastoderma edule to temperature, as indicator of climate change's potential impacts. *Ecological Indicators*, *58*, 95–103. https://doi.org/10.1016/j.ecolind.2015.05.042

Wakashin, H., Seo, E., & Seo, Y. (2018). Accumulation and excretion of manganese ion in the kidney of the Mytilus galloprovincialis. *The Journal of Experimental Biology*, *221*, jeb.185439. https://doi.org/10.1242/jeb.185439

Walne, P. R. (1974). *Culture of Bivalve Molluscs: 50 Years' Experience at Conwy*. Fishing News Books.

Wang, W.-X., & Lu, G. (2017). Chapter 21 - Heavy Metals in Bivalve Mollusks. In D. Schrenk & A. Cartus (Eds.), *Chemical Contaminants and Residues in Food (Second Edition)* (pp. 553–594). Woodhead Publishing. https://doi.org/https://doi.org/10.1016/B978-0-08-100674-0.00021-7

Watanabe, S. (2010). Relationships Among Shell Shape, Shell Growth Rate, and Nutritional Condition in the Manila Clam (Ruditapes philippinarum) in Japan. *Journal of Shellfish Research*, *29*, 353–359. https://doi.org/10.2983/035.029.0210

Weymouth, F. W. (1922). *Fish Bulletin No. 7. The Life-History and Growth of the Pismo Clam (Tivela stultorum Mawe)*.

Wilbur, K. M., & Yonge, C. M. (2013). *Physiology of Mollusca: Volume II* (Vol. 2). Academic Press.

Zieritz, A., & Aldridge, D. (2009). Identification of ecophenotypic trends within three European freshwater mussel species (Bivalvia: Unionoida) using traditional and modern morphometric techniques. *Biological Journal of the Linnean Society*, *98*, 814–825. https://doi.org/10.1111/j.1095-8312.2009.01329.x

Zuykov, M., Pelletier, E., & Harper, D. A. T. (2013). Bivalve mollusks in metal pollution studies: From bioaccumulation to biomonitoring. *Chemosphere*, *93*(2), 201–208. https://doi.org/https://doi.org/10.1016/j.chemosphere.2013.05.001

Zwann, A. de, & Mathieu, M. (1992). Cellular biochemistry and endocrinology. In E. M. Gosling (Ed.), *The Mussel Mytilus: Ecology, Physiology, Genetics and Culture* (pp. 223–307). Elsevier Science Publishers B.V.